

TARGETING TUMOR-SUPPORTIVE CELLS WITH CSF1R SMALL-
MOLECULE INHIBITORS AS A NOVEL TREATMENT STRATEGY FOR
CHRONIC LYMPHOCYTIC LEUKEMIA AND ACUTE MYELOID
LEUKEMIA

By

David K. Edwards V

A DISSERTATION

Presented to the Department of Cell, Developmental and Cancer Biology
and the Oregon Health & Science University

School of Medicine

in partial fulfillment of
the requirements for the degree of

Doctor of Philosophy

April 2018

School of Medicine
Oregon Health & Science University

CERTIFICATE OF APPROVAL

This is to certify that the PhD dissertation of
David K. Edwards V
has been approved

Jeffrey Tyner, Mentor/Advisor

Shannon McWeeney, Co-Mentor

Evan Lind, Member

Paul Spellman, Member

Andrew Weinberg, Member

Molly Kulesz-Martin, External Advisor

Sara Courtneidge, Committee Chair

Table of Contents

1	List of Figures	vi
2	List of Tables	ix
3	Abbreviations.....	x
4	Acknowledgements	xvi
5	Abstract	xx
6	Introduction.....	1
6.1	Hematologic malignancies	1
6.1.1	Acute myeloid leukemia	6
6.1.2	Chronic lymphocytic leukemia	11
6.2	Treatment of AML and CLL	14
6.2.1	Targeted therapy	17
6.2.2	Targeting the tumor microenvironment	21
6.3	Colony stimulating factor 1 receptor (CSF1R)	24
6.3.1	Discovery of CSF1R	24
6.3.2	Structure and function of CSF1R.....	26
6.4	CSF1R and cancer	29
6.4.1	CSF1R clinical trials.....	30
6.4.2	CSF1R in acute myeloid leukemia.....	34
6.4.3	CSF1R in chronic lymphocytic leukemia	36

6.5	Targeting CSF1R in acute myeloid leukemia and chronic lymphocytic leukemia.....	38
7	Targeting of Colony-Stimulating Factor 1 Receptor (CSF1R) in the CLL Microenvironment Yields Antineoplastic Activity in Primary Patient Samples ..	40
7.1	Contribution to Project	41
7.1.1	Conception or design of the work	41
7.1.2	Data collection, analysis, and interpretation.....	42
7.1.3	Article drafting/submission/revision	44
7.2	Abstract.....	45
7.3	Introduction	46
7.4	Results	48
7.4.1	CLL Patient Specimens Are Sensitive to CSF1R-Specific Small-Molecule Inhibitors	48
7.4.2	CD14+ Cell Subpopulation Expresses CSF1R and Is Associated with CSF1R Inhibitor Sensitivity	49
7.4.3	CD14+ Depletion in CLL Patient Samples Decreases Cell Viability and Eliminates CSF1R Inhibitor Sensitivity.....	51
7.4.4	CSF1R Inhibitors Work Synergistically in Combination with Ibrutinib and Idelalisib in a Majority of CLL Patient Samples.....	54
7.5	Discussion.....	55
7.6	Methods.....	58
7.6.1	Patient Sample Acquisition and Processing.....	58
7.6.2	Immunophenotype Analysis of CLL Patient Samples.....	60

7.6.3	Depletion of CD14+ Cells from Primary Patient Specimens	60
7.6.4	Isolating Nurse-Like Cells (NLCs) from Primary Patient Specimens	61
7.6.5	Synergy Calculations between CSF1R Inhibitors and Ibrutinib/Idelalisib	62
7.7	Author Contributions.....	62
7.8	Acknowledgements.....	63
7.9	Funding.....	63
7.10	Conflict of Interest	64
8	CSF1R inhibitors exhibit anti-tumor activity in acute myeloid leukemia by blocking paracrine signals from support cells	86
8.1	Contribution to Project	87
8.1.1	Conception or design of the work	87
8.1.2	Data collection, analysis, and interpretation.....	87
8.1.3	Article drafting/submission/revision	90
8.2	Key Points.....	91
8.3	Abstract.....	91
8.4	Introduction	92
8.5	Methods.....	94
8.5.1	Patient sample acquisition and functional screening	94
8.5.2	Mass cytometry (CyTOF) and flow cytometry analysis of cell surface markers	96
8.5.3	CSF1 expression in plasma and stromal cell conditioned media	97

8.5.4	Cytokine/growth factor analysis.....	97
8.5.5	Cytokine secretion in conditioned media.....	98
8.5.6	Cytokine rescue from GW-2580 sensitivity	98
8.6	Supplemental Methods	99
8.6.1	Patient sample selection	99
8.6.2	Small-molecule inhibitor screening data analysis.....	99
8.6.3	siRNA screening data analysis.....	101
8.6.4	Comparing small-molecule inhibitor and siRNA data	102
8.6.5	Clinical and genetic characteristics.....	102
8.6.6	In-house FLT3-ITD and NPM1 sequencing.....	104
8.6.7	Exome and RNA sequencing.....	104
8.6.8	GW-2580 Sensitivity Survival Analysis.....	106
8.6.9	CyTOF Analysis	107
8.7	Results	108
8.8	Discussion.....	115
8.9	Acknowledgements.....	119
8.10	Authorship Contributions	120
8.11	Disclosure of Conflicts of Interest.....	120
9	Discussion.....	149
10	Appendix	164
10.1	Detailed Protocols Used in Dissertation Research.....	164
10.1.1	Processing Patient Peripheral Blood and Bone Marrow Samples Protocol	166

10.1.2	Electroporation of siRNA Library BioRad (AML Patient Sample) Protocol	173
10.1.3	CSF1R Flow Cytometry Staining Protocol.....	174
10.1.4	CSF1R Inhibition and Stimulation (RNA and Conditioned Media) Protocol	177
10.1.5	Magnetic 30-Plex Luminex Protocol.....	178
10.1.6	Stromal Cell Isolation Protocol.....	181
11	References.....	183

1 List of Figures

Figure 7.1. <i>Ex vivo</i> inhibitor screening reveals CSF1R sensitivity in CLL patient specimens.....	66
Figure 7.2. No genetic or clinical characteristic readily co-segregate with sensitivity to CSF1R inhibition in CLL patient samples.	68
Figure 7.3. CSF1R is not found on CD19+ CLL cells but instead expressed on a CD14+ myeloid subpopulation.	70
Figure 7.4. Sensitivity of CLL cells to CD14+ depletion correlates with sensitivity to CSF1R inhibitors.....	71
Figure 7.5. Synergy between ibrutinib or idelalisib and CSF1R inhibitors in majority of CLL patient specimens.	73
Figure 7.6. CSF1R inhibitor exposure induces apoptosis in CLL primary patient samples.	75
Figure 7.7. Box-and-whisker plots for continuous variables in CLL patient sample comparisons and plots of statistically significant characteristics.	77
Figure 7.8. GW-2580 sensitivity and viability after CD14+ depletion is not correlated with sensitivity to ibrutinib and idelalisib.	79
Figure 7.9. CD14+ depletion significantly impact sensitivity to CSF1R inhibitors but does not impact sensitivity to ibrutinib and idelalisib.	81
Figure 7.10. Representative synergistic and antagonistic dose-response curves from patient specimens exposed to the combination of CSF1R inhibitor and ibrutinib/idelalisib.....	83

Figure 8.1 <i>Ex vivo</i> AML patient sample screen reveals that knockdown/inhibition of CSF1R reduces leukemia cell survival in >20% of samples.	122
Figure 8.2. Resistance to CSF1R inhibitor is associated with adverse prognostic risk gene mutations and cytogenetic abnormalities.	125
Figure 8.3. CSF1R is expressed not on the bulk leukemia population in primary AML patient samples but on a small subpopulation of supportive cells.	126
Figure 8.4. HGF stimulates growth in CSF1R inhibitor sensitive samples and its secretion is regulated by CSF1R activation.	128
Figure 8.5. Sensitivity to CSF1R inhibitors correlates with MET inhibitor sensitivity and is eliminated after external HGF stimulation.	130
Figure 8.6. CSF1R inhibitors induce apoptosis in primary AML patient samples, not healthy donors, and patient sample sensitivity strongly correlates across all inhibitors.	132
Figure 8.7. Individual correlation graphs of CSF1R inhibitor sensitivity for each clinical and genetic characteristic evaluated in this study.	136
Figure 8.8. No correlation between CSF1R inhibitor sensitivity and differences in overall survival or disease presentation.	138
Figure 8.9. CSF1R is not expressed on leukemia blasts from primary AML patient samples.	140
Figure 8.10. CSF1R ^{hi} cells cluster into unique subgroups in AML patient samples that correlate differently with <i>ex vivo</i> GW-2580 response.	145
Figure 8.11. Significant correlation exists between inhibitors of MET in AML patient samples.	147

Figure 8.12. CSF1R inhibitor sensitivity is not associated with CSF1 levels in AML
patient samples or sample-derived stromal cells. 148

2 List of Tables

Table 6.1. Clinical trials with CSF1/CSF1R small molecules or monoclonal antibodies currently in clinical development (as of June 2017).	32
Table 7.1. Statistical analysis of clinical and genetic/cytogenetic characteristics of CLL patient sample cohort evaluated for sensitivity to CSF1R inhibitors.	85

3 Abbreviations

ABL1 – ABL proto-oncogene 1, non-receptor tyrosine kinase

AIDS – acquired immunodeficiency syndrome

AKT – AKT serine/threonine kinase 1

AML – acute myeloid leukemia (or acute myelogenous leukemia)

ALL – acute lymphocytic leukemia

Ara-C – cytarabine

ASXL1 – additional sex combs like 1, transcriptional regulator

ATP – adenosine triphosphate

AUC – area under the curve

AXL – AXL receptor tyrosine kinase

B2M – beta-2 microglobulin

BCL2 – BCL2, apoptosis regulator

BCR – B-cell receptor

BR – bendamustine and rituximab

BTK – Bruton tyrosine kinase

c-fms – cellular feline McDonough sarcoma (or CSF1R)

CCL2 – C-C motif chemokine ligand 2

CCL3 – C-C motif chemokine ligand 3

CCL4 – C-C motif chemokine ligand 4

CCR2 – C-C motif chemokine receptor 2

CEBPA – CCAAT enhancer binding protein alpha

CI – combination index

CLL – chronic lymphocytic leukemia

CLL-IPI – CLL International Prognostic Index

CML – chronic myeloid leukemia

CMML – chronic myelomonocytic leukemia

CN-AML – cytogenetically normal acute myeloid leukemia

CSF1R – colony stimulating factor 1 receptor

CSF1 – colony stimulating factor 1

CTLA-4 – cytotoxic T lymphocyte-associated antigen 4

CXCR2 – C-X-C motif chemokine receptor 2

CXCR4 – C-X-C motif chemokine receptor 4

CXCL12 – chemokine C-X-C motif ligand 12 (or SDF-1)

DLBCL – diffuse large B-cell lymphoma

DNMT3A – DNA methyltransferase 3 alpha

DUSP5 – dual specificity phosphatase 5

ELN – European LeukemiaNet

EMT – epithelial-to-mesenchymal transition

ERK1 – mitogen-activated protein kinase 1

ERK2 – mitogen-activated protein kinase 2

ET – essential thrombocythemia

FAB – French-American-British

FDA – Food and Drug Administration

FeSV – feline sarcoma virus

FIRE – c-fms intronic regulatory element

FISH – fluorescent in situ hybridization

FLT3 – fms related tyrosine kinase 3

FLT3-ITD – fms related tyrosine kinase 3 internal tandem duplication

GAB2 – GRB2 associated binding protein 2

HCST – hematopoietic stem cell transplant

HGF – hepatocyte growth factor

HLA – human leukocyte antigen

HSC – hematopoietic stem cell

IC50 – half maximal inhibitory concentration

IDH1 – isocitrate dehydrogenase (NADP(+)) 1, cytosolic

IDH2 – isocitrate dehydrogenase (NADP(+)) 2, mitochondrial

IFN γ – interferon-gamma

IGHV – immunoglobulin heavy-chain variable region

IKZF3 – IKAROS family zinc finger 3

IL-4 – interleukin 4

IL-6 – interleukin 6

IL-8 – interleukin 8

IL-13 – interleukin 13

IL-34 – interleukin 34

KIT – KIT proto-oncogene receptor tyrosine kinase

KRAS – KRAS proto-oncogene, GTPase

LAM – lymphoid-associated macrophage

LPS – lipopolysaccharide

MAPK – mitogen activated protein kinase

Mb – megabase

MCP1 – monocyte chemoattractant protein 1

MDS – myelodysplastic syndrome

MDS/MPN – myelodysplastic/myeloproliferative neoplasm

MDSC – myeloid-derived suppressor cell

MEK – mitogen-activated protein kinase kinase

MOZ – monocytic leukemia zinc finger protein (or ZNF220 or MYST3)

MPN – myeloproliferative neoplasms

NFKB1 – nuclear factor kappa B subunit 1 (NF- κ B)

NK – natural killer

NLC – nurse-like cell

NOS – not otherwise specified

NPM1 – nucleophosmin 1

NRAS – NRAS proto-oncogene, GTPase

PD1 – programmed death 1

PDL-1 – programmed cell death 1 ligand 1 (or CD274)

PDGFRA – platelet-derived growth factor receptors alpha

PDGFRB – platelet-derived growth factor receptors beta

PI3K – phosphatidylinositol-3-kinase

PI3k δ – phosphatidylinositol-3-kinase delta isoform

PLCG2 – phospholipase C, gamma 2 (phosphatidylinositol-specific)

PMF – primary myelofibrosis

PP2A – Protein phosphatase 2

PTP- ζ – receptor-type protein tyrosine phosphatase- ζ

PV – polycythemia vera

RANTES – C-C motif chemokine ligand 5 (or CCL5)

RBM6 – RNA binding motif protein 6

RNR – ribonucleotide reductase

RPS15 – ribosomal protein S15

RUNX1 – runt related transcription factor 1

SCF – stem cell factor

SERM – selective estrogen receptor modulator

SLL – small lymphocytic leukemia

SM-FeSV – Susan McDonough strain of feline sarcoma virus

SPI1 – Spi-1 proto-oncogene (or PU.1)

STAT5 – signal transducer and activator of transcription 5

TAM – tumor-associated macrophage

TCGA – The Cancer Genome Atlas

TLR – toll-like receptor

TNF – tumor necrosis factor

TNF α – tumor necrosis factor alpha

TNFSF13 – TNF superfamily member 13 (or APRIL)

TNFSF13B – TNF superfamily member 13b (or BAFF)

TP53 – tumor protein p53

TET2 – tet methylcytosine dioxygenase 2

v-fms – viral feline McDonough sarcoma

WASP – Wiskott-Aldrich syndrome protein

WAVE – WASP-family verprolin homologous 2

WHO – World Health Organization

4 Acknowledgements

“A doctorate in science and a theologian's dream.” – R.E.M., “Beat A Drum”

A couple years ago, I wrote about my experience in graduate school for the OHSU StudentSpeak blog. “Science”, I wrote, “the exhausting, elbow-greasy practice of it, is also a blackened altar onto which we sacrifice so much of our lives and our freedom. Science is a jealous god, one who hears the cries of its greatest worshippers and sometimes, more often than we’d like to admit, capriciously holds back its favor and love. We become a wandering people looking to the sky for manna and seeing only thunderclouds forming on the horizon.”

Yeah, not a flattering portrayal. And even though I’m currently writing the concluding sentences of my dissertation, and theoretically demonstrating to the world that I have overpowered that capricious and exacting deity known as Science, I still feel exactly the same.

These years, put simply, were the most harrowing and challenging of my life, both personally and professionally. I love making analogies, and I’ve compared graduate school to dozens of things over the years, but the most accurate description was one I made recently when texting my brother, also a graduate student. Graduate school, I wrote, is like painting a mural, and I’m getting increasingly frustrated by how small my brushes are and how they keep expanding the building I’m painting it on.

Despite all this unbridled negativity, I do believe that my overall experience in graduate school was worthwhile. In that same blog post, I wrote this: “The biggest thing I’ve learned from my experience here is that science is everything. Science

offers us students—most of us overeager, street-dumb twenty-somethings—an unparalleled opportunity to peek behind the curtain of existence. Science allows us to dive deeply into truth-with-a-capital-T and retrieve information to help save the lives of those around us. It’s amazing...and it’s why I entered graduate school in the first place.”

And I still feel exactly the same.

Okay, enough pontificating—I have some people to thank. Surviving and enduring graduate school would not be possible without the help of a significant army of friends, family, and colleagues.

First of all, thank you to the generous patients who literally gave a part of themselves to contribute to scientific research. Their courage and bravery in the face of seemingly unrelenting adversity are inspiring, and nothing in this dissertation would be possible without them.

To everyone in the Druker/Tyner labs, thank you for creating a relaxed, open-hearted environment where there was no animosity or competition between fellow members. I remember a couple years ago when we graduate students were explaining the lab working environment to a postdoctoral candidate interviewing for a position. She was wide-eyed, shaking her head in disbelief. No, we repeated—it’s true. Thank you all for making that truth a reality.

I want to thank the people I have personally mentored in graduate school: to Claire Rosenfeld, the most talented high school research intern I have ever seen; to Riley Roth-Carter, whose determination was often refreshing in the face of repetitive experiments and often confusing results; and, of course, to Angela Rofelty. Angie

spent two years working alongside me, enduring my constant badgering and my grandiose experiments where I used enough controls even to satisfy the most curmudgeonly reviewer. Angie is not only brilliant and hardworking but she's hilarious and patient and kind.

A special thanks to the graduate students who worked alongside me in the Druker/Tyner labs: to Chelsea Jenkins, whose take-no-prisoners attitude toward science has made her successful, and her leave-no-joke-unturned attitude toward me helped me to sharpen my comebacks; to Marilyn Chow, the undisputed Queen of Western Blots, whose persistence is only matched by her generosity and without whom I would've been professionally unmoored; and to Kevin Watanabe-Smith, the good-hearted, more-machine-than-man whiz kid whose partnership with me on my projects was undoubtedly the most rewarding scientific experience of my life.

Still so many people to thank!

Thank you to my dissertation advisory committee—Sara Courtneidge (my committee chair), Shannon McWeeney (my co-mentor), Evan Lind, Paul Spellman, and Andy Weinberg—for their constructive if sobering comments on my research and my professional ambitions. Thank you to the administrators and support staff in the Graduate Program in Molecular & Cellular Biosciences (PMCB), the Department of Cell, Developmental & Cancer Biology (CDCB), and the Cancer Biology Graduate Program, especially Lola Bichler, for enabling me to concentrate on research while everything else was magically—and promptly—handled.

Thank you to Jeffrey Tyner, my mentor and advisor, for overseeing my transformation from science enthusiast and occasional practitioner to fully-fledged

researcher. Jeff is patient, understanding, and incredibly hard-working—and he’s also the greatest scientific salesman I have ever seen. Not only did he teach me how to design good research projects and how constantly to think four or five experiments ahead, he taught me how to present data in a truthful and compelling way. The occasionally disappointing data I showed him during our weekly meetings became intriguing platforms for future experiments. And toward the end of graduate school, when I was starting up collaborations with a half-dozen people and conducting a handful of expensive experiments, he never said no. He gave me complete freedom to maximize my scientific creativity, something I’ll always cherish and appreciate.

And finally, thank you to my friends and family. Thank you to all my classmates and lab mates and non-science friends for the countless late-night meetings and hangouts and events that helped maintain my sanity (though not my original hair color) during these many, many years. Thank you to my parents, David and Adele; to my grandmother, Carol; and my siblings, Steven, Deirdre, and Christianna. (Special thanks to my dad for editing large chunks of this dissertation and making it significantly more readable.) Your love and support for me despite my rambling and incoherent complaints, despite my challenging circumstances, and despite my histrionic tantrums, have made me a better, stronger person. I couldn’t be more grateful.

And, of course, thank you to HsinPei Hsu, my wonderful partner, whose buoyancy and enthusiasm for life always inspire me, and whose abiding commitment and love always bring me home.

5 Abstract

Leukemias comprise a family of hematologic malignancies characterized by the over-proliferation of myeloid precursor cells. Leukemia development depends on multiple factors, including supportive growth signals from non-leukemia cells in the surrounding tumor microenvironment. Identifying these critical supportive cells, and eliminating their support, remains challenging.

This dissertation contains novel research that identifies supportive monocyte/macrophage cells expressing colony stimulating factor 1 receptor (CSF1R) in human chronic lymphocytic leukemia (CLL) and acute myeloid leukemia (AML). These discoveries were made from *ex vivo* screening of CSF1R-specific small-molecule inhibitors in hundreds of primary patient specimens. For both leukemia subtypes, roughly one-quarter of samples are sensitive to CSF1R inhibition or knockdown, and CSF1R inhibitor sensitivity does not strongly correlate with common genetic/clinical characteristics of disease.

In CLL, CSF1R is expressed on nurse-like cells, a population of supportive monocytes, and CSF1R inhibitor treatment eliminated their growth. Combining CSF1R inhibitors with idelalisib or ibrutinib, two small-molecule inhibitors currently used in CLL treatment, was synergistic, suggesting that combination therapy could prove effective in clinical practice. In AML, CSF1R is expressed on a previously undiscovered subpopulation of reprogrammed, supportive monocytes/macrophages whose presence correlates with CSF1R inhibitor sensitivity. This sensitivity correlated with leukemia cell growth after exogenous exposure to HGF and other

cytokines, and direct modulation of CSF1R activity showed concomitant regulation of HGF and other cytokine levels in patient sample conditioned media.

These results identify CSF1R inhibition as a novel therapeutic strategy for CLL and AML, spurring the efforts of forthcoming early-stage clinical trials evaluating its effectiveness in patients.

6 Introduction

This introduction contains a broad overview of the literature relevant to this dissertation, including: (1) a description of hematologic malignancies, with particular focus on acute myeloid leukemia (AML) and chronic lymphocytic leukemia (CLL); (2) the discovery and function of colony stimulating factor 1 receptor (CSF1R); and (3) the contribution of CSF1R in cancer and the ongoing efforts to neutralize CSF1R in clinical trials. Because I undertook two separate projects to investigate CSF1R in leukemia, one in AML and the other in CLL, I have included leukemia subtype-specific introductions available in their corresponding sections in this dissertation (see section 7.3 Introduction for CSF1R in CLL and section 8.4 Introduction for CSF1R in AML).

6.1 Hematologic malignancies

Cancer is the second most common cause of death in the United States, surpassed only by heart disease,¹ and can be found in various tissues throughout the body. The family of cancers that appear in the body's blood-forming tissues are called hematologic malignancies, known colloquially as blood cancers. These blood cancers can appear in the bone marrow and lymphatic vessels and are predominantly found in circulatory and lymphatic systems. Like many other cancer families, blood cancers originate from a rapidly dividing population of progenitor cells that overcome conventional pro-apoptotic signals. The unchecked proliferation of the hematologic malignancy overwhelms the residual population of normal blood cells,

leading to symptoms that include weakness, bone/joint pain, recurrent infections, enhanced bleeding/bruising, and enlarged lymph nodes.

The classification of blood cancer subtypes arose from the conventional understanding of hematopoiesis, or the formation of normal blood cells and tissues. Hematopoiesis begins with the regulated differentiation of hematopoietic stem cells, a group of self-propagating cells that reside in the bone marrow, into two types of progenitor cells: lymphoid (consisting of B cells, T cells, and natural killer (NK) cells, which are critical for adaptive immune system function) and myeloid (consisting of granulocytes, monocytes, erythrocytes, and platelets, which contribute to innate immune system function). The most recognizable “gold standard” classification scheme for hematologic malignancies,² managed by the World Health Organization (WHO), categorizes blood cancers within these two broad categories: lymphocytic leukemias or lymphomas, and myeloid leukemias, respectively.² Titled *The WHO Classification of Hematological Malignancies*, the guidelines were developed by a consortium of researchers and clinicians based on the subtype and morphology of the originating progenitor cell, the presence of specific genetic abnormalities within the tumor cells, and/or the presence of specific cell-surface markers.²

Within the WHO classification scheme,³ the lymphoid tumors can be subcategorized into four groups: small B-cell lymphoid neoplasms, diffuse large B-cell lymphoma, high grade B-cell lymphomas, and mature T-and NK-cell neoplasms.^{2,a} Although small B-cell lymphoid neoplasms are commonly referred to

^a Traditionally, these diseases have been subdivided into Hodgkin lymphoma (HL) and non-Hodgkin lymphoma (nHL), based on the presence of large, multinucleated Reed-Sternberg cells, with nHL

as “low-grade lymphomas” by clinicians, the WHO classification intentionally omits tumor grade for lymphoma classification, hence the preferred term is “small B-cell lymphomas”.⁴ The two most common small B-cell lymphomas are “chronic lymphocytic leukemia/small lymphocytic lymphoma (CLL/SLL)” and “follicular lymphoma”.⁵ The second category, “diffuse large B-cell lymphoma (DLBCL)”, contains the largest number of lymphoma patients.⁵ Although DLBCL can be further subdivided based on cell origin and some clinical characteristics, most of the patients remain uncategorized or “not otherwise specified (NOS)”.³ The other two categories, “high grade B-cell lymphomas” and “mature T-and NK-cell neoplasms”, represent rarer disease subtypes with less well-defined pathological characteristics and few defining genetic alterations.⁴

The WHO classification of myeloid tumors can be broadly subcategorized into acute myeloid leukemia (AML), myelodysplastic syndrome (MDS), myeloproliferative neoplasms (MPN), myelodysplastic/myeloproliferative neoplasms (MDS/MPN), B-lymphoblastic leukemia/lymphoma, and T-lymphoblastic leukemia/lymphoma.² AML is the deadliest hematological malignancy and contains many definitional genetic and cytogenetic abnormalities to distinguish among subtypes.⁶ MDS is characterized as “ineffective hematopoiesis” and defined as presenting with at least 10% dysplasia either in erythrocytes, granulocytes, or megakaryocytes.⁶ MPN contains the uniquely treatable chronic myeloid leukemia (CML), defined and identified by the BCR-ABL1 translocation, as

being the most predominant form. Although there is an explicit “Hodgkin lymphoma” category in the WHO classification, a greater emphasis is placed on progenitor cell type, which I have replicated here.

well as polycythemia vera (PV), primary myelofibrosis (PMF), and essential thrombocythemia (ET). MDS/MPN contains chronic myelomonocytic leukemia (CMML) and additional rare subtypes,⁷ including atypical CML which lacks BCR-ABL1.² The remaining two categories are often grouped together as “acute lymphoblastic leukemia (ALL)” and are subdivided and differentiated based on whether the leukemia originated from B or T cells.⁶

In general, hematologic malignancies share many characteristics that differentiate them from conventional solid tumors like breast and prostate cancers. This distinction presents unique challenges and opportunities to hematology/oncology researchers and clinicians. First, accessing tumor samples from patients is generally easier for liquid tumors, not only because blood cancers rapidly circulate throughout the body but also because blood draws are a routine part of the clinical management of their disease. Second, critical components of tumor evolution such as metastasis and epithelial-to-mesenchymal transition (EMT) are not broadly applicable to blood tumors,^b reducing the imperative to identify their geographical distribution throughout the body. Third, on the whole, hematological malignancies contain many fewer mutations than most solid tumors. In one study reviewing sequencing data from 12 cancer subtypes collected by The Cancer Genome Atlas (TCGA), AML was shown to have the lowest median mutation frequency at 0.28 mutations per megabase (Mb), with all other tumor types having

^b There are rare instances of leukemia that migrates outside of blood vessels into surrounding tissue,⁷ called extramedullary leukemia (EML) or myeloid sarcoma, which does share characteristics with solid tumors.⁸ However, EML is probably not detectable in the majority of leukemia patients and remains poorly understood.

greater than 1 mutation per Mb.⁹ Notably, this analysis excludes pediatric tumors, although leukemia is one of the most prominent childhood cancers— ALL being the most common malignancy in children¹⁰—and the mutation burden of ALL is roughly equivalent to that of AML, a disease found preferentially in older adults.¹¹ Fourth, the molecular profile of hematological malignancies is markedly different from that of solid tumors, with a uniquely high frequency of tumor-type-specific mutations in genes such as fms related tyrosine kinase 3 (FLT3), nucleophosmin 1 (NPM1), DNA methyltransferase 3 alpha (DNMT3A), and tet methylcytosine dioxygenase 2 (TET2).⁹

Having said that, there are important characteristics shared by hematologic malignancies and other cancer subtypes. First, because they are both cancer subtypes, they possess many of the essential “hallmarks of cancer,” including stimulating proliferative signaling, avoiding cell death, and not activating growth suppression pathways.¹² Second, on average, blood cancers possess the same extensive heterogeneity and complex clonal architecture of solid tumors that makes it difficult to achieve lasting clinical benefits in patients with certain hematologic malignancies, including developing resistance to therapy.¹³ Third, both blood cancers and solid tumors have been shown to reprogram surrounding normal tissue, including stromal cells and components of the immune system, to produce a tumor-promotional environment, called the tumor microenvironment, that enhances cancer growth and survival.¹⁴

This dissertation focuses on the contribution of one element of the tumor microenvironment in the two most common leukemias: acute myeloid leukemia (AML) and chronic lymphocytic leukemia (CLL).

6.1.1 *Acute myeloid leukemia*

Acute myeloid leukemia (AML) is the second most common hematological malignancy by incidence and also the deadliest, with an estimated 19,520 new cases and 10,670 deaths occurring in the United States in 2018.¹ AML is a disease commonly found in elderly people (the median age of diagnosis is 68).¹ The incidence of AML is increasing, in large part because the general population is living longer. Another contributor is the increased incidence of “therapy-related AML” caused by cancer treatment, a consequence of DNA-damaging chemotherapy and/or ionizing radiation for patients with prior cancers.¹⁵ As previously mentioned, AML is characterized by the blocked differentiation and increased proliferation of myeloid precursor cells, commonly referred to as “blasts”, inhibiting the growth of normal granulocytes, monocytes, and erythrocytes.

The diagnostic criteria for AML have changed throughout the years, adjusting with advancements in technology and a better understanding of disease biology. The first universal method of categorizing acute leukemias was developed by a cooperative group of seven French, American, and British hematologists in 1976.¹⁶ Called the French-American-British (FAB) classification system, it was created to establish uniform guidelines for separating myeloid and lymphoblastic

leukemias and develop consistent nomenclature of disease subtypes.^{16,c} Their guidelines were based on cell morphology and cytogenetic staining, focusing on cytological features, including cell size, nuclear chromatin, nuclear shape, nucleoli, amount of cytoplasm, basophilia of cytoplasm, and cytoplasmic vacuolation.¹⁶

AML was distinguished from lymphoblastic leukemia based on these characteristics and further subdivided based on the “direction of differentiation” among one or more myeloid cell types and the degree of cell maturation. This subdivision created six categories called M1-M6, with “M” standing for “myeloid”:

- M1: acute myeloblastic leukemia, without maturation
- M2: acute myeloblastic leukemia, with granulocytic maturation
- M3: acute promyelocytic leukemia (APL)
- M4: acute myelomonocytic leukemia; there is an additional M4eo category, which is M4 with bone marrow eosinophilia (increase in eosinophil count)
- M5: subdivided into acute monoblastic leukemia (M5a) and acute monocytic leukemia (M5b)
- M6: acute erythroid leukemias

In later revisions of the FAB classification system, two additional categories were added: M0: acute myeloblastic leukemia, minimally differentiated¹⁷ and M7: acute megakaryoblastic leukemia.¹⁸ Furthermore, to distinguish AML from high-grade

^c Interestingly, the participants of the meeting circulated 150 stained peripheral blood and bone marrow slides from acute leukemias and similar-looking diseases. The hematologists diagnosed each slide separately, met and discussed their differences, and created standards that were applied to a new set of slides deliberately intended to be confusing. They independently achieved an 85% consensus.¹⁶

MDS, the FAB classification system mandated that a diagnosis of AML required the blast percentage to be greater than 30.¹⁶ Overall, the FAB classification strategy was effective in helping researchers determine the relative frequency of AML subtypes and establish consistent examination protocols. However, over time, it suffered from limitations, including low reproducibility and an inability to identify which patients would respond poorly to chemotherapy.¹⁹

Later, with a better understanding of the gene mutations and translocations underlying AML pathogenesis and development, the classification of AML subtypes shifted. The appearance of leukemia cells under the microscope gave way to the presence of genetic abnormalities contained within those cells. Currently, the classification system that best embodies this approach was proposed by the World Health Organization (WHO), first published in 2001.² The WHO classification of myeloid neoplasms, which underwent a revision in 2016,⁶ incorporates many well-known gene mutations and translocations along with the morphologic and cytogenetic characteristics. The number of AML subtypes more than doubled under the WHO classification compared to the FAB classification system; additionally, the diagnostic blast percentage threshold was lowered from 30% to 20%, based on epidemiological data.^{15,d} Overall, this integrative approach to classification has not only improved the reliability and reproducibility of AML diagnoses, but has enhanced our understanding of AML pathobiology.⁶

^d There are two subtypes, “AML with t(8;21)(q22;q22.1); *RUNX1-RUNX1T1*” and “AML with inv(16)(p13.1q22) or t(16;16)(p13.1;q22); CBFβ-MYH11,” that can be classified as AML regardless of blast percentage.

Similarly, determining prognostic risk in AML—the prediction of the risk of relapse when a patient is treated with chemotherapy alone—has incorporated more mutational data along with clinical characteristics. Although there are many different methods employed to calculate prognostic risk, one of the most widely used methods was developed by the European LeukemiaNet (ELN).²⁰ These guidelines were established to identify which genetic abnormalities held the most significance in predicting AML patient outcomes and how best to inform physician decisions during treatment.

The ELN examined survival data from thousands of AML patients and identified four critical characteristics that would minimally subdivide patients by treatment outcome: (1) the presence of specific karyotypic abnormalities; and (2) internal tandem duplications in FLT3, (3) NPM1 mutations, and (4) CEBPA mutations. The guidelines, first published in 2008, were independently validated using a separate European patient cohort.²¹ In 2017, the ELN guidelines for AML prognostic risk were updated, recommending that physicians consider three new karyotypic abnormalities: monosomy 17, monosomal karyotype, and t(9;22); BCR-ABL1.²² They also included mutations in TP53, RUNX1, and ASXL1; biallelic instead of monoallelic CEBPA mutations; and the consideration of FLT3-ITD allele ratio.²²

When a patient is diagnosed with AML, that individual receives a combination of routine cytochemical staining to identify morphology and ascertain the extent of differentiation, as well as full karyotyping and fluorescent in situ

hybridization (FISH) to identify common translocations.¹⁵ The most common prognostically significant translocations include:

- t(8;21)(q22;q22.1); RUNX1-RUNX1T1 (favorable risk)
- inv(16)(p13.1q22) or t(16;16)(p13.1;q22); CBFβ-MYH11 (favorable)
- t(9;11)(p21.3;q23.3); MLLT3-KMT2A (intermediate)
- t(6;9)(p23;q34.1); DEK-NUP214 (adverse)
- t(v;11q23.3); KMT2A rearranged (adverse)
- inv(3)(q21.3q26.2) or t(3;3)(q21.3;q26.2); GATA2,MECOM(EVI1) (adverse)
- t(9;22)(q34.1;q11.2); BCR-ABL1 (adverse)

There are additional cytogenetic abnormalities, including -5 or del(5q), -7, and abnormal 17, whose presence can classify a patient with “AML with myelodysplastic changes”, which constitutes poor prognosis.²⁰

In addition to cytogenetic abnormalities, there are gene mutations that have been identified as prognostically significant over the years. Screening AML patients for these mutations is important because 40-50% of patients have cytogenetically normal AML (CN-AML), meaning that their disease does not present with any detectable cytogenetic abnormalities.²³ As mentioned above, according to the ELN guidelines, the six genes with prognostically significant mutations are FLT3-ITD, NPM1, CEBPA, TP53, RUNX1, and ASXL1.²⁰ There are many additional driver mutations that have been discovered in AML, especially in recent landmark surveys of hundreds of patients using next-generation sequencing.^{24,25} Although the prognostic significance of many of these mutations is unknown, partly because they

are not commonly found in the broader AML population, the increased ubiquity of gene mutation panel screening will help determine whether their presence can predict treatment response.

6.1.2 *Chronic lymphocytic leukemia*

Chronic lymphocytic leukemia is the most common leukemia in the Western world, with an estimated 20,940 new cases in the United States in 2018.¹ However, it has a significantly reduced mortality rate compared to AML, with 4,510 estimated deaths in the United States in 2018.¹ CLL is predominantly found in elderly people, with the median age at diagnosis between 67 and 72 years old, and affects men more than women (1.7:1).²⁶ It is a slow-growing and indolent disease, often lying dormant in the bone marrow for years before undergoing a sudden aggressive transformation (in a process called “blast crisis”). The most common risk factor for CLL is having a family history of the disease—around 10% of CLL cases constitute so-called “familial CLL,” in which the disease is found in two or more individuals in the same family—although minor additional factors, such as ethnicity (there is a lower incidence among East Asians), have been identified.²⁶

The pathogenesis of CLL involves the clonal expansion and proliferation of B cells within the blood and bone marrow, hence the “leukemia” designation. If CLL is found predominantly in the lymph nodes and spleen, it is called small lymphocytic lymphoma (SLL), although both diseases are functionally identical. Some research suggest that the CLL development originates not from B-cell progenitors but from a multipotent hematopoietic stem cell (HSC), although this process remains poorly

understood.²⁷ Recent studies examining the mutational landscape of CLL postulated that the disease might be initiated by a large chromosomal abnormality followed by additional gene mutations that produce a more aggressive disease.^{28,c}

Unlike AML, CLL represents a single disease, according to the WHO classification,² and therefore does not have subtypes defined by common recurrent cytogenetic abnormalities and gene mutations. Additionally, the most common cytogenetic abnormalities in CLL are not translocations but large chromosomal deletions. They include:

- del(13q14), found in ~55% of patients;²⁶ no prognostic significance
- del(11q), found in 25% of advanced-stage patients;²⁶ poor prognosis
- trisomy 12, found in 10-20% of patients;²⁶ unknown prognostic significance²⁹
- del(17p), found in 5-8% of untreated patients;²⁶ poor prognosis

There have been many efforts throughout the years to identify recurrent gene mutations in CLL.^{28,30-32} One recent study identified 44 recurrently mutated genes and 11 recurrent somatic copy number variations.²⁸ Notably, the significance of 26 of those mutated genes had not been previously determined in CLL, and a few of them— RPS15 and IKZF3, for example—had never been previously identified in human cancers.²⁸ These recent discoveries highlight the relative infancy of using genetic mutations to determine prognostic significance in CLL, especially compared to AML.

^c The overall mutation frequency in CLL is relatively low and comparable to that of AML.

There are two commonly used classification systems for CLL clinical staging: the Rai system, published in 1975,³³ and the Binet system, published in 1981.³⁴ Both classification systems were named after the first authors on the original publications, Kanti R. Rai and Jacques-Louis Binet. The Rai system was modified in 1987,³⁵ decreasing the original number of prognostic categories. Both systems subdivide patients into three categories based on clinical characteristics. The modified Rai staging system classifies patients as follows:

- Low-risk disease: lymphocytosis with leukemia cells in the blood and/or marrow (lymphoid cells greater than 30%)
- Intermediate-risk disease: lymphocytosis, enlarged nodes in any site, and splenomegaly and/or hepatomegaly
- High-risk disease: disease-related anemia (hemoglobin less than 11g/dl) or thrombocytopenia (platelet count less than $100 \times 10^9/L$)

The Binet system classifies patients slightly differently, using a combination of the number of “involved areas” (defined as enlarged lymph nodes greater than 1cm in diameter, or organomegaly) and whether the patient has anemia or thrombocytopenia (using very similar numbers as the Rai system).²⁶

Recently, due to a combination of incredibly effective treatments that have been developed for CLL and a greater understanding of which CLL genetic abnormalities are prognostically significant, these staging systems have become insufficient.³⁶ In response, an international working group of researchers developed the CLL International Prognostic Index (CLL-IPI), based on a multivariate analysis of 27 baseline factors in 3,472 patients from Europe and the United States.³⁷ The

CLL-IPI guidelines is built around five characteristics: the presence of mutations/deletions in TP53 (termed “TP53 dysfunction”), the presence of mutations in the immunoglobulin heavy-chain variable region (IGHV), the serum levels of beta-2 microglobulin (B2M), the clinical stage (based on Rai and/or Binet classification), and patient age.³⁷ Each characteristic is assigned a point score:

- del(17p) or TP53 mutation: 4 points
- IGHV mutation: 2 points
- B2M greater than 3.5 mg/L: 2 points
- Clinical stage (intermediate- or high-risk Rai or Binet score): 1 point
- Age greater than 65 years: 1 point

The point values of each characteristic are summed and patients are subdivided into four categories: low risk (0-1), intermediate risk (2-3), high risk (4-6), and very high risk (7-10).³⁷ Although these guidelines have been independently validated,³⁸ demonstrating that they not only predict overall survival but also inform the time to first treatment, additional data will be required to demonstrate their significance in the clinic.

6.2 Treatment of AML and CLL

Due to substantial differences in their clinical presentation—namely, the acute versus chronic nature of their development in patients—AML and CLL have very different treatment strategies. AML is a highly aggressive leukemia, and AML patients are given chemotherapy as quickly as possible, often within days of the initial diagnosis. On the other hand, CLL a slow-growing, indolent leukemia, and

the recommended strategy is “watch and wait”—patients only receive treatment upon disease progression.

The treatment of AML is divided into two categories: induction chemotherapy and consolidation (or post-remission) therapy. The induction phase of treatment is challenging because the clinician is working to deliver enough chemotherapy to achieve complete remission while ensuring that the patient can tolerate the consolidation phase, without which the patient is likely to relapse within 6-9 months.¹⁵ In this way, the induction strategy depends on a variety of characteristics, including patient age, the presence of comorbid conditions that could affect performance status and decrease tolerance to treatment,³⁹ and preexisting myelodysplasia.^{15,f} AML patients are usually separated based on age; they are also considered separately, with patients older than 60 receiving different recommendations offered to patients younger than 60.

Younger AML patients receive the standard induction therapy combining cytarabine (also called Ara-C), a modified cytosine analog, for seven days, and an anthracycline (either daunorubicin, the most common, or idarubicin), a DNA intercalating agent and topoisomerase-II inhibitor, for three days. Nicknamed “7+3”, this treatment strategy has remained the standard induction treatment for over 40 years, underscoring the historical challenge of treating AML.⁴¹ After 7-10 days, a bone marrow aspirate is collected, and additional doses of cytarabine are given,

^f The treatment of acute promyelocytic leukemia (APL), defined by the translocation of the promyelocytic leukemia (PML) gene to retinoic acid receptor alpha (RARA), is dramatically different from standard AML because of the unique ability all-trans retinoic acid (ATRA) possesses to induce differentiation in the blasts of this subtype. Consequently, it should be classified differently from other leukemia subtypes, as has been recommended by independent ELN guidelines.⁴⁰

depending on the presence or extent of residual disease. If a complete remission (no measurable disease) is achieved, then patients receive consolidation therapy consisting of multiple cycles of high-dose Ara-C.¹⁵ This is sometimes accompanied by a hematopoietic stem cell transplant (HSCT), either from the patient's own cells (autologous) or from a donor with acceptable human leukocyte antigen (HLA) matching (allogeneic).¹⁵

Older AML patients either receive standard induction therapy or low-dose Ara-C or hydroxyurea, depending on their performance status, the presence of poor-risk genetic abnormalities, and presence of co-morbidities.¹⁵ They could also receive the same consolidation therapy, depending on their response, although there are many variations in alternative consolidation strategies, including different dosing combinations of Ara-C, anthracycline, and hydroxyurea, an inhibitor of ribonucleotide reductase (RNR).¹⁵ HSCTs are less common in this population due to adverse side effects.¹⁵

The treatment of CLL, as previously mentioned, is dramatically different. Over 90% of CLL patients are initially diagnosed with asymptomatic, early-stage disease, the majority of which contain an indolent disease and often reach normal life expectancy.⁴² Therefore, the standard-of-care treatment is “watch and wait,” where a patient's condition is closely monitored using blood tests and physical exams, and treatment is only considered if symptoms appear or if the patient's condition changes.⁴² Although the monitoring schedule might be adjusted based on the disease staging, the application of newly appreciated prognostic risk markers

(according to the CLL-IWI guidelines) and novel targeted therapies on improving survival in these patients remains poorly understood.⁴²

If patients diagnosed with CLL develop “active disease”, the recommended treatment for patients with a high performance status is FCR, which is the combination of fludarabine, a purine analog, cyclophosphamide, an alkylating agent, and rituximab, a monoclonal antibody targeting CD20.⁴³ For patients that cannot tolerate this aggressive treatment, or for those with very high risk disease classified as previously defined, receiving an alternative CD20-targeting antibody (ofatumumab or obinutuzumab), with its demonstrated higher efficacy and lower toxicity, administered in combination with other chemotherapies is recommended.⁴²

These treatment approaches have demonstrated efficacy in patients with AML and CLL, and have therefore become standard-of-care. However, newer strategies have emerged, specifically new targeted therapies, that have shown promise in recent clinical trials, with some becoming FDA-approved for treatment of these diseases.

6.2.1 *Targeted therapy*

The notion of targeted therapy, or the idea of eliminating only diseased cells within a patient while leaving the surrounding healthy cells unharmed, is commonplace in cancer treatment. It is generally viewed as a natural progression from traditional chemotherapy, which affects all rapidly dividing cells, causing such symptoms in patients as increased susceptibility to infections (reduced leukocytes), gastrointestinal problems (reduced intestinal epithelial cells), and alopecia (reduced

hair follicles). However, its broad adoption required a paradigm shift among clinicians and researchers, which happened gradually following a few key discoveries.

Technically, the first example of targeted therapy was employed in the 1940s with iodine treatment for thyroid cancer. Thyroid cancer cells exclusively uptake ¹³¹I and the tumor is eliminated by the accumulated radioactivity.⁴⁴ Later, in the 1950s, 5-fluorouracil was developed for the treatment of hepatoma, and is currently a mainstay in colorectal cancer treatment, because researchers discovered that the hepatoma demonstrated greater uptake and requirement for uracil relative to normal tissue.⁴⁵ In the 1970s, the creation of tamoxifen fulfilled the more conventional understanding of targeted therapy, in which the therapeutic competitively binds and alters the downstream function of protein uniquely required for cancer survival.⁴⁶ As a selective estrogen receptor modulator (SERM), tamoxifen is used for the treatment of estrogen receptor-positive breast cancer, which requires estrogen to proliferate and survive.⁴⁷

Perhaps the best-known, most quintessential example of targeted therapy is the development of imatinib (commonly known as Gleevec) for the treatment of patients with CML. Unlike most other cancer subtypes, CML is unique because the BCR-ABL1 translocation defines the disease, so developing a kinase inhibitor that fits in the ATP pocket of the resulting fusion protein and inhibiting its downstream function serves as an excellent proof-of-principle for targeted therapies.⁴⁸ Ultimately, imatinib produced remarkable survival benefits in patients with CML.^{49,50}

It is important to mention that targeted therapies include both small-molecule inhibitors and monoclonal antibodies, and their similarities and differences should be discussed. Both small-molecule inhibitors and neutralizing antibodies target growth-factor receptors to prevent downstream signaling and have been developed for (and their effectiveness evaluated in) large-scale clinical trials.⁵¹ There are notable differences between them, however. First, small-molecule inhibitors are significantly smaller than monoclonal antibodies, which helps explain why small-molecules are well distributed across tissues and antibodies are more restricted to plasma and extracellular fluids.⁵² In addition, the circulation half-life for monoclonal antibodies is significantly longer (days vs. hours),⁵² and researchers have speculated that there might be less variance in the degradation time (and therefore less variance in the plasma concentration) of monoclonal antibodies across patients than small-molecule inhibitors.⁵¹

Although the development of imatinib for CML appeared to herald the application of targeted therapies in other hematologic malignancies, there has been little success of targeted therapies to treat patients with AML.⁴¹ There are many possible explanations. First, as previously mentioned, AML is an extremely heterogeneous disease, so targeting a single protein for inhibition would likely be insufficient to eliminate the rest of the leukemia cell population.⁵³ Second, xenotransplantation assays, in which patient cells are injected into recipient mice, can stimulate the growth of functionally different subclones, changing the clonal proportions from the original patient sample and generating erroneous results.⁵⁴ Third, many of the experimental approaches have been problematic, with insufficient

sample size in clinical trials and few human models of certain molecular subsets of AML subsets.⁵³ Fourth, many of these targeted therapies are being investigated with a single-agent approach instead of in combination with existing chemotherapies, greatly limiting their clinical utility and applicability.⁴¹

However, there have been an increasing number of successes for targeted therapies in recent years. Inhibitors against FLT3 mutations or internal tandem duplications (FLT3-ITD), including crenolanib, quizartinib, and sorafenib, have been showing promise. Indeed, multi-kinase inhibitor midostaurin was recently shown to be effective in combination with 7+3 in patients with newly diagnosed FLT3-mutated AML,⁵⁵ leading to its FDA approval in 2017. In addition, the IDH2-specific inhibitor enasidenib was recently shown to be effective against IDH2-mutant relapsed or refractory AML,⁵⁶ and the inhibitor was granted FDA Breakthrough Therapy designation in 2017. There are other targeted therapies under investigation at various stages in clinical development, including gilteritinib (a dual FLT3 and AXL inhibitor), venetoclax (a BCL2 inhibitor), gemtuzumab ozogamicin (an antibody-drug conjugate against CD33), and many others.⁵⁷

In CLL, although most patients are not recommended to receive immediate treatment for their disease, there have recently been substantial recent, exciting developments in targeted therapy. Besides the anti-CD20 antibodies mentioned previously that have become standard-of-care for acute-phase CLL, there is another targeted monoclonal antibody against CD52, alemtuzumab, that was approved for frontline CLL treatment.⁵⁸ However, the drug license was withdrawn in 2012 and remains available only for compassionate use cases.²⁶

There are three prominent small-molecule inhibitors in clinical development for CLL. Two of them target B-cell receptor signaling, which is critically important in CLL cell survival,⁵⁹ and inhibiting their activity has become an active area of clinical investigation.²⁶ The first, idelalisib, is an inhibitor of p110 delta isoform of phosphatidylinositol 3-kinase (PI3K δ), which is required for B cell proliferation and survival and whose activity is required in CLL cells.⁶⁰ Idelalisib induces apoptosis in primary CLL cells without impacting normal T cells or natural killer cells.²⁶ Idelalisib has been tested in combination with ofatumumab, which doubled progression-free survival compared to ofatumumab alone.⁶¹

The second, ibrutinib, is an inhibitor of Bruton tyrosine kinase (BTK), activating downstream NF κ B1 and MAPK pathways, both of which are involved in the signal transduction of the B-cell receptor.⁶² Ibrutinib has been tested extensively and demonstrated efficacy as a single-agent in patients, most recently in a phase 3 clinical trial against ofatumumab in patients with relapsed or refractory CLL.⁶³ It is now considered as a possible frontline treatment for acute, symptomatic CLL.²⁶ In addition, ibrutinib has shown remarkable benefit in combination with other drugs, including: rituximab;^{64,65} bendamustine, an alkylating agent, with rituximab (BR);⁶⁶ and ofatumumab.⁶⁷

6.2.2 *Targeting the tumor microenvironment*

As the number of successful targeted therapies for cancer treatment increased over the past couple decades, a greater understanding of the corruption of normal, healthy cells surrounding the tumor by cancer cells to promote tumor proliferation

and survival has emerged. These surrounding cells and their corresponding supportive cytokines and growth factors were termed the tumor microenvironment, and their interaction with tumor cells has since become a significant focus of tumor biology research.

The first observation that these microenvironmental signals can become hijacked by cancer was made in 1863 by Rudolf Virchow, who discovered that solid tumors also presented with infiltrating leukocytes.⁶⁸ The immune system plays a critical and complicated role in tumor proliferation and evolution. It was discovered that tissues subjected to chronic inflammation from various diseases also exhibited increased incidence of cancer—for example, liver cirrhosis in hepatocellular carcinoma, or long-term colitis and colorectal cancer.⁶⁹ At the same time, immunocompromised or immunosuppressed individuals, including transplant recipients and people with acquired immunodeficiency syndrome (AIDS), also showed higher cancer incidence.^{70,71} These juxtaposing observations highlight the dual, context-dependent roles of the tumor microenvironment in cancer.

To understand the tumor microenvironment in hematologic malignancies, it is important to understand the regulation of hematopoietic stem cells (HSCs) by neighboring cells during normal hematopoiesis. The bone marrow consists of a complex arrangement of nerve bundles, blood vessels, smooth muscle cells, and various other cell types.⁷² In normal hematopoiesis, HSCs exist in a geographically separate area of the bone that is adjacent to blood vessels, commonly referred to as the perivascular niche.⁷³ In the perivascular niche, HSCs receive supportive signals such as CXCL12 or SCF from neighboring cells.⁷⁴ Examples of neighboring cells that

could provide this regulatory signaling include nonhematopoietic cells (osteoblasts, endothelial cells, pericytes, adipocytes, Schwann cells, and nerves) and hematopoietic cells (macrophages, osteoclasts, megakaryocytes, lymphocytes, and neutrophils).⁷²

Hematologic malignancies, and cancer in general, disrupt the normal interaction between these cells and modify the surrounding tissue in such a way that the microenvironment evolves alongside the growing tumor to support and protect it.⁷⁵ Tumor cells accomplish this through a variety of strategies, including: blocking the release of cytolytic granules by neutrophils, reducing the pro-inflammatory phenotype of macrophages, inhibiting the tumor-associated antigen presentation by dendritic cells, and directly inhibiting normal B and T cell responses.⁷⁵ In this way, ordinary macrophages evolve into so-called tumor-associated macrophages (TAMs), which have been shown to promote tumor progression and enhance therapeutic resistance.⁷⁶ Similarly, ordinary myeloid precursors evolve into myeloid-derived suppressor cells (MDSCs), immunosuppressive precursor cells that disrupt multiple pathways of tumor immunosurveillance.⁷⁷ This pattern of phenotypic modification manifests in other cell types, and eliminating or reversing these modifications has been an active, albeit challenging, area of research.⁷⁵

Targeting the tumor microenvironment is an attractive plan of attack, not only because blocking this signaling can overcome the heterogeneous nature of the tumor itself,⁷⁸ but also because the microenvironment is genetically stable and less susceptible to the classic “acquisition of resistance mutation” mechanism of therapy resistance.⁷⁵ Perhaps the most broadly successful approach is blocking the

mechanism by which tumors evade the immune system. One inhibitor, ipilimumab, targets CTLA-4, which activates T cells and thereby promotes an anti-tumor immune response. Ipilimumab has been FDA-approved by demonstrating effectiveness in metastatic melanoma;^{79,80} combining it with other antibodies have also shown promise, including nivolumab,^{81,82} which targets the programmed death 1 (PD1) receptor, and lambrolizumab,⁸³ which blocks the PD1 ligand (PDL-1). Similarly, antibodies that target CD40, a TNF receptor superfamily member that, when targeted, activates antigen-presenting cells and promotes other immune responses,⁸⁴ have demonstrated some efficacy in preclinical pancreatic cancer.⁸⁵

The second approach involves neutralizing tumor-promotional inflammation caused by immune cell recruitment and activity. For example, blocking CCL2-CCR2 signaling reduces the recruitment of inflammatory monocytes and extends overall survival in breast cancer mouse models.⁸⁶ In addition, targeting other components of immune cell recruitment such as CXCR2 (using S-265610) and CXCR4 (using AMD3100) is being actively investigated.⁷⁵ Ultimately, some of the most promising treatment strategies inspired by this approach are inhibitors against a protein ubiquitously expressed on macrophages: colony stimulating factor 1 receptor (CSF1R).⁷⁵

6.3 Colony stimulating factor 1 receptor (CSF1R)

6.3.1 *Discovery of CSF1R*

The first colony-stimulating factor was discovered when researchers were looking into how hematopoietic cells differentiated into mature granulocytes,

monocytes, and macrophages. These researchers already knew that when they isolated bone marrow cells from mice and plated them in soft agar, these cells had the capacity to proliferate extensively and form small colonies. Sometimes, depending on what the cells were incubated with—blood serum, conditioned media, and even urine⁸—these colonies would consist only of granulocytes, or only of macrophages, or a combination of both.⁸⁸ Researchers defined “colony-stimulating factors” as the external additives that are absolutely required to produce these colonies.⁸⁸

In 1977, E. Richard Stanley and Patricia M. Heard, then working at the Ontario Cancer Institute, purified the first colony-stimulating factor, known as colony-stimulating factor 1 (CSF1), through repeated dialysis of conditioned media from L60T mouse fibroblasts.⁸⁸ Stanley’s group discovered that CSF, even at extremely low concentrations, stimulated the formation of macrophage colonies in multiple different cell types.⁸⁹ Using radiolabeled iodine, they confirmed that CSF was binding to a then unknown receptor found almost exclusively on macrophages and their progenitors.⁹⁰

Around the same time, Charles J. Sherr, working at the Viral Pathology Section of the National Cancer Institute, was studying SM-FeSV, a strain of feline sarcoma virus (FeSV) developed by Susan McDonough (SM) and colleagues. At the time, researchers used different strains of FeSVs to discover how they induced sarcomas in their recipient animals. Sherr and colleagues discovered that SM-FeSV

⁸ One study investigated the colony-forming potential of urine samples from patients with a variety of hematological malignancies, including acute leukemia.⁸⁷ Even after waiting 24 hours, half of the samples produced colonies, highlighting the persistence of CSF1R in the bloodstream and beyond.

contained the sequence for a unique transforming gene they called *v-fms* (viral feline McDonough sarcoma).⁹¹ They found that the eukaryotic DNA sequences that were homologous to *v-fms*, which they dubbed *c-fms* (cellular feline McDonough sarcoma), encoded a glycoprotein that showed tyrosine-specific protein kinase activity *in vitro*.⁹²

Eventually, both research groups discovered that there was significant similarity in tissue distribution and biochemical properties between the CSF1 receptor and the glycoprotein encoded by *c-fms*.⁹³ Working together, they discovered that the *c-fms* glycoprotein was expressed at high levels in macrophages, and that rabbit antibodies specific for *v-fms* recognize the murine CSF1 receptor.⁹³ In conclusion, they speculated that “[t]he murine *c-fms* proto-oncogene product and the CSF-1 receptor are therefore related, and possibly identical, molecules”.⁹³ Two years later, the cDNA nucleotide sequence for c-FMS was discovered,⁹⁴ confirming their suspicions and revealing the identity of the receptor, officially called CSF1R but still occasionally referred as c-FMS, as a classical cell-surface tyrosine kinase.

6.3.2 *Structure and function of CSF1R*

CSF1R (colony stimulating factor 1 receptor; also referred to as c-FMS, M-CSF, or CD115) is a 972-amino-acid protein with three topological domains: extracellular (amino acids 20-517), transmembrane (518-538), and cytoplasmic (539-972). The extracellular domain (498 amino acids) is highly glycosylated and contains five immunoglobulin domains, while the intracellular domain consists of a kinase insert domain (73 amino acids) sandwiched between a tyrosine kinase domain (398 amino acids).⁹⁵ CSF1R is located on human chromosome 5 (5q32) and contains 21

introns and 22 exons. It is a member of the class III receptor tyrosine kinase family, which includes PDGFRA and PDGFRB, KIT, and FLT3.

There are two ligands that bind to CSF1R: CSF1 and IL-34 (interleukin 34). IL-34 was later discovered through a large-scale functional screen of the extracellular proteome and was identified as an additional ligand for CSF1R.⁹⁶ Even though both ligands produce a different biological response in CSF1R,⁹⁷ their primary differences are based on how the ligands themselves are regulated and expressed throughout the body. There are three isoforms of CSF1: a secreted glycoprotein, a secreted proteoglycan, and a transmembrane glycoprotein expressed on the surface of cells.⁹⁵ The transmembrane and proteoglycan isoforms of CSF1 have been demonstrated to act locally, although the secreted glycoprotein can circulate through the bloodstream, resulting in humoral regulation.⁹⁸ Additionally, CSF1R appears to be the only receptor for CSF1, based on the observation that the phenotype of CSF1R-deficient mice⁹⁹—including osteopetrosis, or increased bone hardening, and hematologic abnormalities in the peripheral blood, bone marrow and spleen—matches the phenotype of CSF1-deficient mice.⁹⁸ On the other hand, IL-34 is not detectable in normal blood circulation,^{100,101} and has been shown to bind to an additional receptor, PTP- ζ .¹⁰²

CSF1R expression is low on hematopoietic stem cells (HSCs) but increases stepwise as cells differentiate into macrophage progenitors, then monoblasts, promonocytes, monocytes, and macrophages.⁹⁵ This gradual increase in expression occurs through two pathways: (1) the upregulation of the transcription factor SPI1, which binds both to the CSF1R promoter and the so-called FIRE enhancer

element;¹⁰³ and (2) chromatin remodeling and factor assembly at the FIRE enhancer.¹⁰⁴ There are distinct downstream biological functions regulated by CSF1R tyrosine residues, including CSF1R activation/degradation and macrophage survival, proliferation, differentiation, and migration.¹⁰⁵

During macrophage survival, CSF1R degradation is inhibited and PI3K/AKT pathways are activated, signaling downstream to pro-survival proteins.⁹⁵ During macrophage proliferation, there is a CSF1 dose-dependent increase in CSF1R synthesis and CSF1R phosphorylation activates both the MEK and PI3K pathways.^{106,107} During monocyte/macrophage differentiation, CSF1R downstream is different depending on the cell type expressing CSF1R. In multipotent precursor cells, differentiation is promoted through signaling of PLCG2¹⁰⁸ and separately by phosphorylation of ERK1 and ERK2,⁹⁵ which is regulated by DUSP5 in a negative feedback loop.¹⁰⁹ In myeloblasts, monoblasts, and promonocytes, the ERK1/2 pathway is critical in differentiation,¹¹⁰ particularly through the inactivation of PP2A.¹¹¹ Additionally, in these cell types, GAB2 regulates ERK1/2 in a differentiation stage-specific manner, increasing its downstream activity in monoblasts and promonocytes but decreasing its activity in macrophages.¹¹² During migration, CSF1 stimulation produces a rapid membrane ruffling followed by two waves of actin polymerization, regulated by the two actin nucleators WASP and WAVE2, resulting in motility and chemotaxis.⁹⁵

6.4 CSF1R and cancer

To understand the contribution of CSF1R in cancer, it is important to first understand basic macrophage biology. Macrophages, which are found in every tissue in the body, are the most phenotypically plastic cells in the hematopoietic system, which makes defining and classifying macrophages a notoriously challenging task.¹¹³ Perhaps the most classic definition of macrophages—the terminal cells of the mononuclear phagocytic lineage—is incomplete because some macrophages have different origins during development and persist into adulthood.¹¹⁴ Another common method to classify macrophages is by their inflammatory state, which produces two categories.^{115,116} The first is the “classically activated macrophage” or M1, which is thought to be pro-inflammatory and anti-tumorigenic, responding to IFN γ and the activation of toll-like receptors (TLRs). The second is the “alternatively activated macrophage” or M2, which is thought to be anti-inflammatory and pro-tumorigenic, responding to IL-4 and IL-13.^h However, these classical subdivisions do not represent the complexity of macrophages receiving numerous cytokine and growth factor signaling *in vivo*, as recent transcriptional profiling studies of macrophages have demonstrated.^{114,119} Regardless of this complexity, CSF1R exists as the predominant lineage regulator for virtually all macrophages in the body.¹¹³

In cancer, macrophages play a significant role in establishing and maintaining the tumor microenvironment. In response to various cytokines encountered in the

^h Traditionally, CSF1 stimulation is associated with M2 macrophage polarization, although CSF1R is similarly activated in M1 vs M2 phenotype macrophages.^{117,118}

microenvironment (e.g. CSF1, IL-4 and IL-13), they synthesize and secrete inflammatory cytokines (e.g. IFN γ , TNF α and IL-6) which engenders a state of chronic inflammation, although there are other unique signaling partners and molecules depending on the tumor type.¹¹³ In mice, although these pro-tumor macrophages can be subdivided based on the expression of many additional cell-surface markers, they all express canonical macrophage markers, including CSF1R.⁷⁶ In addition, depending on cancer subtype, there are significant differences in terms of the number of macrophages within the tumor and their phenotype, either pro-tumorigenic or anti-tumorigenic.¹²⁰ In 2002, Zhang et al conducted a meta-analysis consisting of 55 studies involving 8,692 patients in order to evaluate the prognostic significance of TAMs in solid tumors.¹²¹ The researchers observed no difference between the proportion of the M1 versus M2 macrophage phenotype and overall survival, highlighting the complexity and tumor-subtype-specific contribution of macrophages to tumor development and treatment response.^{121,i}

6.4.1 *CSF1R clinical trials*

Based on these discoveries showing the contribution of CSF1R-expressing cells on cancer progression and resistance, there is a commensurate focus on clinical trials involving targeting CSF1R activation in cancer. As of June 2017, there are 39 clinical trials completed or in development involving CSF1/CSF1R small-molecule inhibitors or monoclonal antibodies for cancer treatment (see Table 6.1 for complete

ⁱ Zhang et al defined the presence of TAMs as $\geq 20\%$ anti-CD68 cells by immunohistochemistry, and defined M1 by HLA-DR expression and M2 by CD163 expression.¹²¹

list).¹²² These clinical trials can be subdivided into three categories: (1) evaluating the inhibition of CSF1R activity as monotherapy, (2) in combination with chemotherapy regimens, and (3) in combination with immunotherapy regimens.

Slightly more than half of the trials involve small-molecule inhibitors (23/39 or 59%), including PLX3397 (also known as pexidartinib, which is singlehandedly being evaluated in no less than 8 ongoing trials as a monotherapy), ARRY-382, PLX7486, BLZ945, and JNJ-40346527. The remaining clinical trials involve monoclonal antibodies (16/39 or 41%), including emactuzumab, AMG820, IMC-CS4, cabiralizumab, and the CSF1-ligand-targeting antibodies MCS110 PD-0360324. (There are no IL-34-targeting compounds or monoclonal antibodies currently in clinical development.) Broadly, the results that have been published¹²³⁻¹³⁴ suggest that these compounds are well-tolerated, although their efficacy has yet to be determined in large-scale phase 3 clinical trials.¹²²

Table 6.1. Clinical trials with CSF1/CSF1R small molecules or monoclonal antibodies currently in clinical development (as of June 2017).

Modified from Cannarile et al.¹²² See below for list of abbreviations.

Approach	Class	Target	Compound/Class	Combination Partner	Clinical Phase	Sponsor	Indication	ClinicalTrials.gov Identifier	Status/Results	Reference
Monotherapy	Small molecule	CSF1R (and cKIT, Flt3)	Pexidartinib (PLX3397, PLX108-01)	N/A	2	The Christie NHS Foundation Trust	KIT-mutated advanced acral and mucosal melanoma	NCT02071940	Ongoing	-
Monotherapy	Small molecule	CSF1R (and cKIT, Flt3)	Pexidartinib (PLX3397, PLX108-01)	N/A	1/2	Plexikon	Unresectable or metastatic KIT-mutated melanoma	NCT02975700	Ongoing	-
Monotherapy	Small molecule	CSF1R (and cKIT, Flt3)	Pexidartinib (PLX3397, PLX108-01)	N/A	2	Plexikon	Advanced castration-resistant prostate cancer with bone metastasis and high circulating tumor cell counts	NCT01499043	Not yet reported	-
Monotherapy	Small molecule	CSF1R (and cKIT, Flt3)	Pexidartinib (PLX3397, PLX108-01)	N/A	2	Plexikon	Recurrent GBM	NCT01349036	ORR: 0% CBR: 7/38 (18%)	(2014) Butowski et al., J Clin Oncol; (2016) Butowski et al., Neuro Oncol
Monotherapy	Small molecule	CSF1R (and cKIT, Flt3)	Pexidartinib (PLX3397, PLX108-01)	N/A	1/2	NCI	Refractory leukemias and refractory solid tumors, including neurofibromatosis type 1-associated plexiform neurofibromas	NCT02390752	Ongoing	-
Monotherapy	Small molecule	CSF1R (and cKIT, Flt3)	Pexidartinib (PLX3397, PLX108-01)	N/A	2	Plexikon	Relapsed or refractory cHL	NCT01217229	ORR: 1/20 (5%)	(2012) Moskowitz et al., Blood
Monotherapy	Small molecule	CSF1R (and cKIT, Flt3)	Pexidartinib (PLX3397, PLX108-01)	N/A	1/2	Plexikon	Relapsed or refractory FLT3-ITD-positive acute myeloid leukemia	NCT01349049	Ongoing	-
Monotherapy	Small molecule	CSF1R (and cKIT, Flt3)	Pexidartinib (PLX3397, PLX108-01)	N/A	1	Plexikon	Advanced, incurable, solid tumors in which the target kinases are linked to disease pathophysiology	NCT01004861	Ongoing	-
Monotherapy	Small molecule	CSF1R (and Trk)	PLX7486	N/A	1	Plexikon	Solid tumors	NCT01804530	Ongoing	-
Monotherapy	Small molecule	CSF1R	ARRY-382	N/A	1	Array BioPharma	Solid tumors	NCT01316822	ORR: 0% CBR: 4/26 (15%)	(2013) Bendell et al., Mol Cancer Ther
Monotherapy	Small molecule	CSF1R	JNJ-40346527	N/A	1/2	Johnson & Johnson	cHL	NCT01572519	ORR: 1/21 (5%) CBR: 11/21 (52%)	(2015) von Tresckow et al., Clin Cancer Res
Monotherapy	Small molecule	CSF1R	BLZ945	N/A	1/2	Novartis	Solid tumors	NCT02829723	Ongoing	-
Monotherapy	Monoclonal antibody	CSF1R	Emactuzumab (RG7155)	N/A	1	Roche	Solid tumors	NCT01494688	PMR: 5/44 (11%) ORR: 0% CBR: 6/40 (24%)	(2015) Gomez-Roca et al., J Clin Oncol
Monotherapy	Monoclonal antibody	CSF1R	AMG820	N/A	1	Amgen	Solid tumors	NCT01444404	ORR: 1/25 (4%) CBR: 6/25 (24%)	(2016) Papadopoulos et al., Cancer Res
Monotherapy	Monoclonal antibody	CSF1R	IMC-CS4 (LY3022855)	N/A	1	Eli Lilly	Solid tumors	NCT01346358	Ongoing	-
Monotherapy	Monoclonal antibody	CSF1R	IMC-CS4 (LY3022855)	N/A	1	Eli Lilly	Breast and prostate cancer	NCT02265536	Ongoing	-
Monotherapy	Monoclonal antibody	CSF1	MCS110	N/A	1/2	Novartis	Prostate cancer	NCT00757757	Terminated	-
Combination - Chemotherapy	Small molecule	CSF1R (and cKIT, Flt3)	Pexidartinib (PLX3397, PLX108-01)	Androgen-deprivation therapy plus external radiotherapy	1	Plexikon/Daiichi Sankyo	Prostate cancer	NCT02472275	Ongoing	-

[Table 6.1. Clinical trials with CSF1/CSF1R small molecules or monoclonal antibodies currently in clinical development (as of June 2017).]

Combination - Chemotherapy	Small molecule	CSF1R (and cKIT, Flt3)	Pexidartinib (PLX3397, PLX108-01)	Paclitaxel	1	Plexikon/Daiichi Sankyo	Solid tumors	NCT01525602	ORR: 4/23 (17%) CBR: 14/23 (61%)	(2014) Rugo et al., Ann Oncol
Combination - Chemotherapy	Small molecule	CSF1R (and cKIT, Flt3)	Pexidartinib (PLX3397, PLX108-01)	Eribulin	1/2	Plexikon/Daiichi Sankyo	Breast cancer	NCT01596751	Ongoing	-
Combination - Chemotherapy	Small molecule	CSF1R (and cKIT, Flt3)	Pexidartinib (PLX3397, PLX108-01)	Temozolomide plus external radiotherapy	1/2	Plexikon/Daiichi Sankyo	GBM	NCT01790503	Not yet reported	-
Combination - Chemotherapy	Small molecule	CSF1R (and cKIT, Flt3)	Pexidartinib (PLX3397, PLX108-01)	Vemurafenib	1	Plexikon/Daiichi Sankyo	BRAF-mutated melanoma	NCT01826448	Terminated	-
Combination - Chemotherapy	Small molecule	CSF1R (and cKIT, Flt3)	Pexidartinib (PLX3397, PLX108-01)	PLX9486 (KIT inhibitor)	1/2	Plexikon/Daiichi Sankyo	GIST	NCT02401815	Ongoing	-
Combination - Chemotherapy	Small molecule	CSF1R (and cKIT, Flt3)	Pexidartinib (PLX3397, PLX108-01)	Sinolimus	1/2	Plexikon/Daiichi Sankyo	Advanced sarcomas, MPNST	NCT02584647	Ongoing, not yet reported	(2016) Manji et al., J Clin Oncol
Combination - Chemotherapy	Monoclonal antibody	CSF1R	Emactuzumab (RG7155)	Paclitaxel	1	Roche	Ovarian and breast cancer	NCT01494688	Not yet reported	-
Combination - Chemotherapy	Monoclonal antibody	CSF1R	Emactuzumab (RG7155)	Paclitaxel plus bevacizumab	2	Roche	Ovarian cancer	NCT02923739	Ongoing	-
Combination - Chemotherapy	Monoclonal antibody	CSF1	MCS110	Carboplatin plus gemcitabine	2	Novartis	TNBC	NCT02435680	Ongoing	-
Combination - Chemotherapy	Monoclonal antibody	CSF1	PD-0360324	Cyclophosphamide	2	Pfizer	Recurrent platinum-resistant epithelial ovarian, peritoneal, or fallopian tube cancer	NCT02948101	Ongoing	-
Combination - Immunotherapy	Small molecule	CSF1R (and cKIT, Flt3)	Pexidartinib (PLX3397, PLX108-01)	Pembrolizumab (anti-PD1 mAb)	1/2	Plexikon/Daiichi Sankyo	Solid tumors, malignant melanoma GIST, NSCLC, ovarian carcinoma, TNBC, SCCHN, UBC, pancreatic cancer, gastric carcinoma, leiomyosarcoma, cholangiocarcinoma, CRC (MSS)	NCT02452424	Ongoing	(2016) Wainberg et al., J Clin Oncol
Combination - Immunotherapy	Small molecule	CSF1R (and cKIT, Flt3)	Pexidartinib (PLX3397, PLX108-01)	Durvalumab (anti-PDL1 mAb)	1	Astra Zeneca	Pancreatic carcinoma, CRC	NCT02777710	Ongoing	-
Combination - Immunotherapy	Small molecule	CSF1R	ARRY-382	Pembrolizumab (anti-PD1 mAb)	1	Array BioPharma	Solid tumors, melanoma, NSCLC	NCT02880371	Ongoing	-
Combination - Immunotherapy	Small molecule	CSF1R	BLZ945	PDR001 (anti-PD1 mAb)	1/2	Novartis	Solid tumors	NCT02829723	Ongoing	-
Combination - Immunotherapy	Monoclonal antibody	CSF1R	Emactuzumab (RG7155)	Atezolizumab (anti-PDL1 mAb)	1	Roche	Solid tumors, TNBC, gastric cancer, soft tissue sarcoma, UBC, ovarian cancer, NSCLC, melanoma	NCT02323191	Ongoing	-
Combination - Immunotherapy	Monoclonal antibody	CSF1R	Emactuzumab (RG7155)	RG7876 (CD40 agonist mAb)	1	Roche	TNBC, gastric cancer, mesothelioma, CRC, melanoma, pancreatic cancer	NCT02760797	Ongoing	-
Combination - Immunotherapy	Monoclonal antibody	CSF1R	AMG820	Pembrolizumab (anti-PD1 mAb)	1	Amgen	Solid tumors	NCT02713529	Ongoing	-
Combination - Immunotherapy	Monoclonal antibody	CSF1R	Cabiralizumab (FPA008)	Nivolumab (anti-PD1 mAb)	1	FivePrime/BMS	Solid tumors, NSCLC, SCCHN, pancreatic cancer, ovarian cancer, RCC, GBM	NCT02526017	Ongoing	(2016) Brahmer et al., Cancer Immunol Res
Combination - Immunotherapy	Monoclonal antibody	CSF1R	IMC-CS4 (LY3022855)	Durvalumab (anti-PDL1 mAb) or Tremelimumab (anti-CTLA4 mAb)	1	Eli Lilly	Solid tumors	NCT02718911	Ongoing	(2016) Bauer et al., J Immunother Cancer
Combination - Immunotherapy	Monoclonal antibody	CSF1	MCS110	PDR001 (anti-PD1 mAb)	1/2	Novartis	Solid tumors, TNBC, pancreatic cancer, melanoma, endometrial cancer	NCT02807844	Ongoing	-
Combination - Immunotherapy	Monoclonal antibody	CSF1	PD-0360324	Avelumab (anti-PDL1 mAb)	1	Pfizer	Solid tumors	NCT02554812	Ongoing	-

*CBR: clinical benefit rate; cHL: classical Hodgkin lymphoma; CSF1: colony-stimulating factor 1; CSF1R: colony-stimulating factor 1 receptor; CRC: colorectal cancer; CTLA4: cytotoxic T-lymphocyte-associated protein 4; GBM: glioblastoma; di-GCT: diffuse-type tenosynovial giant cell tumor; GIST: gastrointestinal stromal tumor; mAb: monoclonal antibody; MPNST: malignant peripheral nerve sheath tumor; MSS: microsatellite stable; NCI: National Cancer Institute; NHS: National Health Service; NSCLC: non-small cell lung cancer; ORR: objective response rate; PD1: programmed cell death protein 1; PDL1: programmed cell death ligand 1; PMR: partial metabolic response; RCC: renal cell carcinoma; SCCHN: squamous cell carcinoma of the head and neck; TNBC: triple-negative breast cancer; UBC: urothelial bladder carcinoma

6.4.2 *CSF1R* in acute myeloid leukemia

Initially, when considering *CSF1R* genetic abnormalities, the presence of *CSF1R* mutations in acute myeloid leukemia was a controversial issue. The first major study addressing this question used mutant-specific DNA hybridizing probes to two codons critical for *CSF1R* transformation activity and found that 16.7% of AML patients (8/48) contained *CSF1R* mutations.¹³⁵ However, the large-scale study undertaken by TCGA, which analyzed 200 *de novo* AML patient samples using whole-exome sequencing, found no *CSF1R* mutations.²⁴ Indeed, the prevailing hypothesis is that *CSF1R* mutations are extremely rare in acute myeloid leukemia, and that the results from the initial study are indicative of the high false-positive rate of hybridization-based studies.¹³⁶

It should be noted that there are two cell lines that contain *CSF1R* genetic abnormalities. These cell lines require *CSF1R* for their survival and proliferation and are sensitive to *CSF1R* small-molecule inhibitors. The first, GDM-1, is an acute myelomonoblastic leukemia cell line established from a 65-year-old woman.¹³⁷ GDM-1 contains a point mutation (Y571D) in *CSF1R*, resulting in its constitutive activation and phosphorylation.¹³⁸ The second, MKPL-1, is an acute megakaryoblastic cell line established from a 66-year-old man.¹³⁹ MKPL-1 possesses a novel fusion of *CSF1R* to *RBM6*, producing the t(3;5)(p21;q33) *RBM6-CSF1R* translocation, which renders it sensitive to *CSF1R*-targeting small-molecule inhibitors.¹⁴⁰ Neither of these *CSF1R* abnormalities has been reported in patient samples other than the ones from which these cell lines were derived.

One study found a novel population of CSF1R high-expressing leukemia cells in an AML mouse model driven by MOZ fusion proteins.¹⁴¹ These CSF1R^{high} cells demonstrated similar morphology and colony-forming ability as CSF1R^{low} cells, although they had enhanced leukemia-initiating activity, and elimination of these cells resulted in the elimination of AML.¹⁴¹ Mechanistically, CSF1R^{high} cells showed enhanced STAT5 activation in a manner dependent upon the hematopoietic transcription factor SPI1.¹⁴¹ However, although MOZ translocations have appeared occasionally in the literature,¹⁴² the activation of CSF1R by another specific genetic abnormality in AML has not been documented elsewhere.

Recently, a study of 140 Taiwanese colorectal, ovarian, and endometrial cancer patients identified a CSF1R genetic variant (c1085A>G; H362R) that was present in 42.9% of their tumors.¹⁴³ This variant, which was found at the same frequency in healthy Taiwanese (and East Asians in general^j), resulted in reduced CSF1R internalization and phosphorylation after CSF1 stimulation and, paradoxically, increased macrophage sensitivity to CSF1R small-molecule inhibitors. However, since this variant is only found in ~10% of healthy Americans, which comprise the vast majority of our patient population, it is unlikely to be chiefly responsible for the phenotype of CSF1R sensitivity that we observe in leukemia patients. Still, it is worth considering in future studies, especially to confirm that the frequency of this variant in leukemia patients matches that of other cancer types, and

^j Ethnic groupings were classified by 1000 Genomes Project.¹⁴⁴

in identifying patient populations that would benefit from CSF1R inhibitor clinical trials.

6.4.3 *CSF1R in chronic lymphocytic leukemia*

Regarding CSF1R genetic abnormalities, two back-to-back studies^{28,32} performed next-generation sequencing on hundreds of CLL patients (452 CLL patients from Puente et al., 278 from Landau et al.) and found no CSF1R mutations. Additionally, unlike AML, there have been no reported cases of CSF1R translocations or fusion proteins identified in CLL patients. However, the contribution of CSF1R in CLL has received greater attention recently, particularly because of two studies identifying its expression on nurse-like cells (NLCs) that were essential to leukemia cell survival.^k

First, it is important to provide some background information on NLCs. The discovery of NLCs was motivated by the observation that despite their longevity *in vivo*, isolated CLL cells underwent rapid, spontaneous apoptosis upon *in vitro* culture.¹⁴⁵ However, cell survival could be rescued by co-culturing CLL cells with bone marrow stromal cells,^{146,147} suggesting a critical contribution by the tumor microenvironment. Separately, Whitlock and Witte developed a method for long-term culturing of B cells,¹⁴⁸ and observed that B cells migrated underneath a newly-formed layer of bone-marrow-derived stromal cells.¹⁴⁹ A similar observation was

^k These two studies were published a couple of months before we first submitted our manuscript, Targeting of Colony-Stimulating Factor 1 Receptor (CSF1R) in the CLL Microenvironment Yields Antineoplastic Activity in Primary Patient Samples. The researchers perform extremely similar experiments and reach similar conclusions, which is why I discuss their results in some detail.

made in CLL cells,¹⁵⁰ further suggesting that short-range cell contact and growth factor secretion were required for CLL survival. Eventually, these large, adherent cells were discovered to regulate survival through a CXCL12-mediated “nursing” of CLL cells, and were therefore described as “nurse-like cells” (NLCs).¹⁵¹ Later studies characterized NLCs as being the leukemic counterpart of tumor-associated macrophages, expressing CD68 and CD163,^{152,153} enhancing chemoresistance,¹⁵⁴ and mediating CLL survival through additional mechanisms, including upregulating TNFSF13 and TNFSF13B¹⁵⁵ and indirectly stimulating CCL3/CCL4 release from B cells.¹⁵⁶

The first study describing the contribution of CSF1R in CLL, conducted by Ryan Wilcox’s group at the University of Michigan (Polk et al), isolated peripheral blood mononuclear cells (PBMCs) from CLL patients.¹⁵⁷ The researchers exposed them to H27K15, a monoclonal antibody that partially inhibits CSF1R without blocking its internalization or degradation,¹⁵⁸ and observed a decrease in nurse-like cells (NLCs) based on their distinctly high forward- and side-scatter pattern compared to CLL cells.¹⁵⁷ Adding H27K15 significantly decreased cell viability, and combining it with ibrutinib further decreased viability.¹⁵⁷ Notably, instead of testing CSF1R-specific small-molecule inhibitors, Polk et al used pacritinib, a tyrosine kinase inhibitor with multiple targets including CSF1R, and successfully replicated their experiments with the monoclonal antibody using pacritinib.¹⁵⁷

The second study, led by a group of Italian scientists, performed experiments in which they administered clodrolip, a liposomal encapsulation of clodronate used for the *in vivo* depletion of macrophages, to mice with CLL (specifically, Rag2^{-/-}γc^{-/-}

mice injected with MEC1,¹⁵⁹ a CLL cell line).¹⁶⁰ They showed that clondrolip reduces tumor burden, especially in the bone marrow, and demonstrated that this effect was specific for CSF1R using the anti-mouse CSF1R monoclonal antibody 2G2.¹⁶⁰ Interestingly, clondrolip treatment increased the circulation of CD20+ leukemia cells, and combining clondrolip with anti-CD20 monoclonal antibodies produced a distinct survival advantage compared to treating with anti-CD20 antibodies alone.¹⁶⁰

6.5 Targeting CSF1R in acute myeloid leukemia and chronic lymphocytic leukemia

Historically, our laboratory—specifically, the laboratories of Brian Druker and Jeffrey Tyner—has utilized targeted therapies to conduct pioneering research to treat hematologic malignancies. Over many years, our lab has undertaken functional screening of hundreds of patient samples, whereby blood samples are collected from patients with various hematological malignancies and the mononuclear cells are exposed to dose-escalating concentrations of dozens of small-molecule inhibitors. The results from these functional screens revealed that a substantial percentage of AML and CLL patient samples showed sensitivity to CSF1R-specific small-molecule inhibitors. These observations and others spurred an investigation into the mechanism and functional significance of CSF1R in these leukemia subtypes.

Ultimately, this dissertation contains original research investigating the clinical benefit of targeting CSF1R in AML and CLL, and presents the experimental data from two similar, independent projects. The results from the first project—Targeting of Colony-Stimulating Factor 1 Receptor (CSF1R) in the CLL

Microenvironment Yields Antineoplastic Activity in Primary Patient Samples—was published as an article under the same name in *Oncotarget* in March 2018. The results from the second project—CSF1R inhibitors exhibit anti-tumor activity in acute myeloid leukemia by blocking paracrine signals from support cells—was compiled into a manuscript and submitted to *Blood* in March 2018.

To provide essential, project-specific context for these results, each section in this dissertation contains the original Introduction and Discussion sections that were included in their submission. However, a more integrated discussion of these two projects, including a comparison of their similarities and differences, is described in greater detail in section 9 Discussion.

7 Targeting of Colony-Stimulating Factor 1 Receptor (CSF1R) in the CLL Microenvironment Yields Antineoplastic Activity in Primary Patient Samples

David K. Edwards V*, David Tyler Sweeney*, Hibery Ho, Christopher A. Eide, Angela Rofelty, Anupriya Agarwal, Selina Qiuying Liu, Alexey V. Danilov, Patrice Lee, David Chantry, Shannon K. McWeeney, Brian J. Druker, Jeffrey W. Tyner, Stephen E. Spurgeon**, Marc M. Loriaux**

*These authors contributed equally to this work.

**These authors contributed equally to this work.

This article was published in *Oncotarget* in March 2018.

7.1 Contribution to Project

7.1.1 *Conception or design of the work*

The CSF1R-in-CLL project was initiated by Tyler Sweeney (TS), a research associate working under the joint mentorship of Stephen Spurgeon (SES) and Mark Loriaux (ML). Although it was run in parallel to the CSF1R-in-AML project, there was very little interaction between TS and me in the beginning, primarily because of different mentors, different patient sample cohorts, and different initial approaches. (The CSF1R-in-AML project focused on identifying a genetic/clinical marker for CSF1R inhibitor sensitivity after observing CSF1R as a significant hit on the siRNA kinome screen. The CSF1R-in-CLL project focused on evaluating synergy between CSF1R inhibitors and current standard-of-care drugs.)

However, a couple of months before the abstract deadline for the 2015 American Society of Hematology (ASH) meeting, I was approached by TS to help him understand, visualize, and analyze the data he had collected. Because I had spent significantly more time on data analysis for the CSF1R-in-AML project, I helped him prepare an abstract for the conference.

During the months between preparing the abstract and the conference itself, I became more and more involved in the project, overseeing much of its progression and development. We became collaborators, with him providing me with his experimental data and me analyzing and graphing that data. He began receiving informal mentorship from Jeffrey Tyner (JWT), my primary mentor, and attended our weekly meetings. Eventually, the data turned into polished figures, which turned into a complete manuscript.

Because of my significant help with data analysis and visualization, I became co-first authors on the manuscript, with my name listed second. After the manuscript had been submitted and the first round of reviewer comments had been received, TS left to attend graduate school in Virginia. I addressed all the reviewer comments and handled the revisions myself, so although we were still co-first authors, my name was listed first.

7.1.2 *Data collection, analysis, and interpretation*

The experiments handling and processing the CLL samples themselves (i.e. exposure to CSF1R inhibitors, CD14+ cell depletion) were mostly conducted by TS. However, during the revision process, the reviewers suggested two experiments that were performed by me: the effect of CSF1R inhibitors on inducing apoptosis (Figure 7.6) and preventing nurse-like cell growth (Figure 7.4C-D) in primary patient samples.

Figure 7.1. *Ex vivo* inhibitor screening reveals CSF1R sensitivity in CLL patient specimens. The patient sample data on CSF1R was collected and input into the database by others. I designed and created the protocol visualization and the table of CSF1R inhibitor information. I exported the that patient sample data and graphed it, along with identifying and graphing representative sensitive/non-sensitive patient samples. The supplemental figure was made by me.

Figure 7.2. No genetic or clinical characteristic readily co-segregate with sensitivity to CSF1R inhibition in CLL patient samples. Based on my prior experience with extracting information from patient charts, I taught TS how to go

through electronic medical records and enter clinical/genetic information into the database. Once that had finished, I exported the data myself and graphed/formatted it using a combination of the heat map function in Prism 7.0 and Adobe Illustrator. I conducted all statistical analyses and generated the supplemental figure and tables.

Figure 7.3. CSF1R is not found on CD19+ CLL cells but instead expressed on a CD14+ myeloid subpopulation. The antibody cocktails used to identify the CSF1R-expressing subpopulation were created by TS and me in conjunction with the OHSU hematopathology group. TS created the FlowJo figures and I formatted them for the manuscript. Additionally, TS gathered the drug sensitivity and percent CD14+ cells and I graphed and analyzed the resulting data.

Figure 7.4. Sensitivity of CLL cells to CD14+ depletion correlates with sensitivity to CSF1R inhibitors. TS and I developed the CD14-depletion protocol together, although he performed the depletion experiments himself. I performed the nurse-like cell experiment on my own. I designed and created the protocol visualization, devised and conducted the data analysis, and made the supplemental figure.

Figure 7.5. Synergy between ibrutinib or idelalisib and CSF1R inhibitors in majority of CLL patient specimens. TS exposed all of the patient samples to inhibitors and gathered the data. TS used CalcuSyn to determine the synergy scores for each patient sample, and I grouped those scores and used GenePattern to perform hierarchical clustering on them. I visualized and graphed all of the data (including supplemental figure) and performed the relevant statistics.

7.1.3 *Article drafting/submission/revision*

TS and I contributed equally to the initial drafting of the manuscript; TS wrote the Introduction and Discussion sections, while I wrote the Abstract, Results, and Methods sections, along with the Figure Legends. I revised his sections of the manuscript and incorporated them into the final product, which was subsequently revised by JWT and SES.

SES submitted the article to *Clinical Cancer Research*, and upon rejection, TS and I went through the reviewer comments together. He gathered additional data that he had already collected while I made improvements to the graphs and manuscript. SES subsequently submitted it to *Leukemia* and, after getting rejected, I submitted it to *Oncotarget*. The revisions to *Oncotarget*, including rewriting the manuscript and drafting the rebuttal letter, were done by me, with slight assistance from SES and JWT.

7.2 Abstract

In many malignancies, the tumor microenvironment includes CSF1R-expressing supportive monocyte/macrophages that promote tumor cell survival. For chronic lymphocytic leukemia (CLL), these supportive monocyte/macrophages are known as nurse-like cells (NLCs), although the potential effectiveness of selective small-molecule inhibitors of CSF1R against CLL is understudied. Here, we demonstrate the preclinical activity of two inhibitors of CSF1R, GW-2580 and ARRY-382, in primary CLL patient samples. We observed that at least 25% of CLL samples showed sub-micromolar sensitivity to CSF1R inhibitors. This sensitivity was observed in samples with varying genetic and clinical backgrounds, although higher white cell count and monocyte cell percentage was associated with increased sensitivity. Depleting CD14-expressing monocytes preferentially decreased viability in samples sensitive to CSF1R inhibitors, and treating samples with CSF1R inhibitors eliminated the presence of NLCs in long-term culture conditions. These results indicate that CSF1R small-molecule inhibitors target CD14-expressing monocytes in the CLL microenvironment, thereby depriving leukemia cells of extrinsic support signals. In addition, significant synergy was observed combining CSF1R inhibitors with idelalisib or ibrutinib, two current CLL therapies that disrupt tumor cell intrinsic B-cell receptor signaling. These findings support the concept of simultaneously targeting supportive NLCs and CLL cells and demonstrate the potential clinical utility of this combination.

7.3 Introduction

Chronic lymphocytic leukemia (CLL) is the most common leukemia in the Western world, with nearly 19,000 new cases reported annually in the United States.¹⁶¹ The disease is characterized by an accumulation of small mature B-lymphocytes in the lymph nodes, bone marrow and peripheral blood. CLL is predominantly an indolent disease; however, around 25% of patients progress rapidly.¹⁶²

Therapy is generally reserved for patients with symptomatic disease and, until recently, has largely relied on chemo-immunotherapy combination regimens. Introduction of novel targeted therapies that inhibit B-cell receptor (BCR) signaling—such as ibrutinib, a Bruton’s tyrosine kinase (BTK) inhibitor, and idelalisib, a phosphatidylinositol-3-kinase delta isoform specific (PI3k δ) inhibitor—have dramatically improved patient outcomes and treatment options.¹⁶³ However, CLL remains incurable with these classical treatments, and most patients succumb to the disease or its complications.

One significant barrier to treatment is the contribution of the tumor microenvironment, which has been shown to be critical for cancer cell growth and survival. Tumor-associated macrophages (TAMs) have been shown to provide microenvironmental support that maintains tumor cell viability and proliferation in a variety of solid tumor types.¹⁶⁴ These TAMs have protean pro-survival effects including increased angiogenesis, tumor cell invasion, metastasis, and inhibition of immune-mediated anti-tumor responses.¹⁶⁵ TAMs have also been isolated from the

peripheral blood, spleen, and lymph nodes in CLL patients where they have shown to be essential for CLL cell survival in the tumor microenvironment.¹⁶⁶

In this setting, these TAMs, which are known as nurse-like cells (NLCs) or lymphoid-associated macrophages (LAMs), share a similar gene expression profile to TAMs derived from other tumor types.¹⁵² Specifically, these NLCs are derived from CD14-positive monocytes and, in the presence of CLL cells, differentiate into abnormal macrophages,^{153,167-169} which promote CLL cell survival.¹⁶⁷ This has particular clinical relevance given the finding that elevated peripheral blood monocyte count at the time of CLL diagnosis is associated with inferior outcomes.¹⁷⁰

In solid tumors, TAM function has been shown to depend on the receptor tyrosine kinase CSF1R.¹⁷¹ CSF1R, also known as cFMS and M-CSFR, is a member of the type III receptor tyrosine kinase family and is activated by binding of its ligands CSF-1 (M-CSF) or IL-34.^{94,96,172} CSF1R is predominantly expressed on monocytes and tissue macrophages^{90,173} and is required for proliferation,⁸⁹ differentiation,¹⁷⁴ and chemotaxis,¹⁷⁵ all functions critical to TAM activity.

Recent studies suggest an important potential role for targeting CSF1R in CLL. In mice, depletion or targeting of TAMs has been associated with reduction in leukemic burden via reprogramming of the tumor microenvironment.^{160,176} Furthermore, using patient samples, neutralization or inhibition of CSF1R has been shown to inhibit NLC formation and decrease CLL cell viability, a finding mimicked by NLC depletion.¹⁷⁷ Given the role of NLCs in CLL as well as possible therapeutic implications, we evaluated the impact of CSF1R inhibition using highly selective small-molecule inhibitors across a broad spectrum of primary CLL samples.

7.4 Results

7.4.1 *CLL Patient Specimens Are Sensitive to CSF1R-Specific Small-Molecule Inhibitors*

We analyzed primary CLL samples using an *ex vivo* functional screen in which cells were exposed to dose-escalating concentrations of small-molecule inhibitors for 72 hours and then relative numbers of viable cells were assessed to generate dose-response curves (Figure 7.1A). The inhibitors tested included the highly selective CSF1R inhibitors GW-2580 (n = 197) (GlaxoSmithKline) and ARRY-382 (n = 131) (Array BioPharma), the latter of which has completed Phase I clinical testing. Both inhibitors exhibit a high degree of specificity for CSF1R across the kinome, including other class III receptor tyrosine kinases (Figure 7.1B).^{124,178} We observed that a proportion of CLL specimens showed sensitivity to these selective CSF1R inhibitors, with 25.9% (51/197) and 27.5% (36/131) of specimens showing sub-micromolar IC50s (the concentration of inhibitor required to reduce viability to 50%) for GW-2580 and ARRY-382, respectively (Figure 7.1C-D). We confirmed that increased exposure to CSF1R inhibitors induced apoptosis in patient sample cells via annexin V staining (Figure 7.6).

Previous genomic analyses of CLL patients have identified no mutations in CSF1R,^{28,32} nor is CSF1R significantly overexpressed in CLL compared to healthy monocytes. To identify a potential association with known clinical and biological characteristics, we evaluated these characteristics across the cohort of patient specimens that had been screened for CSF1R inhibitor sensitivity (Figure 7.2 and Figure 7.7A; see Table 7.1 and additional supplemental table from published manuscript submission). For GW-2580 and ARRY-382, the IC50 and average area

under the curve (AUC) were calculated for each patient specimen, and the specimens were organized by decreasing sensitivity to GW-2580. As expected, we observed a strong correlation between GW-2580 IC50 and GW-2580 AUC, and between GW-2580 AUC and ARRY-382 AUC ($p < 0.0001$; Figure 7.7B-C). We did not observe an association between specimen type (either from peripheral blood or bone marrow aspirate) and CSF1R inhibitor sensitivity (Figure 7.7D).

We compared the CSF1R inhibitor sensitivity across CLL primary patient specimens with various clinical and genetic characteristics (Figure 7.2 and Figure 7.7E-P). Of the clinical characteristics, lower white blood cell (WBC) count is associated with sensitivity to CSF1R inhibitors. Furthermore, treatment status also significantly correlates with sensitivity to CSF1R inhibition, with relapsed patient specimens showing more resistance compared to specimens obtained from untreated patients. Additionally, of the cytogenetic abnormalities, deletion 11q is found more frequently in CSF1R-resistant patient specimens. However, none of these characteristics are uniformly enriched in the specimens that are sensitive to CSF1R inhibitors, suggesting that other mechanisms might be responsible for inhibitor response.

7.4.2 CD14+ Cell Subpopulation Expresses CSF1R and Is Associated with CSF1R Inhibitor Sensitivity

Since no obvious characteristics of the CLL patient specimens readily cosegregated with CSF1R sensitivity, we examined the contribution of tumor-extrinsic factors. The tumor microenvironment has been shown to be critically important in

the development of CLL and partly responsible for the ineffectiveness of modern chemotherapy regimens.^{179,180} We first assessed the profile of CSF1R expression across various cell populations in fresh CLL patient specimens using flow cytometry conducted by hematopathologists. Consistent with a tumor cell-extrinsic role of CSF1R, we did not find CSF1R expressed on CLL leukemic lymphocytes (CD5+/CD19+), but we did find it expressed on a subpopulation expressing CD14, a surface marker found predominantly on monocytes and macrophages (Figure 7.3A-B).

These findings led to a hypothesis whereby CSF1R inhibitors act indirectly on CLL leukemic cells via direct inhibition of CSF1R-expressing monocytes, suggesting that the presence of varying levels of CSF1R-expressing monocytes may correlate with varying degrees of CSF1R inhibitor sensitivity. Therefore, we wanted to determine whether quantitative levels of CD14 expression correlate with CSF1R sensitivity. We compared the percentages of CD14-positive cells in patient samples, as measured by flow cytometry, to the AUC values for GW-2580 and ARRY-382. We found that a higher CD14-positive percentage of cells is associated with increased sensitivity to CSF1R inhibitors ($p = 0.07$ for GW-2580; $p = 0.01$ for ARRY-382) (Figure 7.3C). These results suggest that the CD14-positive subpopulation of cells is associated with CSF1R inhibitor sensitivity.

7.4.3 *CD14+ Depletion in CLL Patient Samples Decreases Cell Viability and Eliminates CSF1R Inhibitor Sensitivity*

We next wanted to orthogonally validate that the impact of CSF1R inhibition on CLL cell viability is due to the presence (or, rather, the post-inhibitor depletion) of CSF1R-expressing CD14-positive cells. We therefore performed a CD14 antibody depletion experiment with magnetic column cell separation. After depleting CD14-positive cells, we incubated the remaining CD14-negative fraction (“depleted”) and whole mononuclear cells (“non-depleted”) from the same specimen for 72 hours and measured relative numbers of viable cells to compare the impacts of CD14+ depletion versus CSF1R inhibition on cell viability (Figure 7.4A). We confirmed that the depletion protocol itself has no significant effect on overall cell viability by measuring viability pre- and post-depletion (Figure 7.8A).

To quantify the impact of CD14+ depletion, we generated a CD14+ depletion sensitivity ratio that expresses the number of viable cells in CD14+ depleted conditions relative to whole mononuclear cells after 3 days in culture (following normalization to the starting cell viability in order to correct for variance in cell input). A CD14+ depletion sensitivity ratio less than 100 indicates a deleterious effect of CD14+ depletion on the viability of the depleted cells relative to the viability of whole mononuclear cells from the same specimen. The CD14+ depletion sensitivity ratio was compared to CSF1R inhibitor sensitivity in non-depleted cells. We observed a correlation between sensitivity to CD14+ depletion (sensitivity ratio less than 100) and sensitivity to CSF1R inhibition ($p = 0.03$ for GW-2580; $p = 0.06$ for ARRY-382) (Figure 7.4B).

To confirm that this correlation was specific to CSF1R sensitivity and not more generally to overall drug sensitivity, we compared the CD14+ depletion sensitivity ratio against sensitivity to two small-molecule inhibitors that exhibit recurrent efficacy in CLL—ibrutinib, which targets Bruton’s tyrosine kinase (BTK), and idelalisib, which targets phosphoinositide 3-kinase delta (PI3K δ). We confirmed that there is no association between CSF1R inhibitor sensitivity and sensitivity to ibrutinib or idelalisib (Figure 7.8B-C). In addition, we observed no correlation between sensitivity to CD14+ depletion and sensitivity to ibrutinib or idelalisib (Figure 7.8D-E), suggesting that the mechanism underlying the loss of cell viability after CD14+ depletion is specific to CSF1R inhibitor sensitivity and not with sensitivity to any effective small-molecule kinase inhibitor.

Based on our hypothesis that CSF1R inhibition is mediated by the CD14-positive cells, we predicted that CD14+ depletion would prevent any further impact of CSF1R inhibitors on the viability of the remaining cells post-depletion. To test this prediction, we examined the correlation between the change in CSF1R sensitivity imparted by CD14+ depletion relative to the sensitivity to CSF1R inhibitors of the whole mononuclear cell fraction (Figure 7.9A). We determined the degree to which CSF1R dose-response curves were altered after CD14+ depletion versus the CSF1R dose-response curves of whole mononuclear cells from the same specimens. We observed that specimens with higher CSF1R inhibitor sensitivity in whole mononuclear cells were the same ones that showed the greatest decrease in sensitivity after CD14+ depletion ($p = 0.04$ for GW-2580; $p = 0.13$ for ARRY-382) (Figure 7.9B-C). We did not observe this same correlation when comparing ibrutinib

or idelalisib sensitivity (Figure 7.9D-E), again supporting the observation that CSF1R sensitivity is directly connected to the CD14-positive cell population.

In chronic lymphocytic leukemia, CD14-positive monocytes can differentiate into nurse-like cells (NLCs) that provide a critical tumor-promotional and -protective microenvironment for the leukemia. To directly confirm that CSF1R inhibition was targeting the subpopulation of supportive CD14-expressing nurse-like cells (NLCs), we performed long-term culturing experiments to isolate adherent NLCs from the bulk CLL cell population.¹⁶⁷ We exposed primary patient specimens to CSF1R inhibitors before culturing NLCs and measured the change in the number of NLCs that grew on the plate. We found that the addition of 1 μ M GW2580 or ARRY-382 dramatically decreased the number of NLCs compared to untreated cells (Figure 7.4C). Interestingly, for one patient specimen unable to produce a significant number of NLCs even in the untreated condition, the CSF1R inhibitors did not decrease viability, suggesting that their efficacy is dependent on the presence and activity of NLCs within the leukemia (Figure 7.4D).

Overall, these results demonstrate that the depletion of CD14-positive cells, or the removal of these cells after their differentiation into nurse-like cells, results in decreased CLL cell viability and decreased sensitivity to CSF1R inhibitors. They demonstrate that the effectiveness of CSF1R inhibitors is dependent on a paracrine interaction of leukemic cells with CD14-positive/CSF1R-positive supportive monocytes.

7.4.4 CSF1R Inhibitors Work Synergistically in Combination with Ibrutinib and Idelalisib in a Majority of CLL Patient Samples

To determine the potential utility of combining CSF1R inhibitors with currently approved therapies for CLL, we evaluated the sensitivity of patient samples to GW-2580 and ARRY-382 in combination with ibrutinib or idelalisib. CLL primary patient samples were exposed to each CSF1R inhibitor alone and to combinations of each inhibitor with ibrutinib or idelalisib in equimolar concentrations, and combination index (CI) values were calculated (Figure 7.5A).¹⁸¹

We observed a strong synergistic effect when combining CSF1R inhibitors with ibrutinib or idelalisib in the majority of patient specimens (Figure 7.5B-E; see

Figure 7.10 for examples of the drug-dose response curves from representative synergistic and antagonistic patient samples). To assess the possibility that this effect was driven primarily by single-agent sensitivity, we performed unsupervised hierarchal clustering of CI values across the range of drug concentrations, grouping specimens into a spectrum from most to least synergistic. We compared the IC50s of the single agents across the spectrum of patient samples and did not observe any significant association between single-agent sensitivity and combination synergy (Figure 7.5B-E). Moreover, many patient samples that had been resistant to ibrutinib and idelalisib alone became sensitive to the inhibitor in combination with GW-2580 or ARRY-382, suggesting the broad applicability of using CSF1R inhibitors with currently approved inhibitors to target CLL.

7.5 Discussion

The implementation of kinase inhibitors in CLL such as ibrutinib and idelalisib has shown durable response in patients with refractory or poor-risk disease.^{60,182,183} However, as quickly as ibrutinib reached success, a population of patients began to develop resistance,¹⁸⁴ resulting in significantly decreased overall survival.¹⁸⁵ In our study, we focused on therapeutic approaches that would potentially have a lasting, significant impact in treating CLL patients: successfully targeting both leukemic cells and their protective NLCs.

Many solid tumors depend upon microenvironmental support through TAMs,^{68,186} which enhance primary tumor growth and suppress the immune response.¹⁸⁷ There is a similar contribution of the microenvironment in hematologic malignancies, including CLL and lymphoma.^{167,188,189} For example, LAMs, which highly express CSF1R, have been found to support Hodgkin and non-Hodgkin's lymphoma.¹¹⁷ In Hodgkin lymphoma patients treated with standard chemotherapy, higher CSF1R expression was associated with shorter survival.^{190,191} In CLL, the importance of NLCs has been widely demonstrated, and CD14-positive NLC monocytes are critical in maintaining CLL cell viability, and depletion of cells from CLL patient specimens results in leukemic cell death.^{167,188}

In this study, we demonstrated a novel mechanism for targeting of the CLL microenvironment using two highly selective small molecule inhibitors of CSF1R. Through *ex vivo* functional screening of 197 CLL patient specimens, we found that more than 25% of these CLL specimens are highly sensitive to CSF1R inhibition (Figure 7.1). While *ex vivo* screening can result in variability among cell

subpopulations from sample to sample, we aimed to reduce the impact of variability by using a large data set. Furthermore, the variability seen likely reflects the inherent biologic differences across patient samples and therefore potentially represents the variety of drug responses that may be observed *in vivo*.

A comparison of CSF1R sensitivity against various clinical, genetic, and cytogenetic characteristics revealed no major correlations. We did observe a trend toward white cell count correlating with CSF1R sensitivity, and flow cytometric analysis revealed a correlation between CSF1R sensitivity and quantitative levels of CD14-positive cells (Figure 7.3). These interesting correlations are consistent with recently reported clinical data which showed that these characteristics resulted in a shorter time to initiation of treatment and reduced overall survival.¹⁷⁰

Furthermore, we also observed that primary CLL specimens contain a sub-population of CSF1R+/CD14+ cells (Figure 7.3A), suggesting that CSF1R signaling may be an important marker and novel target of the CLL microenvironment. Consistent with these findings, we have also validated the findings that CD14+ depletion deleteriously impacts on CLL cell viability, and we show for the first time in patient samples using selective small-molecule inhibitors that this phenomenon is mimicked by CSF1R inhibition, suggesting a new potential therapeutic route to target the CLL microenvironment.

A recent theme in clinical oncology research and patient care is the need for combination therapies. The contribution of agents targeting tumor-associated macrophage/monocyte lineage cells in these combination regimens has been robustly demonstrated in solid tumors, in which inhibition of microenvironmental

cell types (such as TAMs) dramatically synergizes with tumor-directed therapies via inhibition of microenvironmental rescue signals and induction of immune responses against tumor cells.^{192,193} Our findings extend this concept of targeting TAM-promoted neoplasia into hematologic malignancies. In addition, we show that combinations of CSF1R inhibitors with tumor-directed therapies in CLL (ibrutinib or idelalisib) exhibit strong synergy across numerous CLL patient specimens (Figure 7.5). These data are suggestive of candidate combination therapy regimens for CLL patients that may improve the duration of response and mitigate single-agent drug resistance. Simultaneous targeting of BTK and CSF1R may be of particular interest. Despite the ability of ibrutinib to disrupt CLL cell interactions within their protective niches, inhibiting BTK in NLCs may actually promote CLL cell survival, which may explain the inability of ibrutinib to overcome the protective effects provided by NLCs.^{154,194}

A recent report showing that pharmacologic depletion of macrophages in a CLL cell-line mouse model with a liposomal formulation of a bisphosphonate (clodrolip) or an anti-CSF1R monoclonal antibody (emactuzumab) results in significant anti-leukemic activity.¹⁶⁰ In addition, it has been recently shown that CSF1R is expressed in NLCs and in lymph nodes derived from CLL patients, and that neutralization or inhibition of CSF1R inhibits NLC formation, decreases CLL cell viability, and enhances the anti-tumor effects of ibrutinib.¹⁷⁷ This research further supports the potential for targeting CSF1R in CLL.

Ultimately, these results suggest a treatment strategy whereby CSF1R+/CD14+ cells can be chemically targeted by highly selective CSF1R

inhibitors, and that this targeting deprives CLL cells of crucial microenvironmental support. We propose enhancing this strategy in CLL patients through combination drug approaches by simultaneously giving CSF1R inhibitors, which target NLCs, with BTK and/or PI3K δ inhibitors as well as other agents, which target the leukemia cells themselves.

7.6 Methods

7.6.1 *Patient Sample Acquisition and Processing*

Primary leukemia samples were obtained from CLL patients by informed consent according to a protocol approved by the Institutional Review Board at Oregon Health & Science University. These samples were subsequently processed and exposed to an *ex vivo* small-molecule inhibitor screen as described previously.¹⁹⁵ Briefly, peripheral blood samples were extracted from CLL patients and the fresh mononuclear cells were isolated from whole blood using a Ficoll density gradient. The isolated cells were plated in R20 media consisting of RPMI (#11875; Thermo Fisher, Waltham, MA) with 20% FBS (#S11550; Atlanta Biologicals, Lawrenceville, GA), 1% penicillin-streptomycin (#15140; Thermo Fisher), 2% glutamine (#25030; Thermo Fisher), and 0.1% amphotericin B (#SV3007801; Thermo Fisher).

The mononuclear cells were plated with dose-escalating concentration gradients of small-molecule inhibitors, or a combination of inhibitors following the same fixed concentrations, and incubated for 72 hours at 37°C in 5% CO₂. After incubation, the relative number of remaining viable mononuclear cells in the plate was measured using a tetrazolium-based colorimetric assay (CellTiter AQueous One

Solution Cell Proliferation Assay; Promega, Madison, WI). To determine the degree of apoptosis after exposure to CSF1R inhibitors, the mononuclear cells were plated with either 1uM or 10uM of GW-2580 (GlaxoSmithKline, Brentford, United Kingdom) or ARRY-382 (Array BioPharma, Boulder, CO). The percentage of apoptotic cells was measured after 24, 48, and 72 hours using the Guava Nexin Assay (Merck Millipore, Billerica, MA)

Dose-response curves were generated for GW-2580 (n = 191 specimens) and ARRY-382 (n = 131), along with the BTK inhibitor ibrutinib (n = 84) (AbbVie, North Chicago, IL) and the PI3K δ inhibitor idelalisib (n = 160) (Gilead Sciences, Seattle, WA). Based on cell availability, multiple replicates for each inhibitor dose-response curves were generated on different test plates using our *ex vivo* screen. To calculate an overall drug sensitivity profile for each sample, for each inhibitor replicate, outliers were manually removed and the IC50 and AUC were calculated after fitting the data using a third-order polynomial regression model. Inhibitor curves were removed from further analysis if: (1) AUC < 1100 and (2) $r < 0.4$ (Pearson's correlation coefficient). Additionally, test plates were removed if the percent standard deviation (%stdev) among replicates—calculated as $(\text{mean} \div \text{stdev}) * 100$ —was less than 50%. Similarly, samples were removed if the %stdev among test plates was less than 50%.

Most clinical and genetic information was collected during routine standard-of-care patient sample evaluation obtained using electronic medical records. Some samples that had not been evaluated for the presence of immunoglobulin heavy chain (IGHV) gene mutations during initial treatment were subsequently analyzed using

the IGH Somatic Hypermutation Assay v2.0 (#5-101-0031; Invivoscribe, San Diego, CA). The NCBI IgBLAST tool was used to determine the percent divergence of each clonal sequence, where samples with equal or less than 2% divergence from the germline sequence were considered to have non-mutated IGHV.

7.6.2 *Immunophenotype Analysis of CLL Patient Samples*

Patient sample mononuclear cells that had undergone Ficoll gradient isolation were immunophenotyped to standard clinical specifications by the OHSU Histopathology Shared Resource laboratory. The following antibodies were used: CD3-FITC (#349201; BD Biosciences, Franklin Lakes, NJ), CD5-PC-Cy7 (#348790; BD Biosciences), CD14-APC-H7 (#643077; BD Biosciences), CD19-V450 (#644492; BD Biosciences), CD33-PerCP-Cy-5.5 (#341640; BD Biosciences), CD45-Pacific-Orange (#MHCD4530; Invitrogen, Carlsbad, CA), CD64-PE (#558592; BD Biosciences), and CSF1R-APC (#347306; BioLegend, San Diego, CA). Surface marker analysis was performed on a BD FACSCanto II flow cytometer and the data were analyzed using FlowJo (FlowJo, LLC, Ashland, OR).

7.6.3 *Depletion of CD14+ Cells from Primary Patient Specimens*

Primary patient mononuclear cells were depleted of CD14-expressing cells using MACS MicroBead technology (Miltenyi Biotec, Bergisch Gladbach, Germany). CD14-expressing cells were labeled with magnetic anti-CD14 MicroBeads (#130-050-201; Miltenyi Biotec), resuspended in MACS buffer (phosphate-buffered saline pH 7.2, 0.5% bovine serum albumin, and 2 mM EDTA)

per protocol, and separated with MACS MS columns (#130-042-201; Miltenyi Biotec). Cell viability of CD14+ depleted and non-depleted mononuclear cells was measured using the Guava easyCyte cell counter (Merck Millipore).

Both CD14+ depleted and non-depleted mononuclear cells from the same specimen were plated in R20 cell culture media with or without a concentration gradient of GW-2580 or ARRY-382. Relative numbers of viable cells were measured at 0, 24, and 72 hours after plating using a tetrazolium-based colorimetric assay.

7.6.4 *Isolating Nurse-Like Cells (NLCs) from Primary Patient Specimens*

Long-term NLC culturing experiments were conducted based on established protocols.¹⁶⁷ For each patient specimen, primary patient mononuclear cells were isolated and pipetted into 6 wells of a 24-well plates (1ml at 1.5×10^7 cells/ml in R20 media). Three wells were exposed to inhibitors immediately after plating (1 μ M GW-2580, 1 μ M ARRY-382, and untreated). The cells were incubated for 14 days at 37°C in 5% CO₂, after which the non-adherent cells were removed from all wells by vigorous pipetting and cell viability for each well was calculated using the Guava easyCyte cell counter (Merck Millipore).

For the three pre-treated wells, the remaining adherent NLCs were washed with RPMI media and exposed to 500 μ l 5mM EDTA in PBS for 30 minutes, followed by 100 μ l trypsin for 10 minutes. The cells were spun down, resuspended in R20 media, and counted using a hemocytometer. For the remaining three wells, the non-adherent cells were combined, spun down and resuspended in fresh R20 media. They were pipetted into six wells, three into the original wells containing the

adherent NLCs and three into fresh wells. Wells from each group were either exposed to 1 μ M GW-2580, 1 μ M ARRY-382, or untreated, and incubated for 72 hours at 37°C in 5% CO₂, after which the relative number of viable cells was determined using a tetrazolium-based colorimetric assay.

7.6.5 *Synergy Calculations between CSF1R Inhibitors and Ibrutinib/Idelalisib*

CLL primary patient specimens were exposed to GW-2580/ARRY-382 and ibrutinib/idelalisib, either to each inhibitor alone and in combination with one another in equimolar concentrations. The patient sample cells were incubated for 72 hours and assessed for viability using a colorimetric assay. We used CalcuSyn (Biosoft, Cambridge, Great Britain) to calculate the combination index,¹⁹⁶ which measures the degree of synergy for each combination, and binned each value according to established categories of synergy and antagonism.¹⁸¹ The hierarchical clustering of specimens was performed using the GenePattern platform.¹⁹⁷

7.7 Author Contributions

Conception and Design, B.J.D., J.W.T., S.E.S., and M.M.L.; Development and Methodology, D.K.E.V, D.T.S., A.R., J.W.T., S.E.S., and M.M.L.; Acquisition of data: D.T.S. and H.H.; Analysis and Interpretation of Data, D.K.E.V, C.A.E., A.V.D, and S.K.M.; Resources, A.V.D., P.L., D.C., B.J.D., J.W.T., S.E.S., and M.M.L.; Writing, review, and/or revision of manuscript: D.K.E.V, D.T.S., H.H., C.A.E., A.R., A.A., S.Q.L., A.V.D., P.L., D.C., S.K.M., B.J.D., J.W.T., S.E.S., and

M.M.L.; Study supervision, B.J.D., J.W.T., S.E.S., and M.M.L.; Administrative, technical, or material support: B.J.D., J.W.T., S.E.S., and M.M.L.

7.8 Acknowledgements

Special thanks to the OHSU Pathology Flow Cytometry Lab, especially Randy Eskelin, Haibo Li and Doug Higgins; and to Taylor Rowland and Cody Paiva for conducting the IGHV sequencing. This material is based upon work supported by the National Science Foundation Graduate Research Fellowship Program. Any opinions, findings, and conclusions or recommendations expressed in this material are those of the author(s) and do not necessarily reflect the views of the National Science Foundation.

7.9 Funding

This work was supported in part by The Leukemia & Lymphoma Society. S.E.S. and M.M.L. are supported by SWOG/Hope Foundation. J.W.T. is supported by the V Foundation for Cancer Research, the Gabrielle's Angel Foundation for Cancer Research, and the National Cancer Institute (5R00CA151457-04; 1R01CA183947-01). D.K.E.V is supported by the National Science Foundation Graduate Research Fellowship Program under Grant No. DGE-1448072. A.V.D is supported by the Lymphoma Research Foundation.

7.10 Conflict of Interest

J.W.T. receives research support from Agios Pharmaceuticals, Array Biopharma, Aptose Biosciences, AstraZeneca, Constellation Pharmaceuticals, Genentech, Incyte, Janssen Research & Development, Seattle Genetics, and Takeda Pharmaceuticals, and is a consultant for Leap Oncology. **S.E.S.** receives research support from Bristol-Myers Squibb, Genentech, Janssen, Gilead, and Acerta and has received an honorarium from Gilead. AA receives research funding from CTI BioPharma. PL and DC are employed at Array Biopharma. **A.V.D.:** Millenium Pharmaceuticals: Research Funding; Gilead Sciences Inc.: Research Funding. **B.J.D.:** Fred Hutchinson Cancer Research Center: Research Funding; Bristol-Myers Squibb: Research Funding; Henry Stewart Talks: Patents & Royalties; Millipore: Patents & Royalties; Sage Bionetworks: Research Funding; MolecularMD: Consultancy, Equity Ownership, Membership on an entity's Board of Directors or advisory committees; Gilead Sciences: Consultancy, Membership on an entity's Board of Directors or advisory committees; Cylene Pharmaceuticals: Consultancy, Equity Ownership, Membership on an entity's Board of Directors or advisory committees; AstraZeneca: Consultancy; Novartis Pharmaceuticals: Research Funding; Blueprint Medicines: Consultancy, Equity Ownership, Membership on an entity's Board of Directors or advisory committees; Oregon Health & Science University: Patents & Royalties; CTI Biosciences: Consultancy, Equity Ownership, Membership on an entity's Board of Directors or advisory committees; Leukemia & Lymphoma Society: Membership on an entity's Board of Directors or advisory committees, Research Funding; Oncotide Pharmaceuticals: Research Funding;

Roche TCRC, Inc.: Consultancy, Membership on an entity's Board of Directors or advisory committees; McGraw Hill: Patents & Royalties; ARIAD: Research Funding; Aptose Therapeutics, Inc (formerly Lorus): Consultancy, Equity Ownership, Membership on an entity's Board of Directors or advisory committees. All other researchers have no relevant conflicts to disclose.

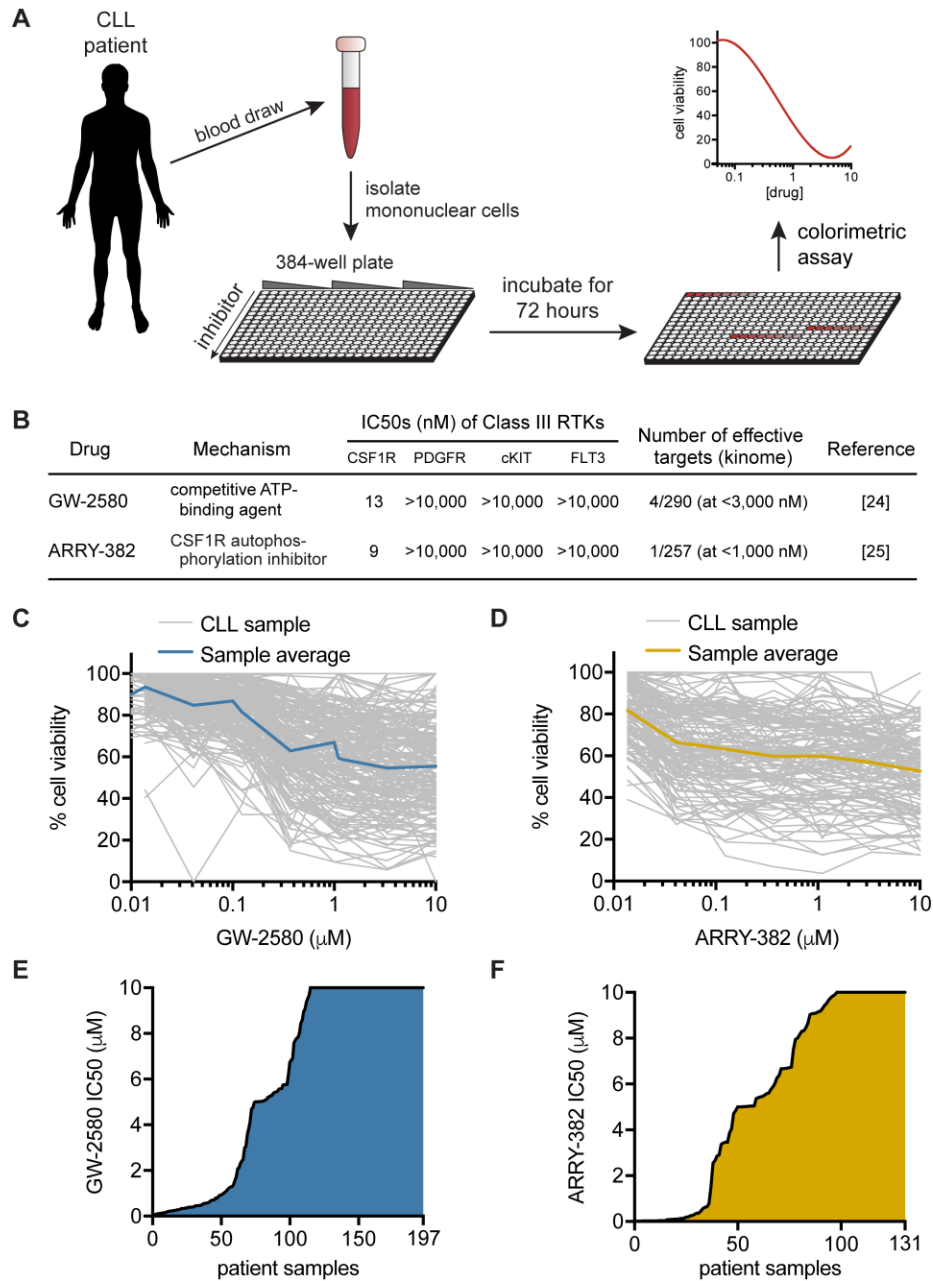


Figure 7.1. *Ex vivo* inhibitor screening reveals CSF1R sensitivity in CLL patient specimens.

(A) Mononuclear cells isolated from peripheral blood or bone marrow of CLL patients were added to 384-well plates containing dose-escalating concentrations of small-molecule inhibitors. Following incubation for 72 hours, the relative number of

remaining viable mononuclear cells was evaluated by subjecting cells to a colorimetric cell viability assay.

(B) GW-2580 and ARRY-382 are highly specific small-molecule inhibitors of CSF1R (and not other class III receptor tyrosine kinases). Data from [24] Davis et al.¹⁹⁸ and [25] Wright et al.¹⁹⁹

(C-D) CLL primary patient specimens were exposed (C) GW-2580 and (D) ARRY-382, as described in (A), and dose-response curves for each specimen were included along with an average dose-response curve for all specimens.

(E-F) Waterfall plot of the IC₅₀ values for each patient specimen after exposure to (E) GW-2580 and (F) ARRY-382. The IC₅₀ was calculated from the dose-response curve using a cubic logarithmic regression, and each specimen was positioned in order of increasing IC₅₀.

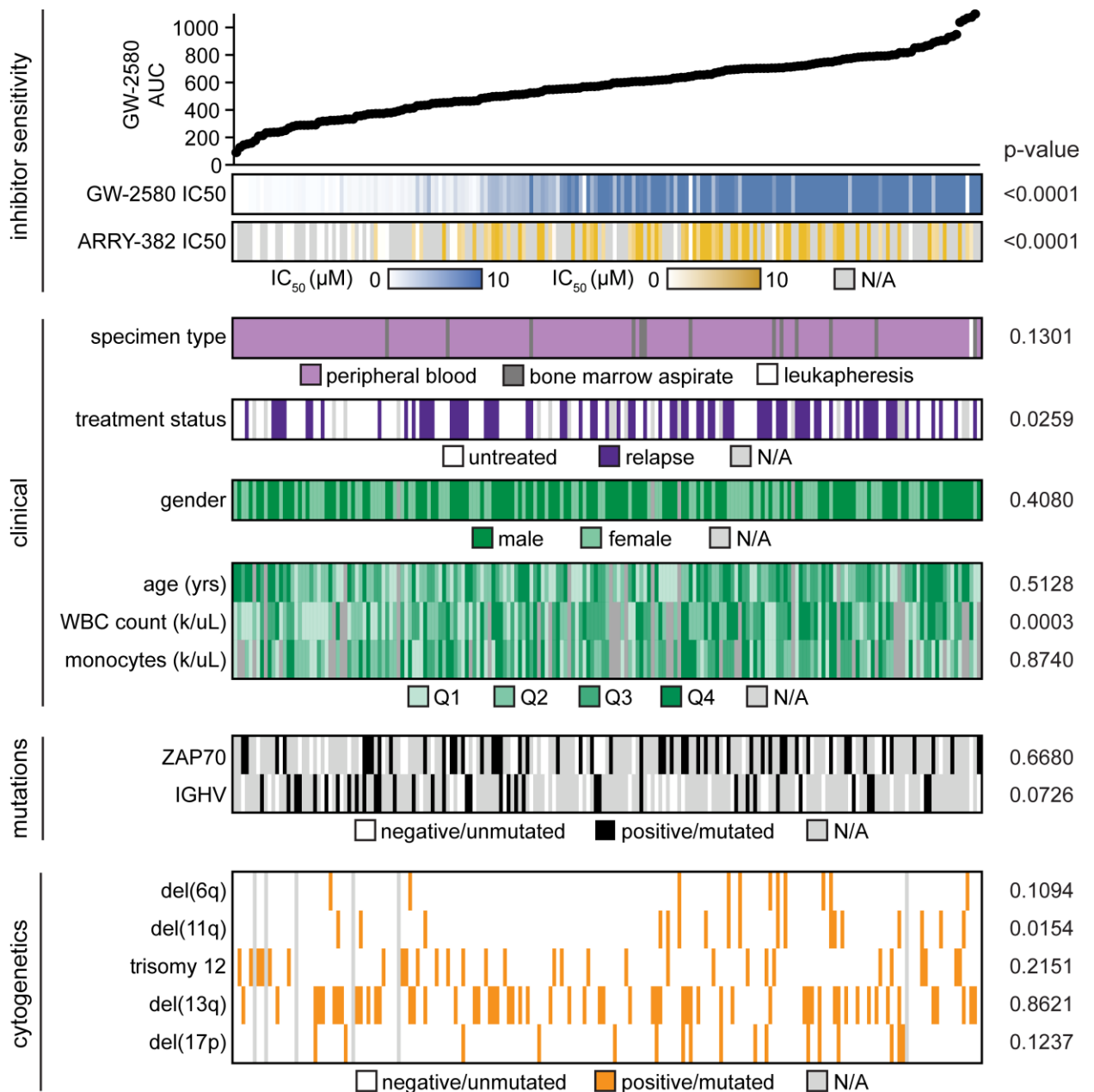


Figure 7.2. No genetic or clinical characteristic readily co-segregate with sensitivity to CSF1R inhibition in CLL patient samples.

The 197 CLL patient specimens that were evaluated by *ex vivo* inhibitor screening in Figure 7.1 were ordered by increasing AUC for GW-2580, which was calculated using a cubic logarithmic regression model. Various demographic, clinical, and genetic/cytogenetic characteristics of each patient were determined (the continuous

variables are broken into quartiles) and each characteristic was evaluated for statistical significance (see Figure 7.7, Table 7.1, and additional large supplemental table from published manuscript).

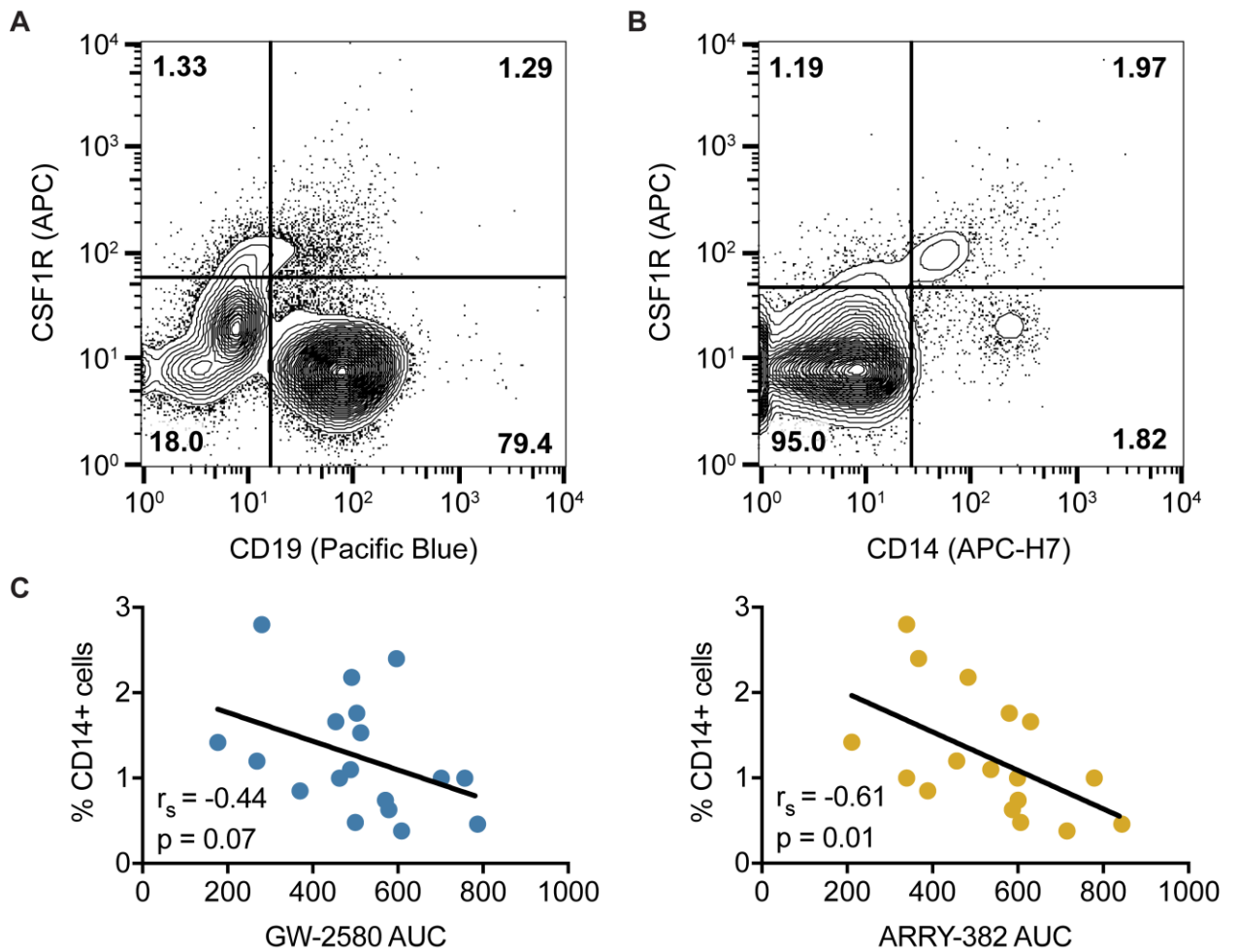


Figure 7.3. CSF1R is not found on CD19+ CLL cells but instead expressed on a CD14+ myeloid subpopulation.

(A-B) Mononuclear cells isolated from CLL patients were subjected to flow cytometry using antibodies specific for CSF1R and CD19, with CSF1R expression (A) not observed in CD19+ lymphocytes (CLL cells) but (B) observed in a subpopulation of CD14+ cells.

(C) Sensitivity to CSF1R inhibitors, as determined in Figure 7.1 and Figure 7.2, was correlated with percentage of CD14-positive cells as determined in Figure 7.3B.

Statistics were calculated using Spearman's rank correlation.

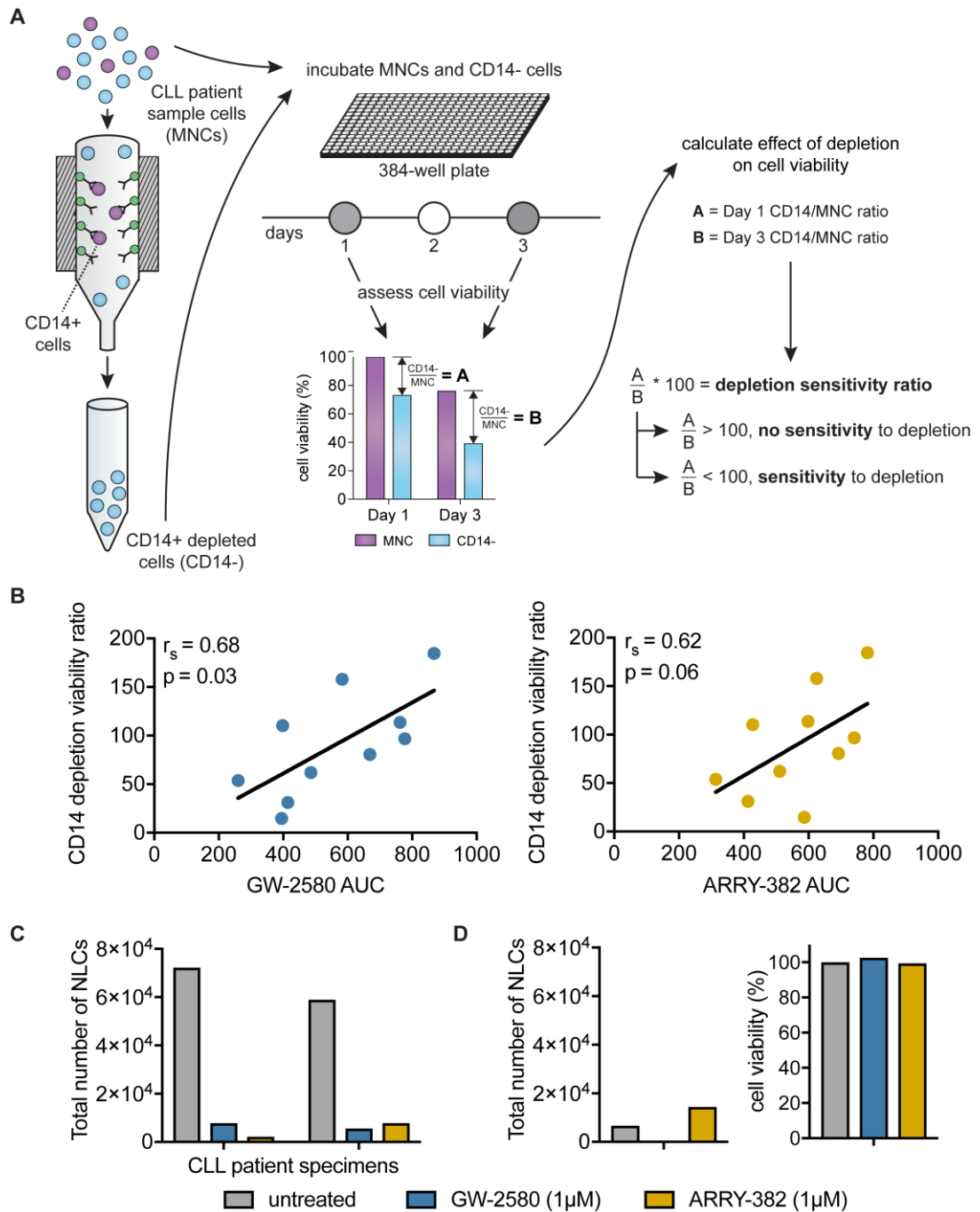


Figure 7.4. Sensitivity of CLL cells to CD14+ depletion correlates with sensitivity to CSF1R inhibitors.

(A) CD14+ cells were depleted from patient specimens using magnetic cell-separation columns, and incubated in 384-well plates for 72 hours. The CD14+

depletion sensitivity ratio was calculated by comparing the relative remaining numbers of viable cells in depleted versus non-depleted conditions using a colorimetric assay. The ratio of cell viability readings in depleted to non-depleted cells at 72 hours was normalized to the same ratio at the start of the experiment to control for variance in cell input.

(B) The CD14⁺ depletion sensitivity ratio was generated for a panel of primary CLL patient samples as described in (A). This ratio was compared to GW-2580 and ARRY-382 AUCs. Statistics determined by Spearman's rank correlation.

(C) Primary CLL patient samples cells were exposed to CSF1R inhibitors and were subjected to long-term culture conditions to produce nurse-like cells (NLCs). The number of NLCs was quantified using a hemocytometer.

(D) For one primary patient sample that did not produce NLCs, the addition of CSF1R inhibitors did not have a significant impact on cell viability compared to untreated control.

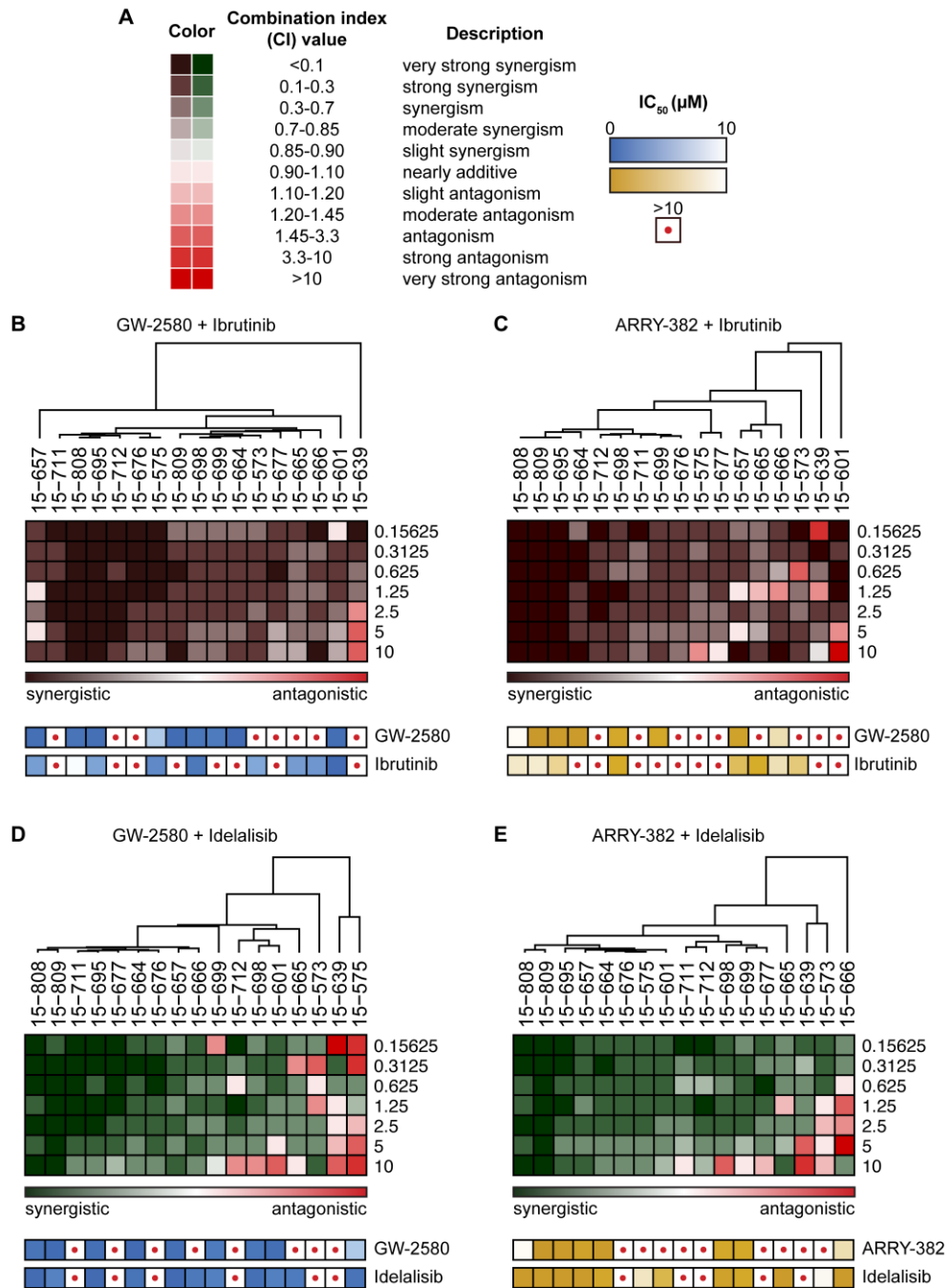


Figure 7.5. Synergy between ibrutinib or idelalisib and CSF1R inhibitors in majority of CLL patient specimens.

(A) Mononuclear cells from CLL patient specimens were cultured with dose gradients of single-agent CSF1R inhibitors, ibrutinib, or idelalisib, as well as equimolar ratio dose gradients of CSF1R inhibitors combined with ibrutinib or

idelalisib. After a 72-hour incubation, relative numbers of remaining viable cells were assessed using a colorimetric cell viability assay, and synergy calculations were generated from the dose-response curves.

(B-E) A hierarchically clustered heat map was generated showing the combination indices at increasing concentrations of inhibitors (rows) in CLL patient samples (columns) for (B) GW-2580 with ibrutinib; (C) ARRY-382 with ibrutinib; (D) GW-2580 with idelalisib; and (E) ARRY-382 with idelalisib. The single-agent sensitivity (IC₅₀) to each drug used in the combination is included (depicted as a heat map) below the corresponding patient sample.

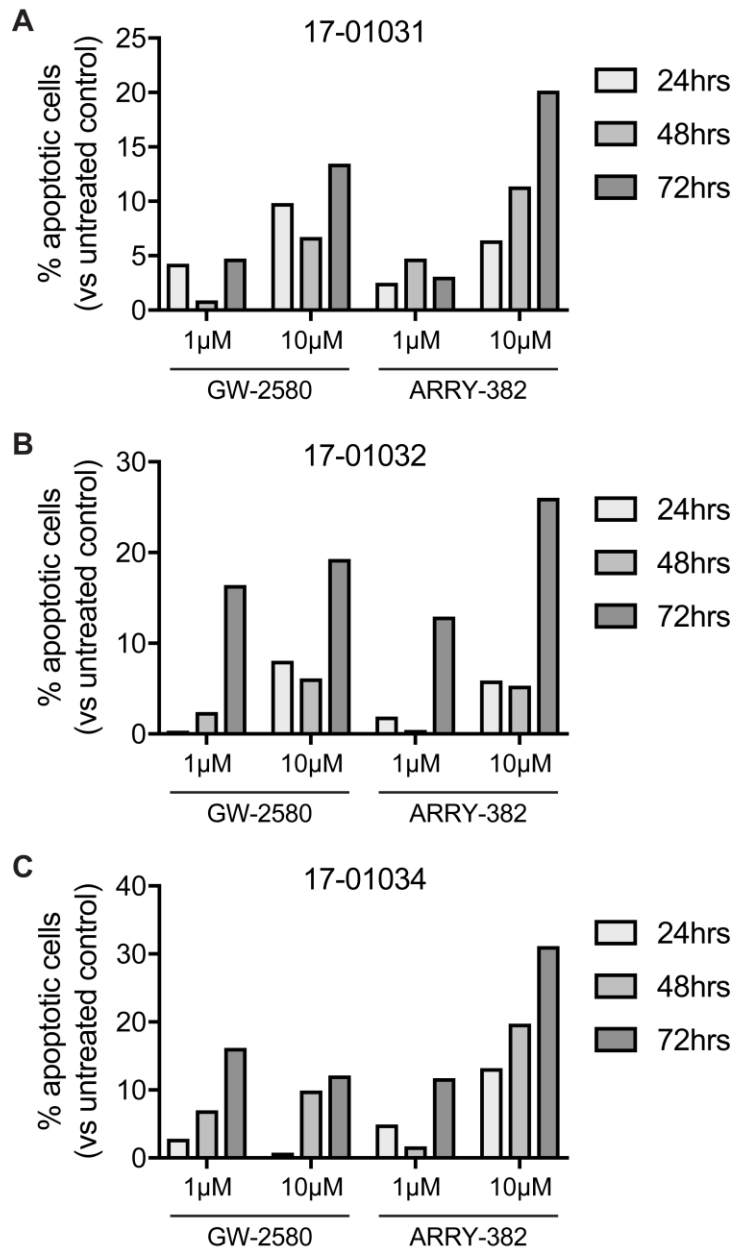


Figure 7.6. CSF1R inhibitor exposure induces apoptosis in CLL primary patient samples.

(A-C) Percent apoptosis after exposure to GW-2580 and ARRY-382 at 24, 48, and 72 hrs in three CLL primary patient samples: (A) 17-01031, (B) 17-01032, and (C) 17-01034. The percentage of apoptotic cells for each patient sample was normalized

to untreated control cells to account for sample-specific variations in cell viability over time.

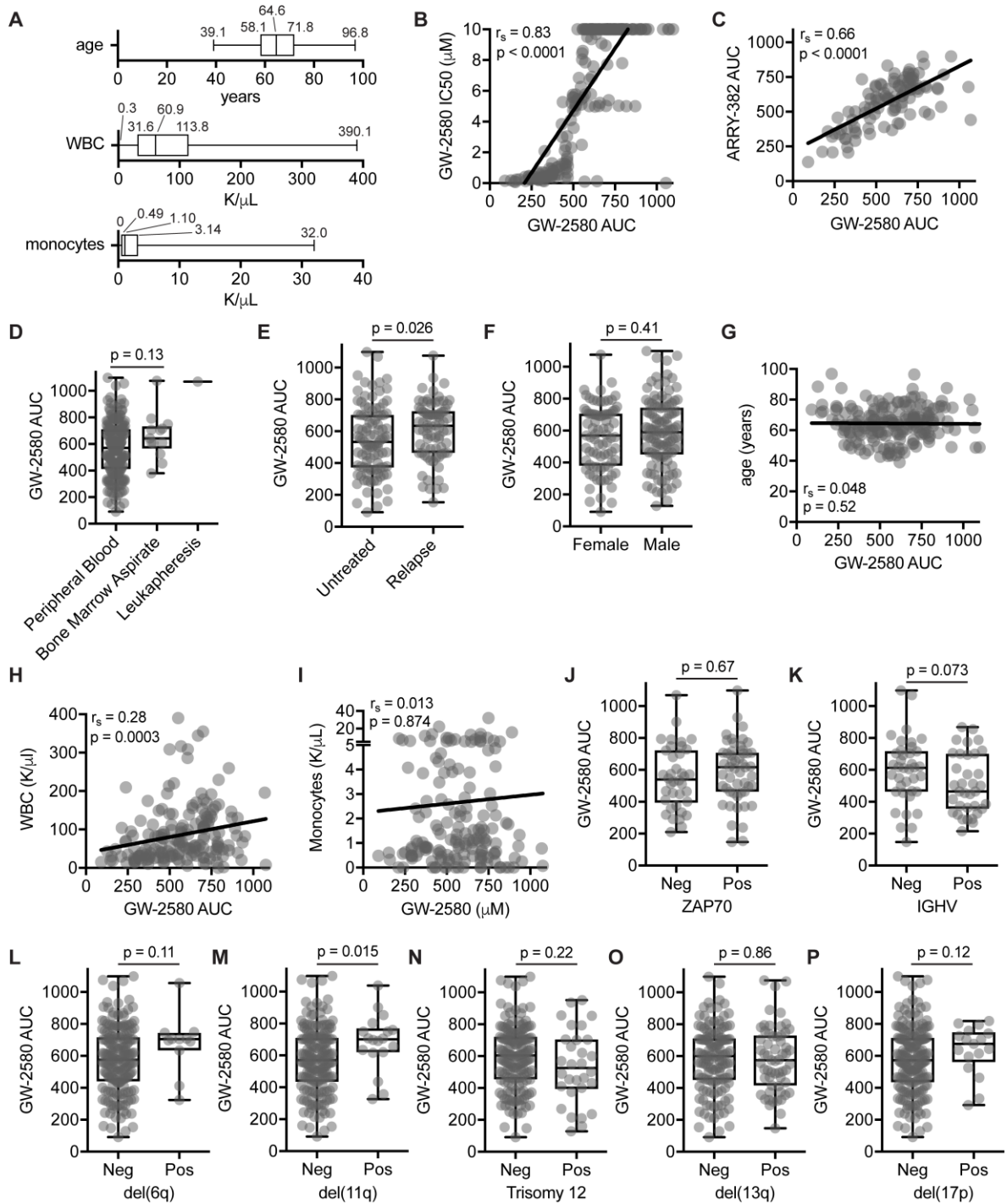


Figure 7.7. Box-and-whisker plots for continuous variables in CLL patient sample comparisons and plots of statistically significant characteristics.

(A) Box-and-whisker plots of the clinical characteristics measured by continuous variables that are displayed in Figure 7.2.

(B-C) Correlation between GW-2580 area under the curve (AUC) in CLL patient samples and (B) GW-2580 IC50 and (C) ARRY-382 AUC.

(D-P) Association or correlation between GW-2580 AUC and (D) specimen type; (E) treatment status; (F) patient gender; (G) age; (H) white blood cell count (WBC); (I) monocyte count; and the presence/absence of (J) ZAP70 overexpression, (K) IGHV mutations, (L) del(6q), (M) del(11q), (N) trisomy 12, (O) del(13q), and (P) del(17p). Statistics for (D-F; J-P) was evaluated using Mann-Whitney U test; statistics for (G-I) were evaluated using Spearman's rank correlation.

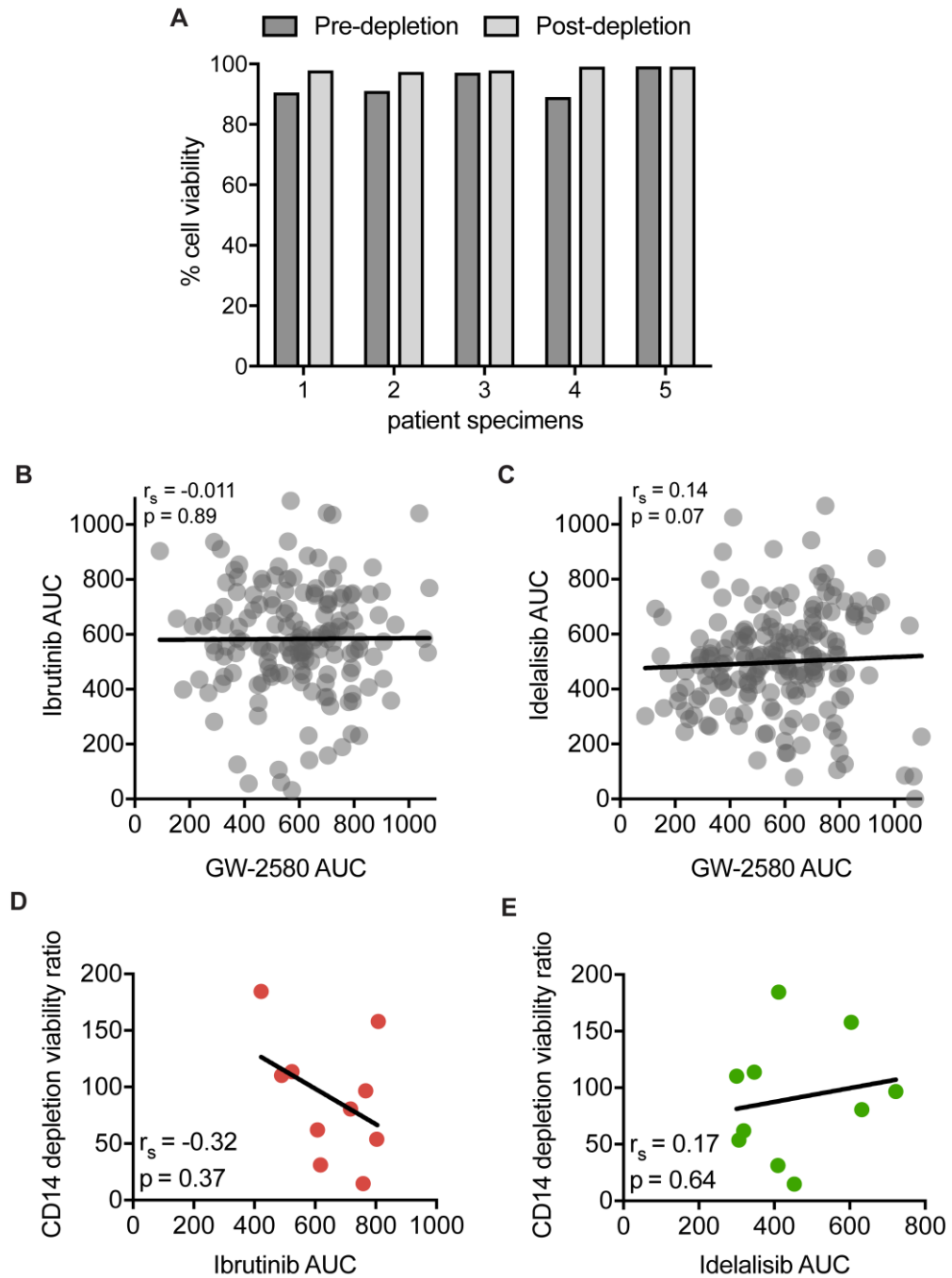


Figure 7.8. GW-2580 sensitivity and viability after CD14+ depletion is not correlated with sensitivity to ibrutinib and idelalisib.

(A) No significant difference in overall cell viability between CLL patient specimens before and after depletion protocol, as measured by Guava easyCyte cell counter.

(B-C) Correlation between GW-2580 area under the curve (AUC) in CLL patient samples and the AUC values for (A) ibrutinib and (B) idelalisib.

(D-E) CD14+ depletion viability ratio compared to area under the curve (AUC) for (A) ibrutinib and (B) idelalisib. Statistics for (B-E) determined by Spearman's rank correlation.

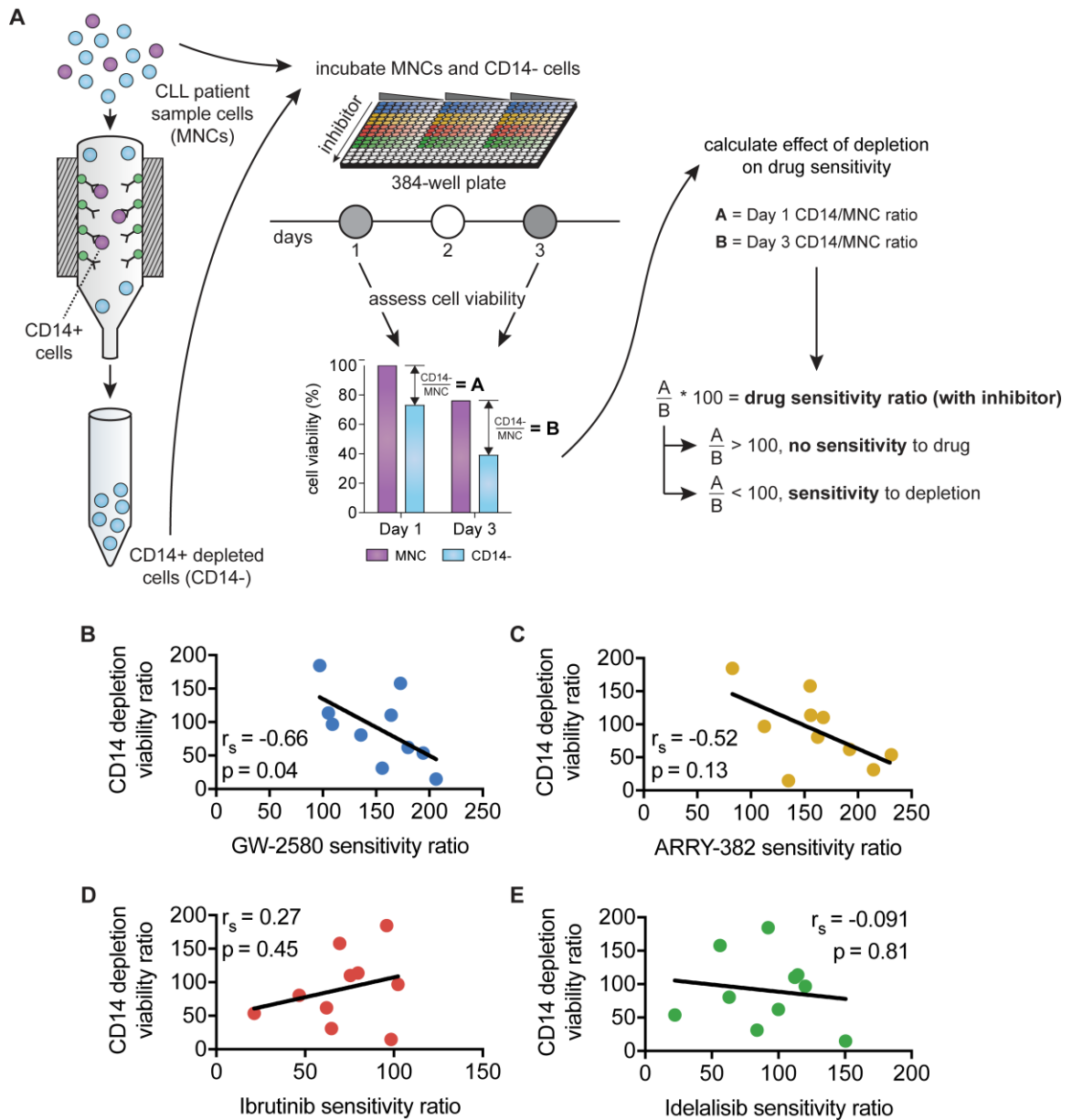


Figure 7.9. CD14+ depletion significantly impact sensitivity to CSF1R inhibitors but does not impact sensitivity to ibrutinib and idelalisib.

(A) CD14+ depleted and whole mononuclear cells were plated with dose-escalating concentrations of inhibitors and incubated for 72 hours. The drug sensitivity ratio

was calculated by comparing sensitivity to inhibitors of CD14+ depleted versus whole mononuclear cells.

(B-E) There is a correlation or trend between the drug sensitivity ratio and the cell viability ratio for CD14+ cell depletion after exposure to CSF1R inhibitors—(B) GW-2580 and (C) ARRY-382—but not to (D) ibrutinib and (E) idelalisib. Statistics determined by Spearman's rank correlation.

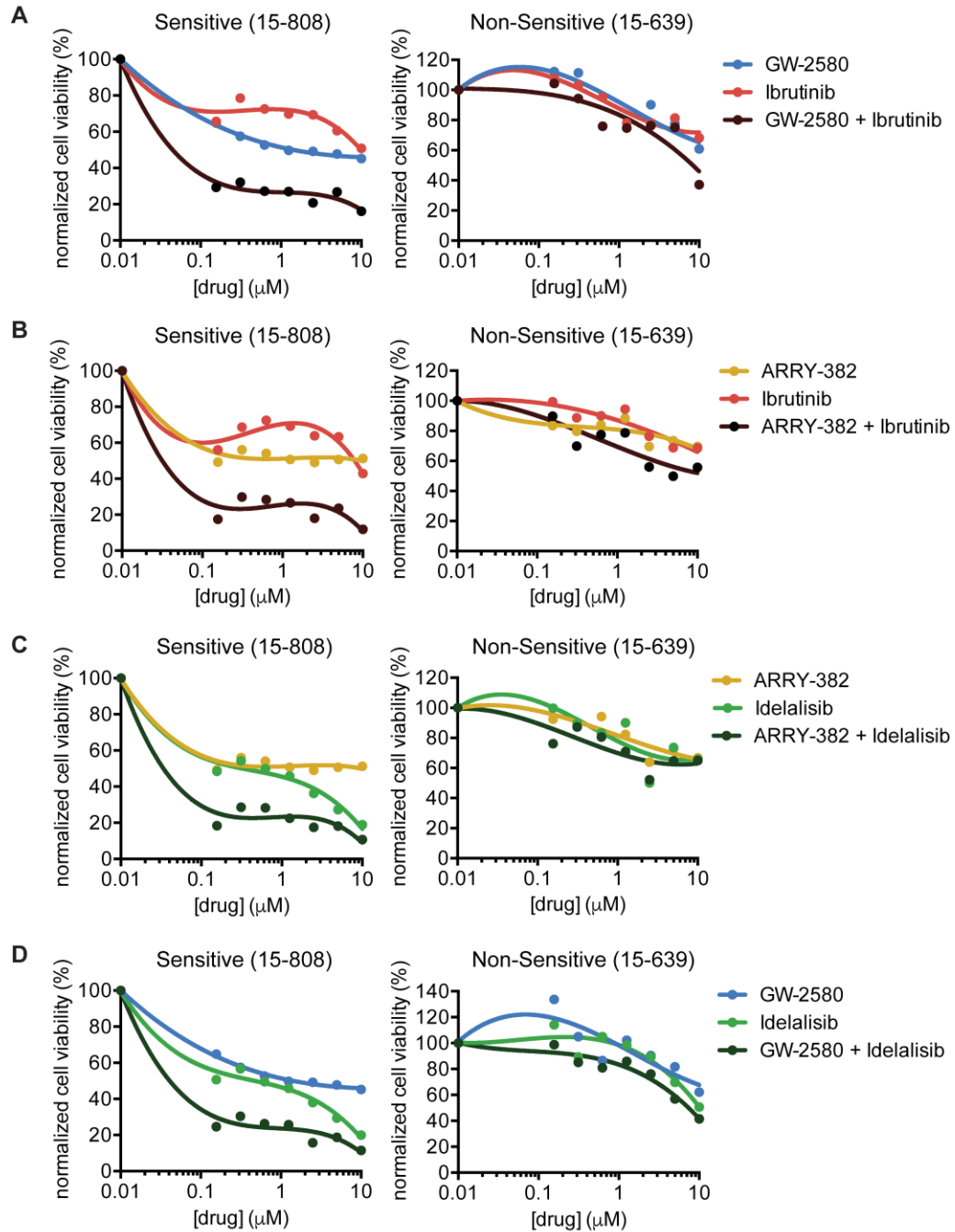


Figure 7.10. Representative synergistic and antagonistic dose-response curves from patient specimens exposed to the combination of CSF1R inhibitor and ibrutinib/idelalisib.

Dose-response curves for each single agent inhibitor and combination for (A) GW-2580 and ibrutinib, (B) ARRY-382 and ibrutinib, (C) ARRY-382 and idelalisib, and

(D) GW-2580 and idelalisib in which the combination was synergistic (Specimen 15-808) and non-synergistic (Specimen 15-639).

Table 7.1. Statistical analysis of clinical and genetic/cytogenetic characteristics of CLL patient sample cohort evaluated for sensitivity to CSF1R inhibitors.

Category	Samples with available data (%)	Statistical test	Correlation coefficient	P-value
Inhibitor sensitivity				
GW-2580 IC50	197 (100)	Spearman's rank correlation	0.8291	<0.0001
ARRY-382 IC50	102 (52)	Spearman's rank correlation	0.5790	<0.0001
Clinical				
treatment status	177 (90)	Mann-Whitney test	--	0.0259
gender	193 (98)	Mann-Whitney test	--	0.4080
age	185 (94)	Spearman's rank correlation	0.0484	0.5128
WBC (K/ μ L)	171 (87)	Spearman's rank correlation	0.2761	0.0003
monocytes (K/ μ l)	159 (81)	Spearman's rank correlation	0.0127	0.8740
Mutations				
IGVH	73 (37)	Mann-Whitney test	--	0.0726
ZAP70	89 (45)	Mann-Whitney test	--	0.6680
Cytogenetics				
del(6q)	191 (97)	Mann-Whitney test	--	0.1094
del(11q)	191 (97)	Mann-Whitney test	--	0.0154
trisomy 12	191 (97)	Mann-Whitney test	--	0.2151
del(13q)	191 (97)	Mann-Whitney test	--	0.8621
del(17p)	191 (97)	Mann-Whitney test	--	0.1237

8 CSF1R inhibitors exhibit anti-tumor activity in acute myeloid leukemia by blocking paracrine signals from support cells

David K. Edwards V, Kevin Watanabe-Smith, Angela Rofelty, Alisa Damnernsawad, Ted Laderas, Adam Lamble, Evan F. Lind, Andy Kaempf, Motomi Mori, Mara Rosenberg, Amanda d'Almeida, Nicola Long, Anupriya Agarwal, David Tyler Sweeney, Patrice Lee, David Chantry, Marc Loriaux, Shannon K. McWeeney, and Jeffrey W. Tyner

Presented in abstract form at the 57th annual meeting of the American Society of Hematology, Orlando, FL, December 7, 2015.²⁰⁰

A version of this chapter was submitted to *Blood* in March 2018.

8.1 Contribution to Project

8.1.1 *Conception or design of the work*

The CSF1R-in-AML project was my primary project throughout graduate school. It was an outgrowth of the RAPID (RNAi-assisted protein target identification) functional screen, a technique developed by my mentor, Jeffrey Tyner (JWT). The RAPID screen exposes primary AML patient sample cells to siRNAs against the tyrosine kinome (and NRAS/KRAS) to identify which kinases are critical to cell viability. The lab had already screened hundreds of patient samples using this technique and observed that the siRNA that significantly decreased cell viability in the largest number of samples was siCSF1R.

Over the years, there had been attempts in our group to understand the role of CSF1R in acute myeloid leukemia. However, they were unsuccessful in identifying the mechanism behind CSF1R sensitivity or predicting which patients would respond to CSF1R small-molecule inhibitors. My investigations into answering these two questions became the basis for my dissertation research.

As with many dissertation projects, a significant amount of work (CD14+ depletion followed by CSF1R inhibitor sensitivity in primary patient samples, CSF1R activation and regulation in AML cell lines) is not included here. Most of that work was conducted by me, although some of the earlier work was done in conjunction with Angela Rofelty (AR), a former technician in our lab.

8.1.2 *Data collection, analysis, and interpretation*

Figure 8.1 *Ex vivo* AML patient sample screen reveals that knockdown/inhibition of CSF1R reduces leukemia cell survival in >20% of samples.

The patient samples used in this analysis have been screened for inhibitor and siRNA sensitivity over the course of many years by a team of dedicated technicians, so I did not collect this data myself. I developed a method to quality-filter the data from the RAPID functional screen, which I did in partnership with Kevin Watanabe-Smith (KWS), a postdoctoral fellow in our group. I decided how to measure the correlation between CSF1R inhibitor sensitivity and siCSF1R impact and calculated it with KWS. The drug sensitivity data was determined using probit regression by Andy Kaempf (AK), a biostatistician in Tomi Mori's group. I designed the figure layout and graphed the results, with some assistance from KWS, and built the supplemental figure.

Figure 8.2. Resistance to CSF1R inhibitor is associated with adverse prognostic risk gene mutations and cytogenetic abnormalities. A significant amount of the patient sample information, including demographics, treatment history, and diagnostic test results, is stored in a massive online database. When I arrived, the clinical and genetic annotations for the patients in the database had received sporadic attention from JWT and others. I worked to comprehensively update the database for months, receiving some assistance from Matt Siegel, a clinical fellow who was doing a research rotation in our lab. I entered in the information from hundreds of patient sample records into a database, creating a standardized hierarchy of assigning specific diagnosis. In addition, I designed and built an automated decision tree to compute prognostic risk based on established guidelines. I selected which clinical

and genetic characteristics to compare and, working with KWS, extracted that information from the database. I graphed and visualized that information myself (both the primary heatmap and the individual graphs included in the supplemental material) and conducted all statistical tests. Additionally, for the survival data, I worked with Mara Rosenberg (MR), a medical student with a computational biology background. She exported the data for me based on my instructions, and I graphed and visualized it (including the supplemental data) with her feedback.

Figure 8.3. CSF1R is expressed not on the bulk leukemia population in primary AML patient samples but on a small subpopulation of **supportive cells**. The CyTOF data was generated by Evan Lind (EL), an assistant professor and close collaborator (and member of my dissertation advisory committee), and analyzed by Ted Laderas (TL), an assistant professor. Working with both of them, I provided guidelines for how to represent and visualize the data, and both TL and I summarized and graphed the data included in the figure. Although the CSF1R^{hi} cell clustering was performed by TL, I performed the downstream analysis, including its significance in drug sensitivity and distribution across patient samples. The flow cytometry data was generated by AR and me. The samples were evaluated by Mandy Gilchrist (MG) at OHSU's flow cytometry core. The gating, data analysis, and visualization was performed by me, with some feedback from Marc Loriaux (ML), a hematopathologist.

Figure 8.4. HGF stimulates growth in CSF1R inhibitor sensitive samples and its secretion is regulated by CSF1R activation. The cytokine/growth factor data was the result of a collaboration between me and Anupriya Agarwal (AA), an assistant

professor. (I was second author on the original manuscript.) The raw data was combined with the GW-2580 sensitivity data and KWS and I analyzed and graphed the data. The conditioned media experiments were performed by me, as was the Luminex assay (with assistance from Bri Garcia at OHSU's flow cytometry core) and all of the downstream data analysis and visualization. The experiments evaluating the CSF1 levels in the plasma were performed by AR and me. In addition, I modified an existing protocol for isolating stromal cells from AML patient samples and, working with AR, performed this isolation on dozens of samples. AR and I performed the CSF1 level experiments of stromal cell conditioned media. The data was analyzed and graphed by me.

Figure 8.5. Sensitivity to CSF1R inhibitors correlates with MET inhibitor sensitivity and is eliminated after external HGF stimulation. AK performed the probit regression analysis on the MET inhibitors and I analyzed the data.

8.1.3 *Article drafting/submission/revision*

I drafted the entire manuscript myself and, after incorporating revisions from JWT and other co-authors, submitted it to *Blood* in March 2018.

8.2 Key Points

- CSF1R inhibition reduces cell viability in more than 20% of AML patient samples and is expressed on a subpopulation of supportive cells.
- CSF1R activation stimulates paracrine cytokine secretion (e.g. HGF), suggesting that CSF1R is novel target of the AML microenvironment.

8.3 Abstract

To identify new therapeutic targets in AML, we performed small-molecule and siRNA screens of primary AML patient samples. In 23% of samples, we found sensitivity to inhibition of CSF1R, a receptor tyrosine kinase responsible for survival, proliferation, and differentiation of myeloid-lineage cells. Sensitivity to the CSF1R inhibitor GW-2580 was found preferentially in *de novo* and favorable risk patients, and resistance to GW-2580 was associated with reduced overall survival. Using flow cytometry, we discovered that CSF1R is not expressed on the majority of leukemic blasts but instead on a subpopulation of supportive cells. Comparison of CSF1R-expressing cells in AML versus healthy donors by mass cytometry (CyTOF) revealed the expression of unique cell-surface markers. The quantity of CSF1R-expressing cells correlated with GW-2580 sensitivity.

Exposure of primary AML patient samples to a panel of recombinant cytokines revealed that CSF1R inhibitor sensitivity correlated with a growth response to CSF1R ligand, CSF1, and other cytokines, including an alternative growth factor, HGF. The addition of CSF1 increased the secretion of HGF and other cytokines in conditioned media from AML patient samples, while adding GW-2580 reduced their

secretion. In untreated cells, HGF levels correlated significantly with GW-2580 sensitivity. Finally, recombinant HGF and HS-5-conditioned media rescued cell viability after GW-2580 treatment in AML patient samples. Our results suggest that CSF1R-expressing cells support the bulk leukemia population through the secretion of HGF and other cytokines. This study identifies CSF1R as a novel therapeutic target of AML and provide a mechanism of paracrine cytokine/growth factor signaling in this disease.

8.4 Introduction

Acute myeloid leukemia (AML) is the deadliest hematological malignancy, with 10,670 estimated new deaths from the disease in the United States in 2018.¹ One of the factors complicating AML treatment is its genetic heterogeneity, with hundreds of drivers collectively observed across AML patient tumors and an average of ~5-15 somatic mutations observed within each patient tumor.^{24,25} The use of genetically targeted therapies to treat AML has produced some clinical responses, but the development of disease resistance and relapse remains a continuous problem, in part because of the presence of multiple genetic subclones of leukemia cells in each patient.^{41,201}

To overcome the inherent genetic complexity of AML, researchers have investigated methods of targeting the supportive leukemia microenvironment.²⁰² Indeed, the development of resistance in AML is driven by multiple factors, including external signals from the bone marrow microenvironment.²⁰³ Leukemia cells disrupt normal hematopoietic stem cell growth,²⁰⁴ and changes in the

microenvironment are sufficient to induce leukemia or myelodysplastic syndromes.²⁰⁵ The modification and reprogramming of multiple cell types in the bone marrow niche have been shown to enhance AML tumor cell proliferation and survival, including mesenchymal stromal cells (MSCs),²⁰⁶⁻²⁰⁸ osteoblasts,^{209,210} and T cells.²¹¹⁻²¹³

In solid tumors, a key contributor to the microenvironment is supportive monocytes/macrophages, also known as tumor-associated macrophages (TAMs).²¹⁴ TAMs express a variety of proteins, including colony stimulating factor 1 receptor (CSF1R), which signals downstream through PI3K/AKT and MEK/ERK and promotes cell proliferation and differentiation.²¹⁵ There have been significant efforts to target and eliminate TAMs in solid tumors, and many ongoing clinical trials exist using CSF1R small-molecule inhibitors and monoclonal antibodies.¹²² More recently, the same phenomenon has been shown in chronic lymphocytic leukemia (CLL), where targeting CSF1R-expressing nurse-like cells (NLCs) has shown efficacy in mouse models^{157,160} and *ex vivo* patient samples.²¹⁶ Recently, it was shown in mouse models that AML induces an increase in monocytes/macrophages in the bone marrow and spleen that supports a pro-tumorigenic microenvironment.²¹⁷ However, the biological significance of supportive monocyte/macrophages, including the possibility of targeting and eliminating these cells, has never before been demonstrated in humans.

Using functional screening of *ex vivo* primary AML patient samples, we report for the first time that CSF1R signaling is essential for the survival of AML samples. CSF1R sensitivity is not confined to a particular clinical or genetic subtype, although

it is less prevalent in patients with adverse risk features. Using mass cytometry (CyTOF) and conventional, fluorescence-based flow cytometry, we found that CSF1R surface expression is not found on the tumor cells themselves but instead confined to a small subpopulation of supportive monocyte/macrophage-like cells that show evidence of phenotypic reprogramming. Samples with CSF1R inhibitor sensitivity show increased response to CSF1 and HGF growth factor stimulation, and HGF secretion was directly modulated after stimulation or inhibition of CSF1R in sensitive samples. These data indicate that CSF1R is a novel therapeutic target in AML and provide evidence for paracrine signaling from CSF1R-expressing supportive cells, suggesting that CSF1R small-molecule inhibitors would be broadly effective in treating AML.

8.5 Methods

8.5.1 *Patient sample acquisition and functional screening*

Primary AML samples were obtained from patients by informed consent according to a protocol approved by the Oregon Health & Science University Institutional Review Board, and processed as described previously.²¹⁸ Briefly, peripheral blood, bone marrow, and leukapheresis samples were extracted from patients with AML. The mononuclear cells (MNCs) were isolated from whole blood by Ficoll density gradient and plated in media containing RPMI with 20% FBS, 1% penicillin-streptomycin, 2% glutamine, and 0.1% amphotericin B. MNCs underwent two functional screens, depending on available cell number. First, MNCs were exposed to dose-escalating concentration gradients of small-molecule inhibitors²¹⁹—

including GW-2580, ARRY-382, JNJ-28312141, crizotinib, foretinib, and SGX-523—and incubated for 72 hours at 37°C in 5% CO₂. Second, MNCs were electroporated with a library of 93 siRNAs collectively targeting the tyrosine kinome (plus NRAS/KRAS), as described previously,^{220,221} and incubated for 96 hours at 37°C in 5% CO₂. After incubation, the relative number of remaining viable mononuclear cells for each screen was measured using a tetrazolium-based colorimetric assay (CellTiter AQueous One Solution Cell Proliferation Assay; Promega, Madison, WI).

The half maximal inhibitory concentration (IC₅₀) and area under the curve (AUC) were determined for each sample using probit regression analysis (see Supplemental Methods). Within each patient sample, a “hit” for a specific siRNA was determined if its cell viability was at least 2 standard deviations less than the mean computed across all siRNAs tested ($z\text{-score} \leq -2$).^{11,12}

To evaluate apoptosis, MNCs were exposed to either GW-2580 or ARRY-382 at 10µM, and apoptosis was measured after 24, 48, and 72 hours by Annexin V staining (Guava Nexin Assay; Merck Millipore, Billerica, MA). The percentage of apoptotic cells from untreated control wells was subtracted from the drug-exposed wells to accommodate sample-specific variation in overall cell viability.

Most of these samples originated from the Beat AML program, a collaborative, multi-institutional project that evaluated a cohort of 672 tumor specimens collected from 562 patients. For more information about the selection of our patient sample cohort, see Supplemental Methods.

8.5.2 *Mass cytometry (CyTOF) and flow cytometry analysis of cell surface markers*

MNCs were isolated from primary AML patient samples and evaluated for a variety of cell surface markers using mass spectrometry-based flow cytometry, as described previously.²²² Briefly, 3×10^6 cells from primary AML bone marrow aspirates were stained with a custom-built panel of 16 metal-conjugated antibodies for cell surface markers (including a cell viability stain, a DNA intercalator for doublet removal, a core panel of 13 well-established phenotypic markers, and a variety of other markers of myeloid cells and their major subsets). The samples were run on a CyTOF Mass Cytometer (DVS Sciences, Markham, Ontario), and the resulting FCS files were processed and visualized. Automated gating was performed using the openCyto pipeline and comparison of the population percentages of expressed surface markers was performed using various Bioconductor packages.²²³⁻²²⁵

For conventional flow cytometry, MNCs were stained with Live/Dead Aqua (L34957; Thermo Fisher, Waltham, MA), CD45-PerCP (304025; BioLegend, San Diego, CA), CD34-PE-CF594 (562383; BD Biosciences, Franklin Lakes, NJ), and CSF1R-APC (347306; BioLegend), according to manufacturer's instructions. Surface marker analysis was performed on a BD FACSCanto II flow cytometer and the data were analyzed using FlowJo (FlowJo, LLC, Ashland, OR). Blast gating was performed under the direction of a hematopathologist.

8.5.3 *CSF1 expression in plasma and stromal cell conditioned media*

Blood plasma was isolated from peripheral blood samples and bone marrow aspirates and flash-frozen. Stromal cells were isolated from red blood cell (RBC) pellets from post-Ficoll primary AML patient samples. RBC pellets were incubated with ammonium-chloride-potassium (ACK) lysis buffer for 30 minutes and plated onto 15cm dishes in MEM-alpha with 20% FBS, 1% penicillin-streptomycin, 2% glutamine, and 0.1% amphotericin B. The plates were cultured for at least 2 weeks at 37°C in 5% CO₂, with media changed every 7 days to remove non-adherent cells. When the plate was ~70% confluent, conditioned media was collected and flash-frozen. The levels of CSF1 and IL34 were determined using the Human M-CSF and IL-34 Quantikine ELISA Kits (R&D Systems, Minneapolis, MN), respectively, according to manufacturer's instructions.

8.5.4 *Cytokine/growth factor analysis*

We analyzed data assessing cytokine growth response *ex vivo* in AML patient samples.²²⁶ Briefly, mononuclear cells isolated from primary AML patient samples were exposed to low, medium, or high doses of 94 cytokines, chemokines, and growth factors (see Carey et al²²⁶ for details). After 72 hours of incubation, cell viability was measured using a tetrazolium-based colorimetric assay (CellTiter AQueous One Solution Cell Proliferation Assay; Promega). For each cytokine, the growth response was compared to positive (HS-5-conditioned media and previously published combinations of IL-6, IL-11, FLT-3L, SCF, GM-CSF, G-CSF, and/or SCF^{227,228}) and negative (no cytokine) controls. Each sample was labeled as a

“responder” for specific cytokines that significantly increased cell growth over control wells, and a “non-responder” for cytokines that did not.²²⁶ These samples were also screened for sensitivity to small-molecule inhibitors as described above. For each cytokine, the log₂ fold change (mean AUC for responders divided by mean AUC for non-responders) was calculated and an unpaired Student’s t-test conducted to compare sensitivity to GW-2580 between these two groups.

8.5.5 *Cytokine secretion in conditioned media*

Primary AML patient samples were added to 12-well plates (1ml at 1x10⁶ cells/well) and treated with 10μM GW-2580, 100ng/ml CSF1 (Peprotech, Rocky Hill, New Jersey), or remained untreated. The plates were incubated for 48 hours, after which the cells from each condition were centrifuged and the conditioned media was collected and flash-frozen in liquid nitrogen. The levels of cytokines, chemokines, and growth factors were measured using the Human Cytokine Magnetic 30-Plex Panel for the Luminex platform (Thermo Fisher).

8.5.6 *Cytokine rescue from GW-2580 sensitivity*

Primary AML patient samples were exposed to GW-2580 as described above. Cells were incubated either with HGF (1μg/ml), the maximum concentration used in Carey et al,²²⁶ or conditioned media from the human marrow stromal cell line HS-5²²⁹ at a 1:1 ratio with normal media. Cells were incubated for 3 days and viability was evaluated by colorimetric assay.

8.6 Supplemental Methods

8.6.1 *Patient sample selection*

There are 672 samples and 562 patients in the final Beat AML patient sample cohort, of which 447 samples had received either small-molecule inhibitor screening or RNAi-assisted protein target identification (RAPID) screening (see the Beat AML manuscript, currently in preparation, for a more comprehensive list of samples). For the CSF1R small-molecule inhibitor analysis, we removed any samples that were not diagnosed as “ACUTE MYELOID LEUKAEMIA (AML) AND RELATED PRECURSOR NEOPLASMS,” leaving 637 samples from 532 patients. Then, we removed samples without seven-dose-point GW-2580 inhibitor sensitivity data, leaving 345 samples from 315 patients. Finally, we removed duplicate samples from the same patient (the earliest sample was selected), leaving 315 samples. For the RAPID analysis patient sample selection process, see “siRNA screening data analysis”. See the supplemental table,¹ available upon request and included in the manuscript submission, for complete details of clinical and genetic annotations.

8.6.2 *Small-molecule inhibitor screening data analysis*

The tetrazolium-based colorimetric assay produced absorbance values (optical density) that were used to calculate cell viability. For each sample, the wells treated with inhibitors were normalized to the average viability in each plate’s untreated

¹ This table contains the complete table of clinical and genetic characteristics of 302 patients with AML evaluated in this study. For each patient, the specimen ID, diagnosis and specific diagnosis (according to the WHO classifications of hematological malignancies), and clinical and genetic factors are included. For translocations and mutations, 0 = absent, 1 = present, and NA = not available.

control wells. These normalized values were confined to a 0-100 range to produce a response variable that represented the percentage of the average control well viability. Viability percentages for each sample/drug pairing, plated on a seven-dose dilution series (10 μ M, 3.33 μ M, 1.11 μ M, 0.307 μ M, 0.124 μ M, 0.0412 μ M, and 0.0137 μ M), were modeled using probit regression after log-transforming the dose concentration to enhance model fit. Roughly 60% of the seven-dose sample/drug profiles included same-plate replicates at each dose. For these profiles with two or three observed response values (viability percentages) per dose point, a single probit model was fit.

Two measures of drug efficacy, IC50 and AUC, were calculated based on the fitted probit curve. The IC50, or half-maximal inhibitory concentration, was defined as the lowest concentration within the plated dose range with a predicted viability \leq 50%. The AUC, defined as the area under the fitted probit curve over the plated dose range, was computed by integration and later rescaled by the maximum possible area to produce values between 0 and 100. The probit model could not be used for dose-response profiles with a single constant viability value of either 0 or 100. In the first scenario (viability values all equal 0), the IC50 was set to the minimum plated dose and the AUC was set to 0. In the second scenario (viability values all equal 100), the IC50 was set to the maximum plated dose and the AUC was set to the maximum possible area (equal to 286.27 for the 7-dose series, although renormalized to 100).

8.6.3 *siRNA screening data analysis*

From the complete dataset of 332 patient samples that underwent RNAi-assisted protein target identification (RAPID) screening,²³⁰ we selected those who were part of the Beat AML project (n = 257). Each sample was analyzed on 96-well plates, which were run in triplicate. The mean viability for each siRNA was calculated from the triplicate values and normalized based on the median of the mean absorbance values for all siRNAs (excluding the blank well). A z-score for each siRNA was calculated by comparing this triplicate-averaged mean viability to the mean viability of all siRNAs.

The dataset was further filtered using the following steps: (1) within-siCSF1R variance; (2) plate-to-plate variance; and (3) optical density variance. First, for within-siCSF1R variance, the standard deviation for the siCSF1R triplicate values needed to be less than 20% of the average of means (the average of the mean absorbance values for all siRNAs). Second, for plate-to-plate variance, the standard deviation of the absorbance values within a single plate needed to be less than 30% of the average of means (which averages all three plates). Third, for optical density variance, the mean optical density (mean_{OD}) and standard deviation optical density (stdev_{OD}) across all three plates were evaluated using the following criteria based upon a blinded visual inspection of the data: if $\text{mean}_{\text{OD}} < 0.04$, then did not pass; or if $0.04 \leq \text{mean}_{\text{OD}} \leq 0.075$ and $\text{stdev}_{\text{OD}} > 30\%$ of mean_{OD} , then did not pass; or if $\text{stdev}_{\text{OD}} > 50\%$ of mean_{OD} , then did not pass. If any one of those three variance filtering criteria was not met, the siRNA screening results from that sample were discarded.

In total, 162 samples passed all three variance filtering criteria. Five of those 162 samples (09-00427, 09-00438, 09-00453, 09-00456, and 09-00496) were run on older versions of the panel and therefore do not have viability testing for ABL1, CSK, EPHA8, FES, FYN, LMTK2, NTRK2, RET, and TNK1 siRNAs. Therefore, for these kinases, the data was analyzed for the remaining 157 samples.

For the samples who passed the variance filtering criteria, an siRNA “hit” for a particular sample was considered to be less than or equal to two standard deviations below the mean viability for all siRNAs ($z\text{-score} \leq -2$).

8.6.4 *Comparing small-molecule inhibitor and siRNA data*

The comparison between GW-2580 sensitivity and siRNA response was conducted in R. For each unique patient in our dataset that underwent both the RAPID and small-molecule inhibitor screen ($n = 162$), a linear regression was performed between GW-2580 AUC and the siCSF1R z-score, and the slope and p-value were obtained. This regression was repeated for each siRNA on the panel and represented as the negative log of the uncorrected p-value versus the slope of the linear regression line.

8.6.5 *Clinical and genetic characteristics*

Clinical data was obtained from the clinical annotations included in the Beat AML project dataset. Age was calculated by subtracting the date of AML diagnosis from the date of birth. The prognostic risk calculation was determined using an automated decision tree that we developed to evaluate prognostically significant mutations and cytogenetic abnormalities based on the newly revised European

LeukemiaNet guidelines.²³¹ Briefly, the karyotype and presence or absence of *FLT3*-ITD, *NPM1*, *CEBPA*, *TP53*, *RUNX1*, and *ASXL1* mutations were extracted from our dataset. Entries with incomplete information were excluded, including karyotypes that did not follow standardly defined nomenclature.²³² Regular expressions were used to identify prognostically significant abnormalities (including common monosomies/translocations) within a karyotype. In addition, the presence of complex karyotype and monosomal karyotype, as previously defined,²² along with the number of cytogenetic abnormalities, was determined. Cases of acute promyelocytic leukemia were classified as Favorable risk based on separate ELN guidelines.⁴⁰ For samples with a karyotype, the presence of common cytogenetic abnormalities was determined using regular expressions (see above).

The presence of gene mutations: For patients treated at Oregon Health & Science University, the results of GeneTrails testing, a mutation panel test that combines amplicon-based DNA library preparation with semiconductor sequencing, were included. The results from similar mutation panels were included from patients from Stanford University (GeneTrails), The University of Utah (ARUP Myeloid Panel), The University of Texas Southwestern (Foundation Medicine), and The University of Miami (Genoptix). In addition, for many patients, the *NPM1* or *FLT3*-ITD mutations were determined using in-house testing methods (see “In-house *FLT3*-ITD and *NPM1* sequencing” for protocol). Some patients also received exome sequencing (see “Exome and RNA sequencing” for analysis protocol), from which only non-synonymous mutations that had not failed subsequent custom-capture and

RNA-sequencing validation steps were selected (described in detail in the forthcoming Beat AML manuscript).

8.6.6 *In-house FLT3-ITD and NPM1 sequencing*

After the mononuclear cells were isolated from the AML patient samples, cell pellets were flash-frozen in liquid nitrogen. DNA was extracted using the DNeasy Blood and Tissue kit (#69506; Qiagen, Hilden, Germany) according to the manufacturer's protocol. FLT3-ITD and NPM1 detection was performed using mutations-specific primers as described previously,²³³ and analyzed by capillary electrophoresis using a QIAxcel High Resolution Kit (Qiagen) according to the manufacturer's protocol.

8.6.7 *Exome and RNA sequencing*

After the mononuclear cells were isolated from the AML patient samples, cell pellets were flash-frozen in liquid nitrogen, and DNA was extracted using the DNeasy Blood and Tissue kit (Qiagen).

For exome sequencing, Illumina Nextera capture probes were used and the libraries were run on a HiSeq 2500 System using a paired-end, 100-cycle protocol. The initial data processing and alignments were performed using an in-house analysis pipeline. Briefly, the FASTQ files were aggregated for each flowcell and each sample into single files for reads 1 and 2. The Burrows-Wheeler Aligner algorithm BWA-MEM²³⁴ (v0.7.10-r789) was used to align the read pairs for each sample-lane FASTQ file, with the flowcell/lane information preserved as part of the

read group of the resulting SAM file. The Genome Analysis Toolkit²³⁵ (GATK; v3.3) and the bundled Picard pipeline (v1.120.1579) were used for alignment post-processing. The files in the Broad Institute's bundle 2.8 were used, including their version of GRCh37. The following steps were performed for each sample-lane SAM file: sorting/conversion to BAM via SortSam; marking both lane-level standard and optical duplicates via MarkDuplicates; read realignment around indels via RealignerTargetCreator/IndelRealigner; and base quality score recalibration. The resulting BAM files were aggregated by sample and an additional round of MarkDuplicates was conducted. For genotyping, the BAM file for each AML sample was realigned at the sample level and genotyped for single nucleotide variations using Mutect²³⁶ (v1.1.7) and VarScan2²³⁷ (v2.4.1), with indels identified via VarScan2. Each VCF file was annotated using the Variant Effect Predictor²³⁸ (v83) against GRCh37. The resulting VCF files were filtered to include only those annotated to genes and converted to MAF using vcf2maf (v1.6.6) (<https://github.com/mskcc/vcf2maf>). The complete analysis protocol will be described in the final publication of the BeatAML dataset, which is currently in preparation.

For RNA sequencing, libraries were constructed using the SureSelect Strand Specific RNA Library Prep system (Agilent, Santa Clara, CA) and the *Bravo* Automated Liquid Handling Platform (Agilent). Libraries are validated using the 2100 Bioanalyzer (Agilent) and combined to generate 4 samples per lane, with a targeted yield of 200 million clusters. Combined libraries were denatured, clustered with the cBot System (Illumina), and sequenced on the HiSeq 2500 System using a

paired-end, 100-cycle protocol. For each sample, FASTQ files were aggregated into single files for reads 1 and 2. Alignment was performed using Subjunc²³⁹ (v1.4.6), and the resulting SAM files were analyzed by featureCounts²⁴⁰ (v1.4.6) and reads summarization was performed.

8.6.8 *GW-2580 Sensitivity Survival Analysis*

We selected Beat AML patients having high-quality clinical data (defined as having received a manual chart review from our data manager), having been screened for sensitivity to GW-2580, and having been diagnosed either with *de novo* AML, secondary AML (transformed from a prior hematologic malignancy), or relapsed AML. Of those patients within the analysis cohort, 202 had samples with seven-point drug curves for GW-2580: 158 with *de novo* AML, 24 with secondary AML, and 20 with relapsed AML. The area under the curve (AUC) for GW-2580 was calculated for each patient sample via probit regression as described above. GW-2580 AUC was compared across the three diagnostic subgroups using the Kruskal-Wallis test with Dunn's multiple comparisons test (at $\alpha = 0.05$). Of those patients with GW-2580 AUC data, 173 were unique patients that contained complete clinical status information (both last follow up date and survival status). Overall survival (OS) for this cohort was calculated from the date of disease diagnosis until date of death or last known follow-up and estimated using the Kaplan-Meier estimator. OS among diagnosis subgroups was compared using the log-rank test.

Patients were determined to have relapsed AML if they had recurrence of disease after attaining complete remission, as defined by $\geq 5\%$ blasts in their bone

marrow or peripheral blood, or if they developed extramedullary disease. Time to relapse was calculated as number of days from the date of diagnosis to the date of relapse as confirmed by laboratory testing. Of the 199 patients in our sample cohort, 41 patients relapsed after their initial sample collection. All survival data analysis was conducted using R (v3.4.0) (<http://www.R-project.org>).

8.6.9 *CyTOF Analysis*

The original dataset (currently in submission) consisted of 98 primary AML samples and 11 healthy donors. From this dataset, we only selected unique samples that also contained GW-2580 inhibitor data (when a patient had two samples with inhibitor data, the earlier sample was selected), resulting in 66 primary AML samples.

Hierarchical clustering of the CSF1R^{hi} cells was performed, with the Euclidean distance as the distance metric and using the complete linkage method (performed using the `dist` and `hclust` functions, respectively, in R). Due to computational demands, for samples with ≥ 2000 CSF1R^{hi} cells, only 2000 cells were randomly selected from the complete population and used for clustering. The heatmaps were generated with an unweighted dendrogram by row only (each row is an individual CSF1R^{hi} cell), with red signifying high arcsinh values and black signifying low values (performed using the `heatmap.2` function within `gplots` in R). The clusters that defined CSF1R^{hi} cell phenotypes were determined by cutting the dendrogram tree into several groups at a specified cut height (17 for AML samples; 15 for healthy donor samples), performed using the `cutree` function in R.

Based on a blinded visual inspection of the data, a cluster was considered “positive” for a cell-surface marker if there were $\geq 30\%$ of cells with $\text{arcsinh} \geq 3$; and considered “low” for a marker if there were $\geq 50\%$ of cells with $\text{arcsinh} \geq 2$. If there were ≥ 7 markers classified as either “positive” or “low”, the phenotype was summarized as “various”. When calculating the overall percentage of cells within each CSF1R^{hi} cluster, for samples with ≥ 2000 CSF1R^{hi} cells, the total number of CSF1R^{hi} cells within each cluster was extrapolated from the proportion identified in the clustering analysis.

8.7 Results

To identify new therapeutic targets and effective drugs against acute myeloid leukemia, we performed functional screening on primary AML patient samples (Figure 8.1A). We screened mononuclear cells from patient samples with small-molecule inhibitors, or an siRNA library targeting the human tyrosine kinome, and measured cell viability after short-term culture. We observed that the siRNA that significantly reduced cell viability in the largest number of samples among our filtered patient sample population ($n = 157$ or 162 ; see Supplemental Methods) was siCSF1R (Figure 8.1B), the specificity of which has been validated previously.¹⁴⁰

We next compared these siRNA screening results in samples that were also evaluated for sensitivity to CSF1R small-molecule inhibitors as a means of orthogonal validation. We chose three inhibitors with single-digit nanomolar sensitivity (by IC₅₀) to CSF1R: GW-2580, ARRY-382, and JNJ-28312141 (Figure 8.1C). We confirmed that GW-2580 and ARRY-382 induce apoptosis in primary

AML patient samples (Figure 8.6A-B). As a quality control check, we examined the sensitivity profiles of these inhibitors across patient samples and observed a highly significant correlation for each pairwise comparison of inhibitors (Figure 8.6C-E). Notably, we did not observe GW-2580 sensitivity in MNCs isolated from 5 healthy donors (Figure 8.6F-J), which had also been observed previously,²⁴¹ highlighting the unique therapeutic responsiveness of AML samples. Both GW-2580 and ARRY-382 have extreme specificity for CSF1R, having no interaction with other Class III receptor tyrosine kinases.^{198,199} Because GW-2580 had the highest specificity for CSF1R among the other inhibitors, it was used to exclusively represent CSF1R inhibitor activity in all subsequent experiments.

We observed a significant correlation between the z-score for siCSF1R and GW-2580 area under the curve (AUC), suggesting that siCSF1R efficacy (lower z-score) correlates with greater sensitivity to GW-2580 (lower AUC) (Figure 8.1D). (Unless otherwise specified, drug sensitivity was quantified using AUC because of its effectiveness in combining drug potency and efficacy.²⁴²) To confirm that this correlation was specific for siCSF1R, we performed the same correlation calculation from Figure 1D for each tyrosine kinase siRNA, which includes all other Class III receptor tyrosine kinase family members. We found that siCSF1R had the strongest, most significant correlation with GW-2580 sensitivity compared to all other siRNAs (Figure 8.1E), suggesting that CSF1R is the operational target of inhibition underlying CSF1R inhibitor sensitivity. Collectively, our screening of 315 AML patient samples for sensitivity to GW-2580 (Figure 8.1F) revealed a wide range of

responses, with many highly sensitive samples as well as samples that were completely resistant (Figure 8.1G-H).

To determine if sensitivity to CSF1R inhibitors correlated with prominent genetic abnormalities or clinical characteristics found in patients with AML, we analyzed patient samples from the Beat AML cohort that had been subjected to small-molecule inhibitor screening, many of which had whole exome sequencing and detailed clinical annotations (manuscript describing the full Beat AML cohort is in review). We compared the distribution of GW-2580 sensitivity as it related to demographic or clinical factors of disease (specimen type, age, gender, white blood cell count, and prognostic risk) and genetic factors (common translocations and mutations found in AML²⁴) (Figure 8.2A). Overall, we found a significant association between CSF1R inhibitor resistance and poor prognostic markers, including cytogenetic abnormalities (complex karyotype, inversion 3, and monosomy 5/deletion 5q), gene mutations (*TP53*, *NRAS*, and *KRAS*), and ELN adverse prognostic risk (Figure 8.2A and Figure 8.7A-C).

To evaluate the relationship between CSF1R inhibitor sensitivity and clinical response, we analyzed the patients with high-quality treatment data and GW-2580 functional screening data within our sample cohort (n = 202 samples from 199 patients). We subdivided this patient population based on disease presentation: *de novo*, secondary, and relapsed AML. We classified CSF1R inhibitor sensitivity based on the GW-2580 AUC for each sample compared to the total population: “sensitive” samples were below the 20th percentile, “indeterminate” samples between the 20th and 80th percentiles, and “resistant” samples above the 80th percentile. We observed

that the relapsed AML samples had a higher GW-2580 AUC than *de novo* AML samples ($p = 0.040$), while there was no difference between the GW-2580 AUC of secondary AML versus *de novo* AML (Figure 8.2B and Figure 8.8A). In addition, we observed that overall survival was different among the CSF1R inhibitor subgroups (Figure 8.2C), although there was no difference between the sensitive and indeterminate categories. This observation of CSF1R inhibitor resistance correlating with worse survival showed a similar trend within *de novo*, secondary, and relapsed disease groups, although it did not achieve statistical significance at $\alpha = 0.05$ (Figure 8.8A-D). We observed no correlation between median time to relapse and GW-2580 sensitivity (Figure 8.8E).

We next wanted to understand the mechanism of action of CSF1R inhibitors in AML. Since CSF1R mutations are not observed in AML,²⁴ and we did not observe any single genetic biomarker that could biologically explain sensitivity to CSF1R inhibitors, we examined CSF1R expression patterns in AML patient samples. In healthy individuals, CSF1R cell-surface expression is found only on macrophages and committed macrophage precursor cells.²⁴³ This prompted us to determine whether CSF1R inhibitor sensitivity correlated with CSF1R expression on AML tumor cells or on healthy macrophage-lineage cells that might be interacting with the tumor cells. Therefore, we analyzed mass cytometry (CyTOF) data on the expression levels of 16 cell surface markers, including CSF1R, on 66 AML patient samples and 11 healthy donors (Figure 8.3A) (methods reviewed in Lambie et al,¹³ full dataset in submission) as well as conducted conventional flow cytometry on cells from 2 patient samples.

Our initial examination of CSF1R expression using conventional flow cytometry, which allowed for traditional gating of leukemic blasts, revealed negligible expression of CSF1R on leukemic blasts, suggesting that CSF1R expression is confined to a subpopulation of non-leukemic cells (Figure 8.9). Using CyTOF data, we found that the percentage of CSF1R^{hi} cells ($\text{arcsinh} \geq 3$) was relatively low throughout the AML patient dataset (mean of 1.4% in total cells), and was comparable to that of the healthy donor samples (Figure 8.3B and Figure 8.10A). We observed no association between the percentage of CSF1R^{hi} cells and FLT3-ITD status or FAB morphology (Figure 8.10B-C). CSF1R^{hi} cells most often co-express myeloid-specific markers in patients with AML (Figure 8.3C) and in healthy donors (Figure 8.3D), suggesting that these CSF1R-expressing cells are of a monocyte/macrophage-lineage.

We investigated the relationship between the frequency of CSF1R^{hi} cells and CSF1R inhibitor sensitivity. We found an association between the overall percentage of CSF1R^{hi} cells and GW-2580 sensitivity (Figure 8.3E), with more sensitive samples having a higher percentage of CSF1R^{hi} cells than resistant samples (Figure 8.3F-G). We further combined CSF1R^{hi} cells from every sample in our dataset (separate combinations for AML and healthy donor samples) and subdivided the cells based on the co-expression of common hematopoietic-population-defining cell surface markers and markers associated with myeloid-derived suppressor cells (MDSCs)²⁴⁴ (Figure 8.3A). Ultimately, these cells clustered into 6 subgroups in patients with AML and 7 subgroups in healthy donor samples (Figure 8.3H-I and Figure 8.10B-C). We found that CSF1R^{hi} cells in AML samples were enriched for co-expression of

CD33 and HLA-DR compared to healthy donors (which predominantly co-expressed CD11c and CD16; Figure 8.3J), showing evidence of CSF1R^{hi} phenotypic reprogramming in AML. We correlated the percentage of each CSF1R^{hi} subgroup with the GW-2580 AUC of the corresponding sample, identifying a possible correlation between AML cluster 2 (CSF1R+, CD45+, CD33+, HLADR+) and GW-2580 sensitivity (Figure 8.10D-E). Overall, these results suggest that CSF1R^{hi} cells in AML constitute a population of supportive cells that contribute to sensitivity to CSF1R inhibitors.

Next, we wanted to identify the cytokines or growth factors being secreted by this population of CSF1R-expressing supportive cells. We recently performed a study²²⁶ in which we incubated primary AML patient samples with various cytokines and growth factors, and classified each sample either as a “responder” (molecule increased cell growth) or a “non-responder” (molecule had no effect). For each of these cytokines/growth factors, we compared sensitivity to GW-2580 for responders and non-responders. We determined the fold change (the ratio of mean AUC values) between responder samples and non-responder samples to examine whether CSF1R inhibitor sensitivity correlated with responsiveness to any recombinant cytokine/growth factor, which could indicate an operational role for that cytokine/growth factor in mediating the signal between CSF1R^{hi} cells and AML tumor cells. We identified cytokines and growth factors that showed a negative log₂ fold change, meaning that the cytokine-responsive samples were more sensitive to GW-2580 than the samples that were non-responsive to the cytokine (Figure 8.4A). The four cytokines and growth factors that correlated most significantly with CSF1R

inhibitor sensitivity were LPS, RANTES, CSF1, and HGF (Figure 8.4B). The identification of CSF1 in this group reinforces our previous data suggesting that GW-2580 sensitivity occurs specifically because of inhibition of CSF1R and also suggests that the CSF1R inhibitor sensitivity involves a ligand-dependent mechanism.

To further study the cytokines and growth factors that are operationally important in mediating a paracrine signal between leukemia cells and CSF1R-expressing monocyte/macrophage support cells, we treated primary AML patient samples (n = 15) either with CSF1, GW-2580, or nothing (remained untreated). We collected cell supernatants to study changes in cytokine levels that were impacted by positive or negative perturbation of CSF1R signaling (Figure 8.4C). We calculated the change in cytokine levels in conditioned media after CSF1 stimulation (CSF1-treated minus untreated control) and after CSF1R inhibition (GW-2580-treated minus untreated control), ranking each cytokine in order of decreasing median value (Figure 8.4D-E). To identify the cytokines that both increased after CSF1 stimulation and decreased after CSF1R inhibition, we subtracted the inhibition ranking from the stimulation ranking (Figure 8.4F).

The top three cytokines that we identified were IL-8, MCP-1, and HGF. The identification of IL-8 and MCP-1 in this context is not unexpected, as similar results have been observed in blood from healthy donors.²⁴⁵ However, HGF has not been previously associated as a CSF1/CSF1R-driven growth factor. We observed a significant correlation between GW-2580 sensitivity and baseline levels of HGF in conditioned media from untreated patient samples (n = 10; 5 samples showed no detectable HGF) (Figure 8.4G). We examined our small-molecule inhibitor dataset

of *ex vivo* AML patient samples to determine whether there was a correlation between CSF1R inhibitor sensitivity and sensitivity to inhibitors of the HGF receptor, MET. Using three small-molecule inhibitors with sensitivity to MET (crizotinib, foretinib, and SGX-523), whose response in AML patient samples significantly correlates with one another (Figure 8.11A-C), we observed a strong correlation between their response and the response to GW-2580 (Figure 8.5A-C).

We performed a rescue experiment where primary AML patient samples were treated with GW-2580 for 72 hours and incubated either with HGF or conditioned media from the human marrow stromal cell line HS-5. We observed that HGF significantly rescued viability in 1 sample (Figure 8.5D), suggesting its importance in CSF1R inhibitor sensitivity. However, we also observed that HS-5-conditioned media rescued viability in 4 samples (Figure 8.5D-G), emphasizing that multiple factors are likely mediating CSF1R inhibitor sensitivity in the majority of samples.

Overall, our results suggest that, for roughly one quarter of primary AML patient samples, a small subpopulation of CSF1R-expressing cells secretes necessary survival molecules, including HGF, to the bulk population of leukemia cells. By adding small-molecule inhibitors of CSF1R, we can nullify these signals and kill the leukemia cells (Figure 8.5H).

8.8 Discussion

The results of our research suggest that using CSF1R inhibitors or neutralizing agents to eliminate supportive monocytes/macrophages may be an effective treatment for a subset of patients with AML. This aligns with existing

research in solid tumors, in which eliminating tumor-associated macrophages (TAMs) can be effective against a variety of tumor subtypes.²⁴⁶ However, whereas data from solid tumors generally suggests that a combinatorial approach is required for efficacy,¹²² we observe single-agent sensitivity to CSF1R inhibitors in our *ex vivo* patient samples.

Although GW-2580 sensitivity did correlate with individual genetic and prognostic markers—there was a slight correlation with the presence of *NPM1* and *IDH2* mutations, the significance of which is not understood—we observed a strong association between multiple adverse-risk markers and GW-2580 resistance. We believe that these CSF1R-inhibitor-resistant samples are potentially resistant to any known treatment, targeted or otherwise, which would explain the ineffectiveness of CSF1R inhibitors. In addition, perhaps the presence of NRAS/KRAS mutations in the leukemia cells, being downstream from the receptor tyrosine kinase signaling, obviates the contribution from upstream CSF1R activity. It should be noted that, in forthcoming early-stage clinical trials using CSF1R inhibitors in patients with AML, the targeted patient population will likely have relapsed/refractory disease, reducing the number of candidates we predict would exhibit a clinical response to CSF1R inhibitors.

Even though having a higher percentage of CSF1R^{hi} cells correlated with increased GW-2580 sensitivity, we observed no difference in overall survival between patients whose samples were sensitive or resistant to CSF1R inhibitors. In most solid tumor types, higher TAM density is generally associated with both late-stage clinical presentation and reduced overall survival, although exceptions exist in ovarian and

colorectal cancer.¹²¹ Our data suggests that AML reflects the complexity underlying the prognostic significance of TAMs, in that having more supportive monocyte/macrophages is correlated with favorable prognostic risk but shows no difference in overall survival.

There is extraordinary plasticity in the functional activity of TAMs, whose phenotype changes depending on tumor subtype and the surrounding tissue microenvironment.¹²² Our results indicate that CSF1R^{hi} cells show extensive reprogramming in AML patient samples compared to healthy donor samples, particularly through the increased cell-surface expression of HLA-DR and CD33. HLA-DR is an MHC class II molecule whose expression is found on pro-inflammatory, classically activated TAMs. Enrichment of HLA-DR-expressing TAMs has been shown to correlate with better overall survival in non-small cell lung cancer²⁴⁷ and ovarian cancer.²⁴⁸ CD33, a sialoadhesin molecule generally expressed on myeloid-lineage cells, has been identified as a marker on myeloid-derived suppressor cells (MDSCs),^{249,250} but the role of CD33+ supportive monocytes/macrophages remains poorly understood.²⁵¹ Overall, the functional significance of the various CSF1R^{hi} cell populations identified in this study reflects the complexity of TAM phenotypes, which often defy the traditional M1/M2 classification,²¹⁴ and provide yet another distinct supportive-cell surface marker phenotype that has been identified in many other cancers.²⁵²

One remaining question is the extent to which CSF1R ligand(s) contribute to CSF1R inhibitor sensitivity. We demonstrate that the addition of CSF1 to AML patient samples increases leukemia cell growth preferentially in samples sensitive to

CSF1R inhibition (Figure 8.4A-B), suggesting a ligand-dependent mechanism. We did not find an association between the level of CSF1 in patient sample plasma (22 bone marrow aspirates; 27 peripheral blood) and GW-2580 sensitivity (Figure 8.12A-D) (IL-34 could not be detected in 28 samples; data not shown). Because CSF1 is known to be secreted by bone marrow stromal cells,²⁵³ we isolated mesenchymal stromal cells from primary AML patient samples and measured the concentration of CSF1 in stromal cell conditioned media by ELISA. There was no association between the level of CSF1 and the GW-2580 sensitivity of the samples from which the stromal cells were isolated (Figure 8.12E), suggesting that the CSF1 ligand-dependent mechanism could be a localized, autocrine stimulation of CSF1R^{hi} cells.

The contribution of HGF signaling to this supportive-cell-dependent phenotype is intriguing, considering that autocrine HGF signaling has been previously identified in AML by Kentsis et al.²⁵⁴ They found HGF and MET co-expression on 58/138 AML patient samples by immunohistochemistry, and 5/13 samples showed phosphorylated MET on CD34-selected primary blasts by capillary isoelectric focusing electrophoresis nanoimmunoassay.²⁵⁴ In addition, while we do not know the mechanism of crosstalk between the AML tumor cells and the supportive CSF1R^{hi} cells, there is evidence that interferon beta stimulates HGF production in monocytes.²⁵⁵ Notably, our data supports a paracrine signaling mechanism in which supportive cells not only secrete HGF but other cytokines, as evidenced by the rescuing of cell viability after GW-2580 exposure using HS-5-conditioned media. There are likely multiple cytokine/growth factor pathways responsible for the CSF1R-dependent leukemia cell survival. Perhaps CSF1R-

sensitive AML comprises an earlier stage of disease development, with dependence upon signaling from CSF1R^{hi} supportive cells for their survival. Eventually, possibly due to a genetic perturbation, the disease becomes modified, with AML cells either producing their own supportive cytokines (including HGF) or gaining independence from supportive signaling entirely through the acquisition of adverse-risk mutations. Indeed, this model is consistent with our observation of a higher proportion of CSF1R-resistant cases carrying adverse risk features of disease.

Overall, we have identified a new role for tumor-supportive cells in AML biology as well as a novel therapeutic approach for targeting survival signaling essential for leukemia survival. Based on our findings, we propose using CSF1R inhibitors as a promising targeted therapeutic agent against AML.

8.9 Acknowledgements

Special thanks to Mandy Gilchrist and Brianna Garcia from the OHSU Flow Cytometry Core for technical assistance; Daniel Bottomly and Beth Wilmot for conducting Beat AML exome sequencing; and Cristina Tognon and Elie Traer for assistance with Beat AML patient samples. Additional thanks to Stephen Kurtz, Christopher Eide, Quinn Roth-Carter, Riley Roth-Carter, and Chris Cheng.

This work was supported by The Leukemia & Lymphoma Society. J.W.T. received grants from the V Foundation for Cancer Research, the Gabrielle's Angel Foundation for Cancer Research, and the National Cancer Institute (1R01CA183947, 1U01CA217862, and 1U54CA224019). D.K.E.V was supported

by the National Science Foundation Graduate Research Fellowship Program (DGE-1448072).

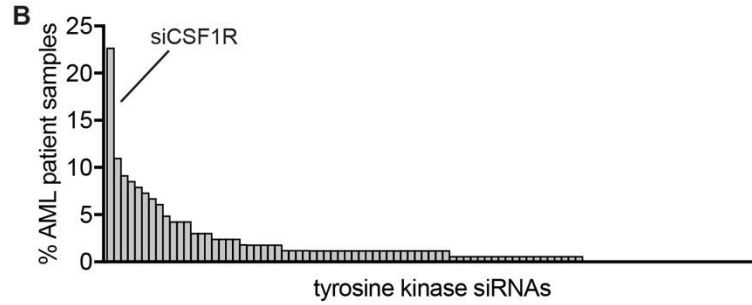
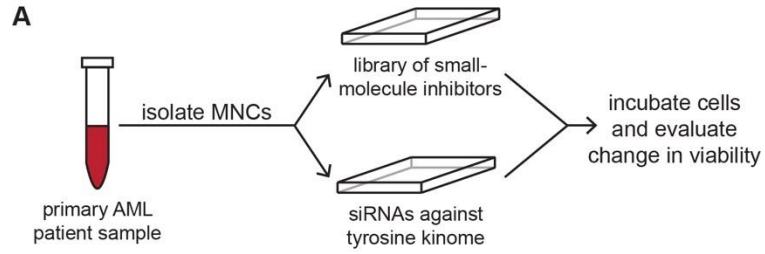
8.10 Authorship Contributions

Conceptualization: D.K.E.V and J.W.T.; *Methodology:* D.K.E.V and J.W.T.; *Formal Analysis:* D.K.E.V, K.W-S., T.L., A.K., M.M., M.R., N.L., M.L., and S.K.M.; *Investigation:* D.K.E.V, K.W-S., A.R., A.D., A.A., M.R., A.d'A., A.L., and E.F.L.; *Resources:* A.A., P.L., D.C., and J.W.T.; *Writing – Original Draft:* D.K.E.V; *Writing – Review & Editing:* D.K.E.V, K.W-S., A.R., A.D., T.L., A.L., E.F.L., A.K., M.M., M.R., A.d'A., N.L., A.A., D.T.S., P.L., D.C., M.L., S.K.M., and J.W.T.; *Visualization:* D.K.E.V, K.W-S., T.L., M.R., D.T.S., M.L. and J.W.T.; *Supervision:* S.K.M. and J.W.T.; *Funding Acquisition:* D.K.E.V and J.W.T.

8.11 Disclosure of Conflicts of Interest

J.W.T. receives research support from Aptose, Array, AstraZeneca, Constellation, Genentech, Gilead, Incyte, Janssen, Seattle Genetics, Syros, and Takeda, and is a co-founder of Leap Oncology.

All other authors have no conflict of interest to disclose.



C

Drug	K_d/IC_{50} of Class III RTKs (nM)				Number of effective targets (kinome)	Ref
	CSF1R	PDGFR	cKIT	FLT3		
GW-2580	2.2	none	none	none	4/386 (at <3,000 nM)	[1]
ARRY-382	9	none	none	none	1/257 (at <1,000 nM)	[2]
JNJ-28312141	3.2	27.5	3.6	17	150/386 (at <3,000 nM)	[1]

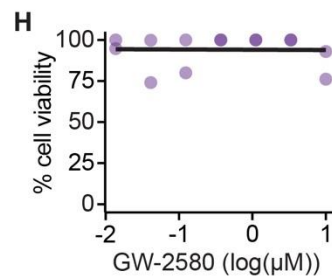
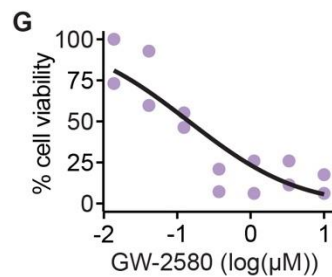
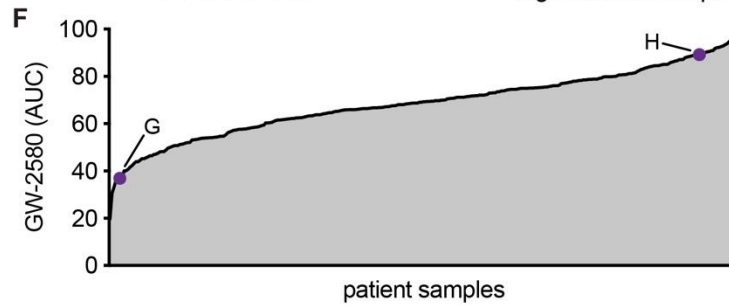
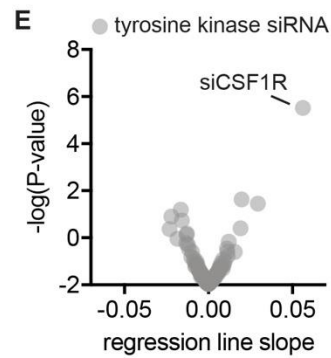
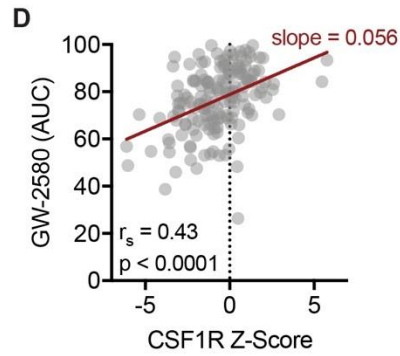


Figure 8.1 *Ex vivo* AML patient sample screen reveals that knockdown/inhibition of CSF1R reduces leukemia cell survival in >20% of samples.

(A) Schematic of screening primary AML patient samples against small-molecule inhibitors and siRNAs against the tyrosine kinome to identify new therapeutic targets.

(B) siRNA tyrosine kinome screen (n = 93 kinase siRNAs) identifies CSF1R as the top “hit” in primary AML patient samples (n = 157 or 162) to significantly reduce cell viability.

(C) High degree of specificity among the CSF1R-targeted small-molecule inhibitors GW-2580, ARRY-382, and JNJ-28312141, compared to other Class III receptor tyrosine kinases. Data from [1] Davis et al¹⁹⁸ and [2] Wright et al¹⁹⁹.

(D) Strong correlation observed between GW-2580 area under the curve (AUC) and z-score of the viability from siCSF1R compared to that of other tyrosine kinase siRNAs (n = 162 patient samples). Significance determined by Spearman’s rank correlation.

(E) siCSF1R has the strongest correlation and most significant association with GW-2580 AUC in the siRNA tyrosine kinome screen. Slope of linear regression line calculated for each siRNA as indicated in (D) was plotted against the p-value, determined by significance test for linear regression.

(F) Profile of sensitivity to GW-2580 across the cohort of primary AML patient samples (n = 315). The relative position of representative dose-response curves (G) and (H) are indicated.

(G-H) Representative dose response curves for a (G) sensitive and (H) non-sensitive primary AML patient sample to GW-2580.

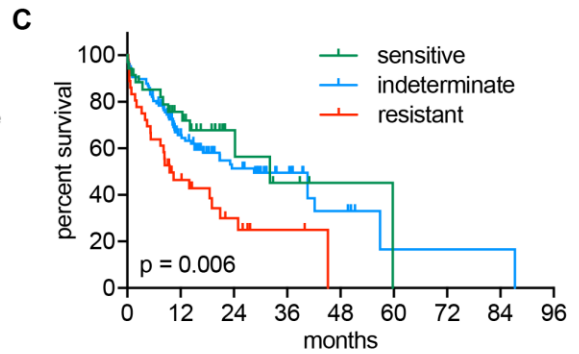
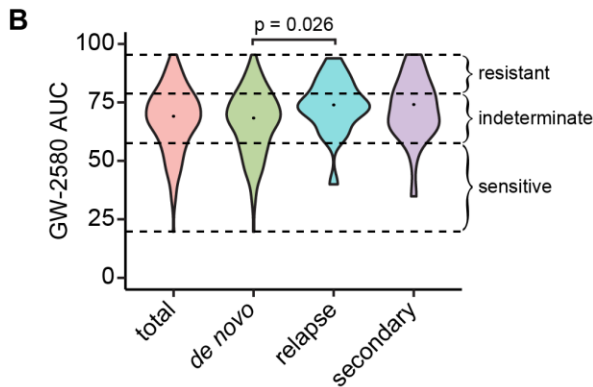
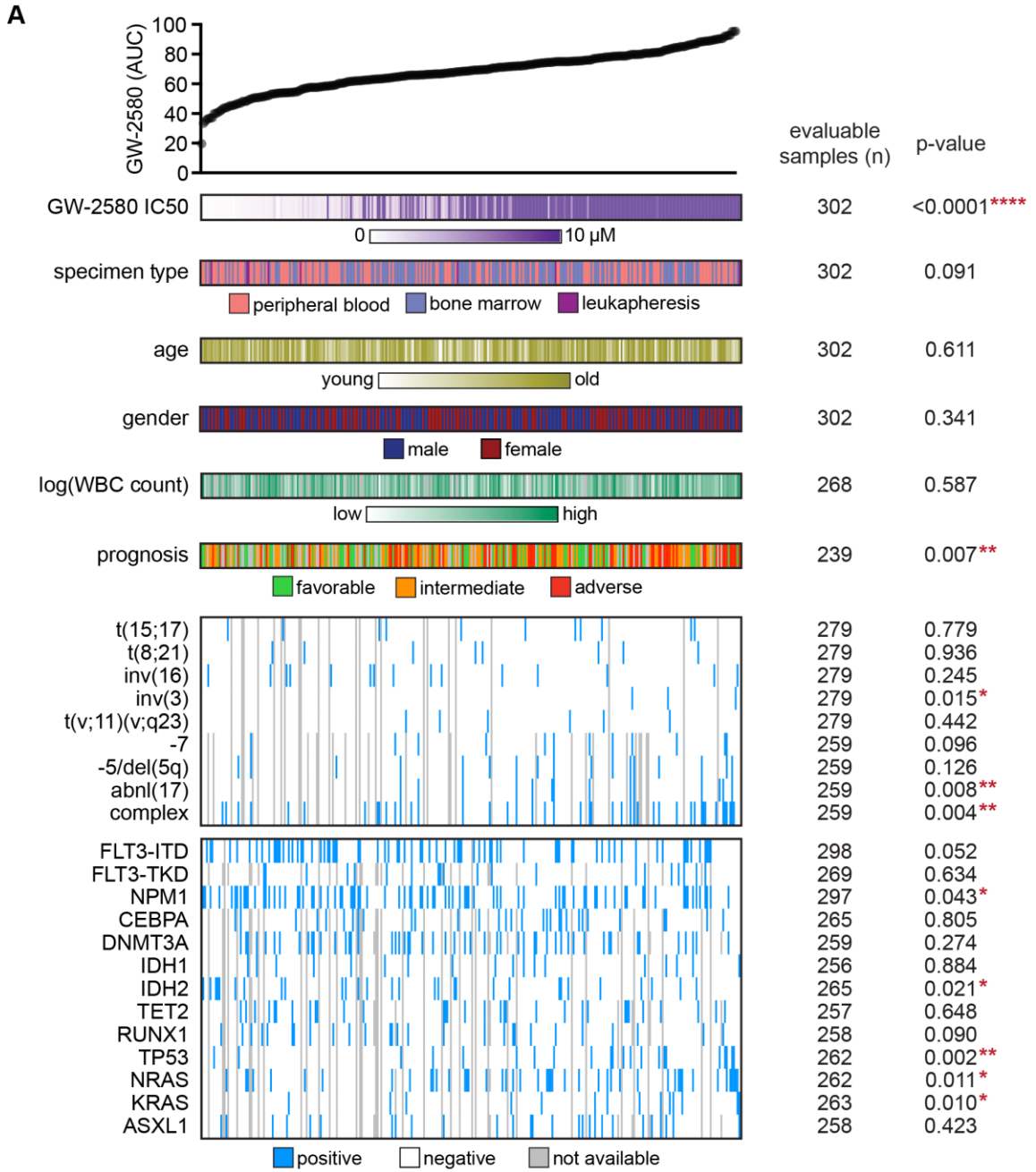


Figure 8.2. Resistance to CSF1R inhibitor is associated with adverse prognostic risk gene mutations and cytogenetic abnormalities.

(A) GW-2580 AUC from primary AML patient samples (n = 315) was compared for a multitude of clinical and genetic characteristics, with number of samples with evaluable data and the p-value listed for each characteristic. Prognostic risk was determined using the European LeukemiaNet guidelines for acute myeloid leukemia (see Döhner et al²⁰). The presence/absence of translocations was determined from karyotype. Only translocations that were found in ≥ 2 patients were considered. Mutational data was collected either by targeted sequencing (OHSU GeneTrails panel using Ion Torrent), whole exome sequencing, or targeted PCR-based methods (FLT3-ITD and NPM1). Significance was determined using either Mann-Whitney or Kruskal-Wallis tests (for categorical variables) or Spearman's rank correlation (for continuous variables).

(B) GW-2580 AUC among the patient population with clinical data (n = 202 samples from 199 patients), subdivided into *de novo* (n = 158), secondary (n = 24), and relapsed (n = 20) AML disease presentation categories. Statistics were calculated on subdivided categories by Kruskal-Wallis test with Dunn's multiple comparisons test.

(C) Kaplan-Meier survival curve of patients with AML with both clinical and survival data (n = 173), grouped by the response of their corresponding *ex vivo* primary sample to GW-2580: sensitive (0-20th percentile), indeterminate (20th-80th), and resistant (80th-100th). Statistics determined by log-rank test.

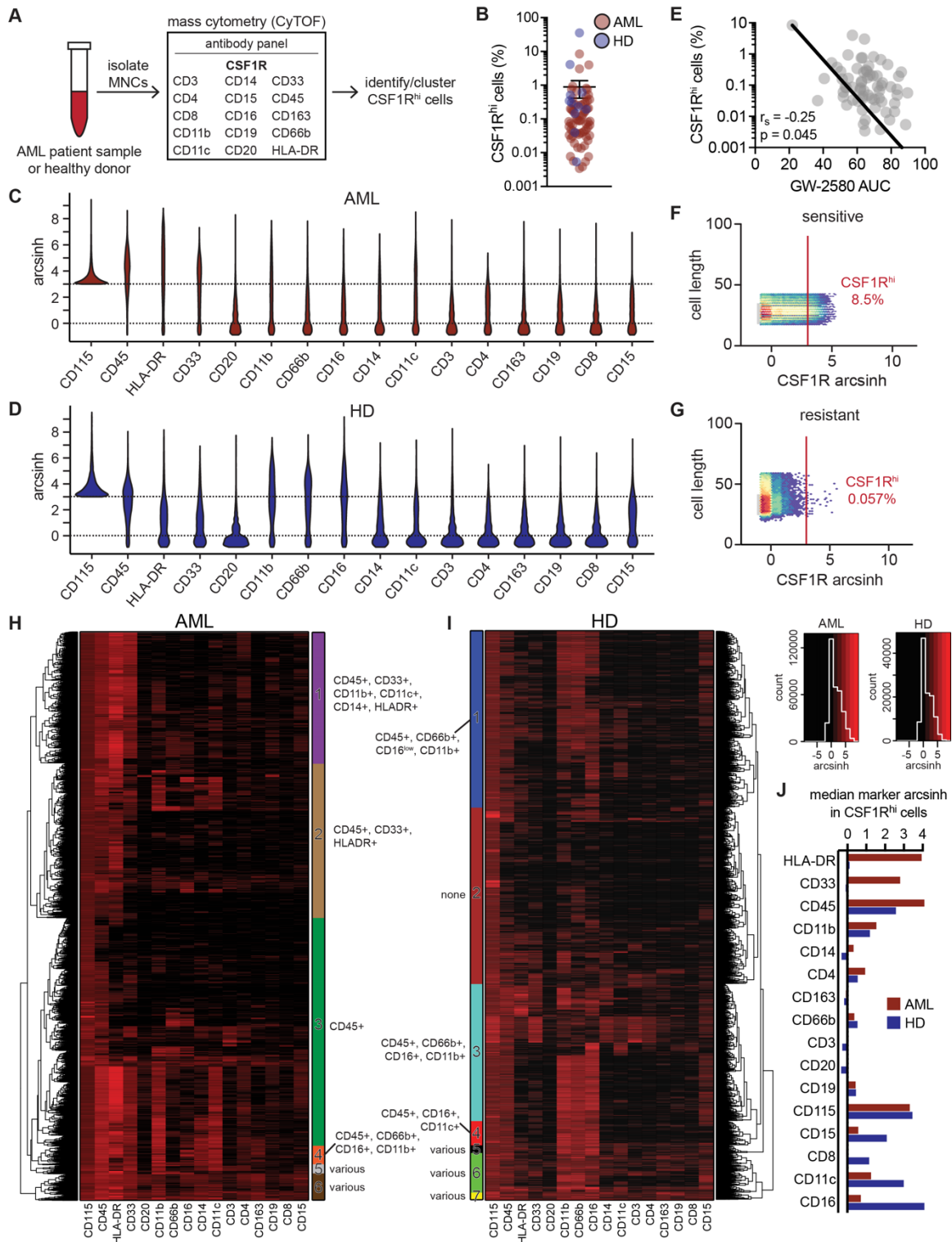


Figure 8.3. CSF1R is expressed not on the bulk leukemia population in primary AML patient samples but on a small subpopulation of supportive cells.

(A) Schematic diagram of CyTOF analysis to profile CSF1R^{hi} cells in primary AML patient samples.

(B) Percentage of CSF1R^{hi} cells in primary samples from patients with AML (n = 66) and healthy donors (n = 11).

(C-D) Violin plots of expression intensity of other cell surface markers in CSF1R^{hi} cells from (C) AML patient and (D) healthy donor samples.

(E) Correlation of the proportion of CSF1R^{hi} cells in primary AML patient samples with the sample's response to GW-2580. Significance determined by Spearman's rank test.

(F-G) Representative CyTOF plots of CSF1R expression in primary AML patient samples that show (F) sensitivity and (G) resistance to GW-2580.

(H-I) Heatmap of cell surface marker expression among all CSF1R^{hi} cells in (H) primary AML patient sample cohort and (I) healthy donors. Subgroups of CSF1R^{hi} cells determined by unsupervised hierarchical clustering of surface marker expression. Dashed red line indicates the dendrogram cutoff height.

(J) Cell-surface marker expression (median arcsinh) in CSF1R^{hi} cells for AML patient and healthy donor samples.

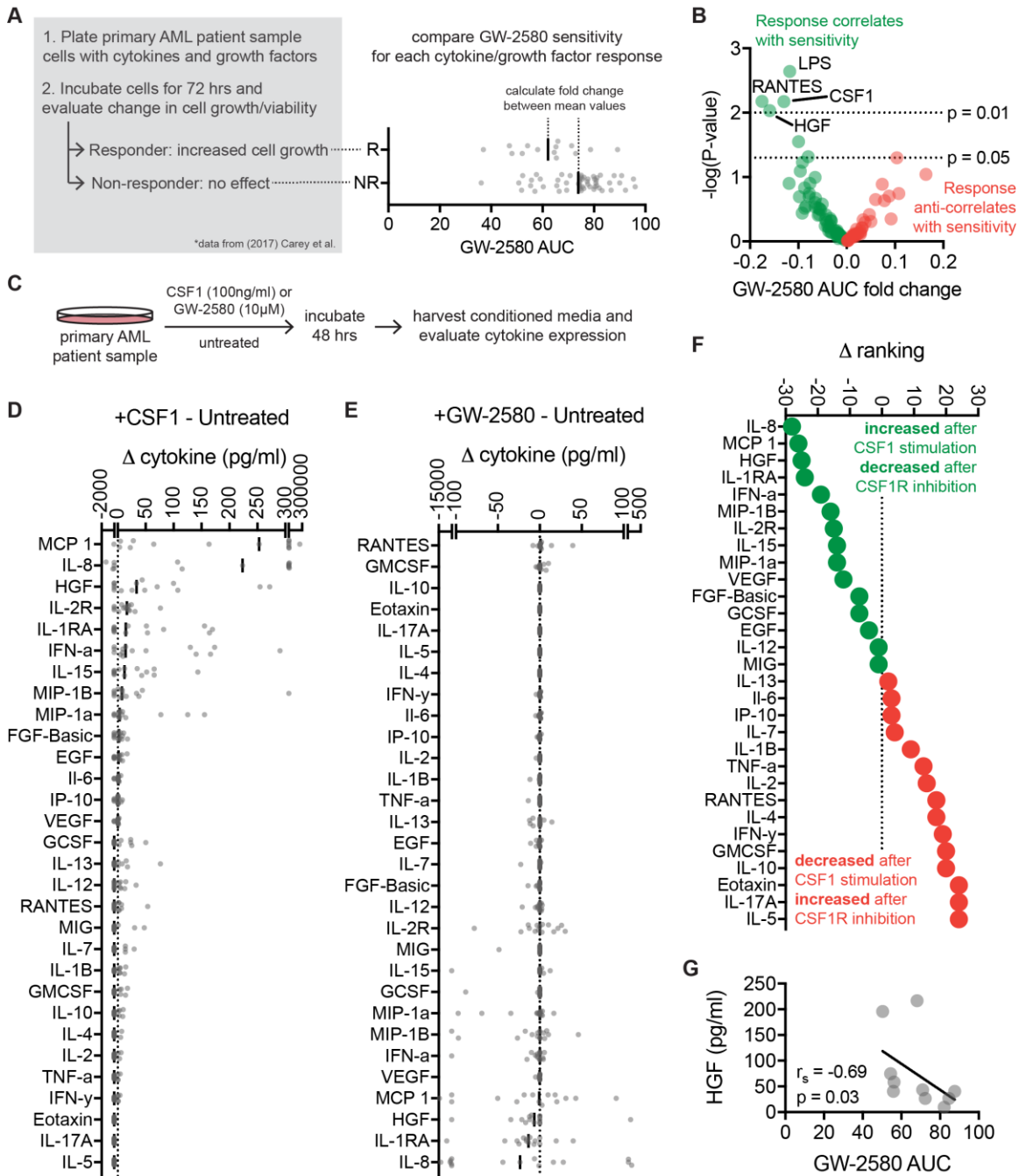


Figure 8.4. HGF stimulates growth in CSF1R inhibitor sensitive samples and its secretion is regulated by CSF1R activation.

(A) Schematic of analysis connecting cytokine growth assay results (data from Carey et al²²⁶) with CSF1R inhibitor sensitivity.

(B) Cytokines and growth factors that increase AML cell growth are significantly associated with sensitivity to GW-2580. Data represents \log_2 fold change of GW-2580 AUCs between responders and non-responders (n = 68 primary AML patient samples and 94 cytokines/growth factors) versus the unadjusted p-value, determined by Student's t-tests.

(C) Schematic of evaluating cytokine secretion after stimulation/inhibition of CSF1R in primary AML patient samples (n = 15).

(D-E) Change in cytokine levels in conditioned media of primary AML patient samples after (D) CSF1R stimulation and (E) CSF1R inhibition. Cytokine levels for each patient sample are normalized to untreated and ranked by median value.

(F) Difference in rank order of cytokines from (D) and (E) identifies cytokine secretion profile associated with up-regulated and down-regulated CSF1R activity.

(G) Baseline HGF levels in primary AML patient samples correlate with GW-2580 sensitivity (n = 10). Significance determined by Spearman's rank correlation.

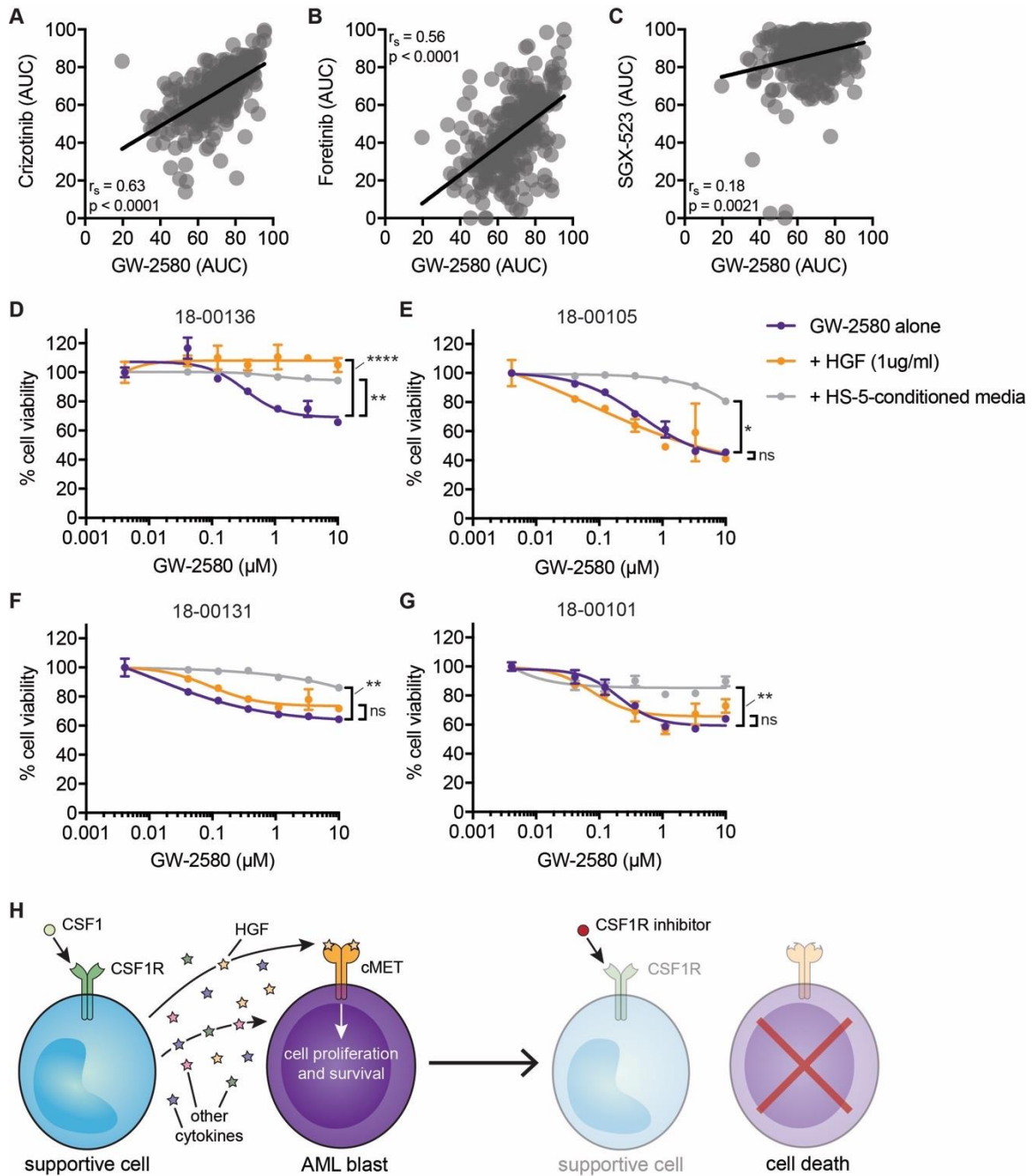


Figure 8.5. Sensitivity to CSF1R inhibitors correlates with MET inhibitor sensitivity and is eliminated after external HGF stimulation.

(A-C) Strong correlation in primary AML patient samples ($n = 315$) between GW-2580 sensitivity and sensitivity to three MET inhibitors: (A) crizotinib, (B) foretinib, and (C) SGX-523. Significance determined by Spearman's rank correlation.

(D-G) GW-2580 dose-response curves for 4 primary AML patient samples treated with recombinant HGF (1 μ g/ml), HS-5-conditioned media, or untreated. Error bars represent mean \pm SEM (n = 4 replicates); non-linear curve fitting conducted using least squares regression. Significance determined by one-way ANOVA on the area under each curve with Dunn's test for multiple comparisons.

(H) Model of CSF1R inhibitor sensitivity in primary AML patient samples resulting from paracrine secretion of cytokines by CSF1R-expressing supportive cells.

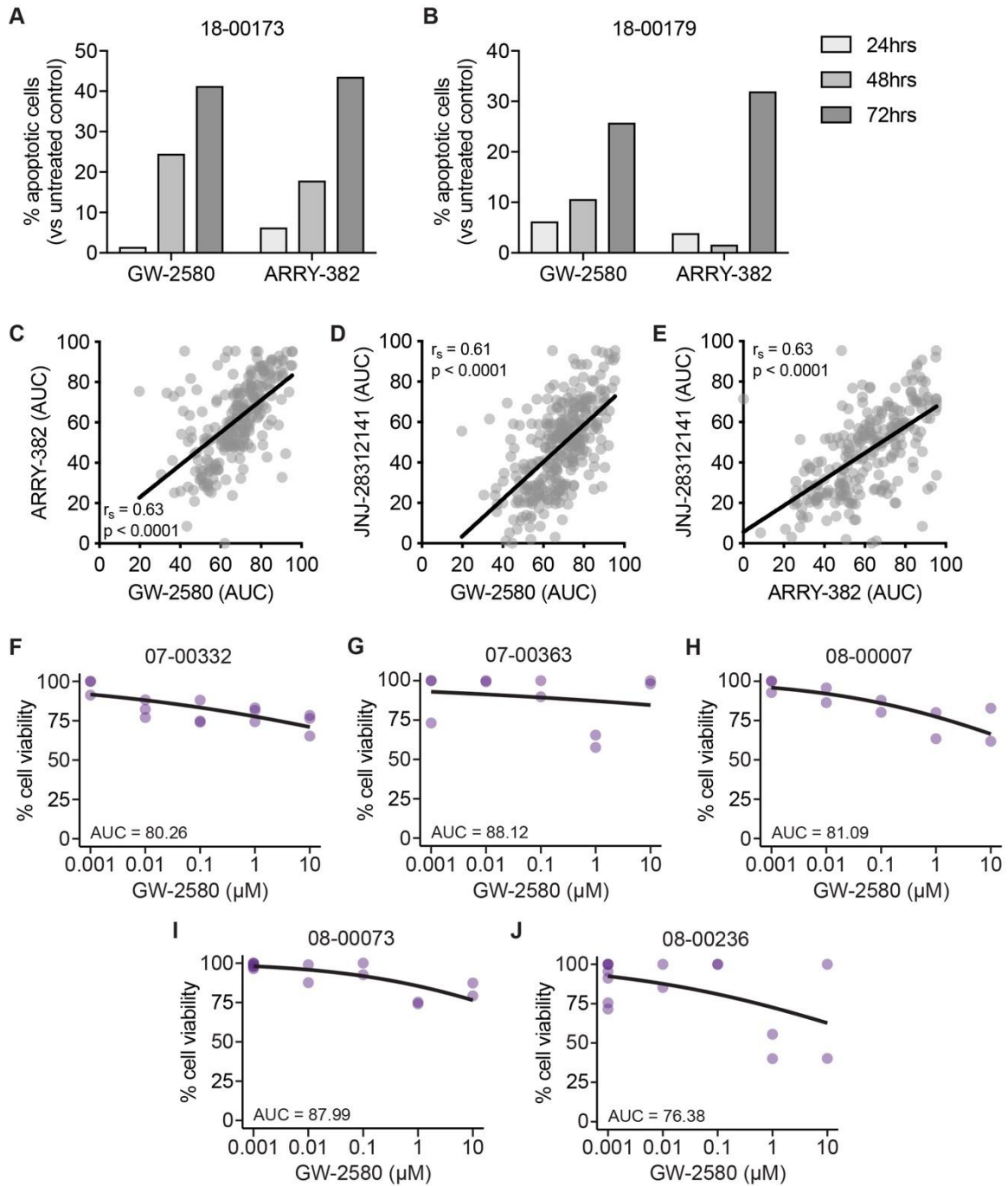


Figure 8.6. CSF1R inhibitors induce apoptosis in primary AML patient samples, not healthy donors, and patient sample sensitivity strongly correlates across all inhibitors.

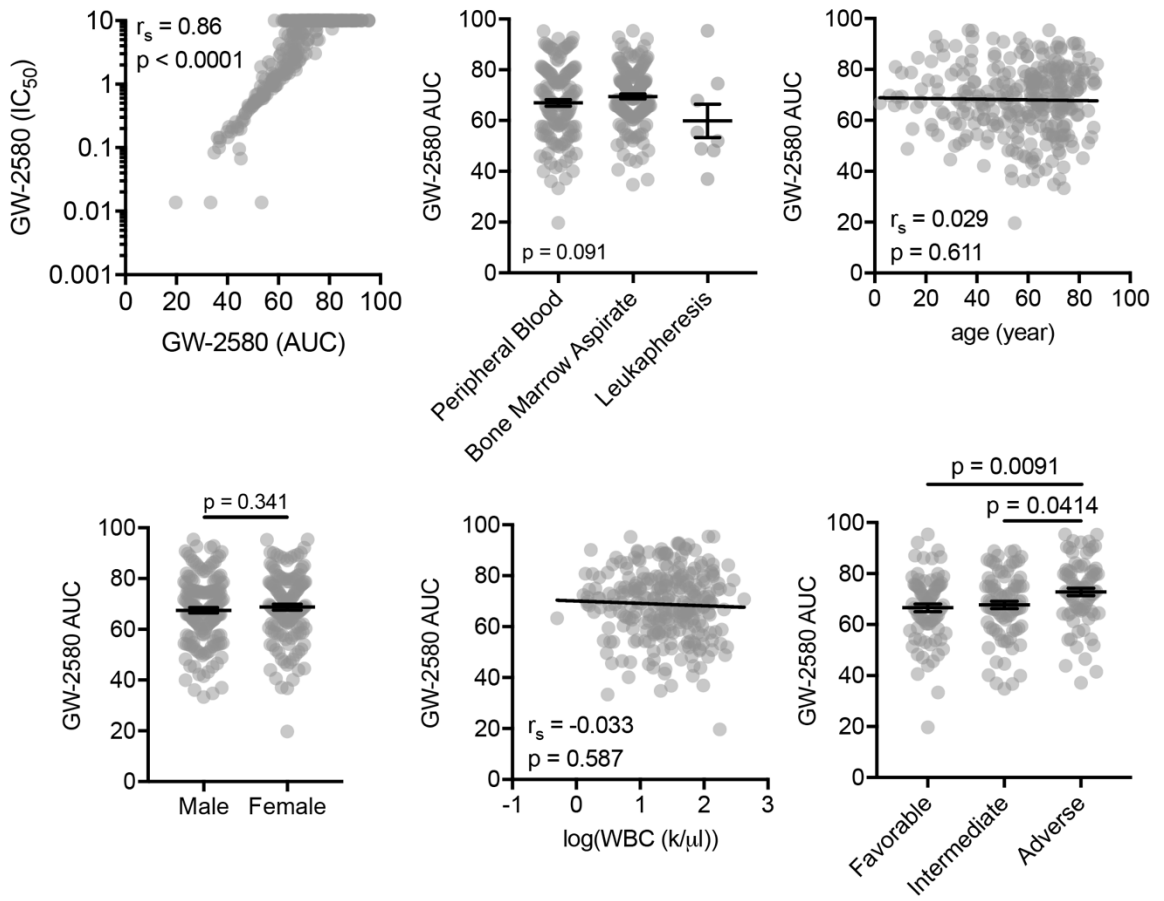
(A-B) Percent apoptosis after 24-, 48-, and 72-hour exposure to 10 μ M GW-2580 or ARRY-382 in two primary AML patient samples: (A) 18-00173 and (B) 18-00179.

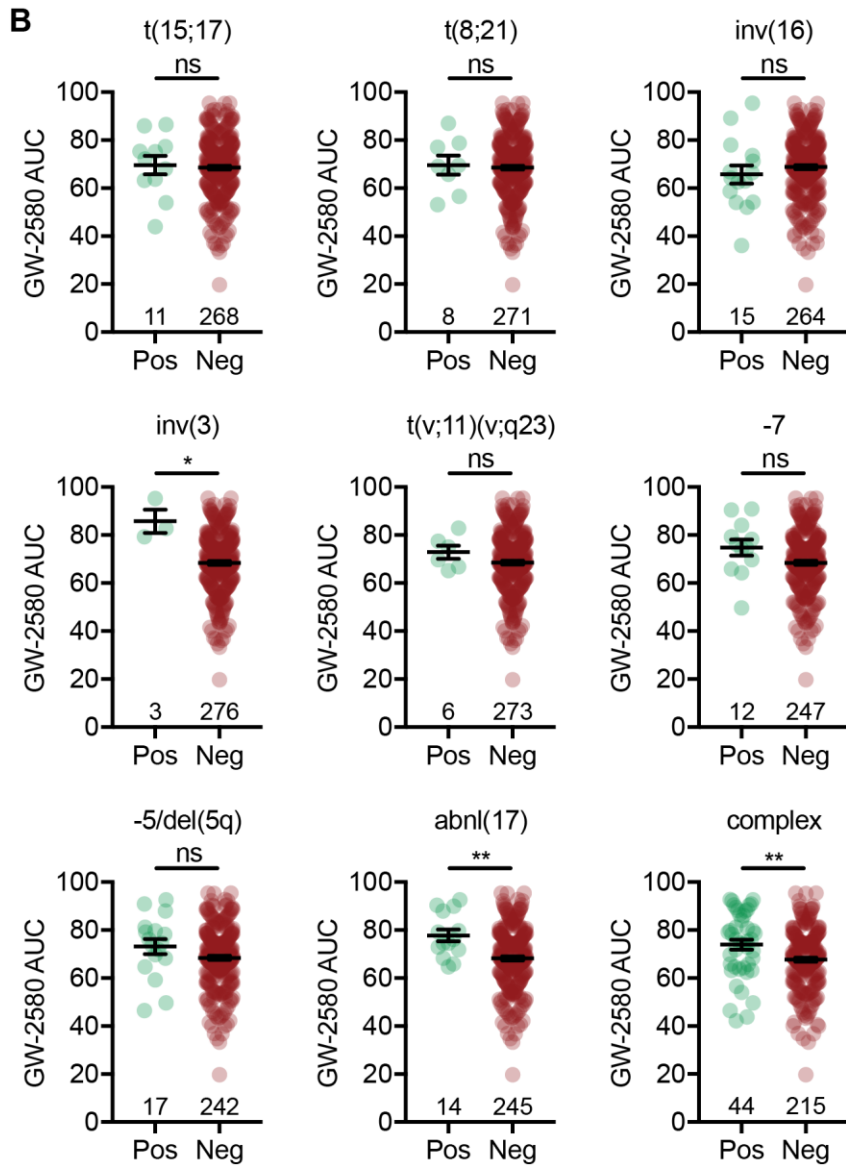
The percentage of apoptotic cells for each patient sample was normalized to untreated control cells to account for sample-specific variations in cell viability.

(C-E) Spearman correlation and associated p-value for (A) GW-2580 AUC vs. ARRY-382 AUC (n = 244 patient samples); (B) GW-2580 AUC vs. JNJ-28312141 AUC (n = 305 samples); and (C) ARRY-382 AUC vs. JNJ-28312141 (n = 243 samples).

(F-J) GW-2580 dose-response curves for MNCs isolated from five healthy donors: (F) 07-00332, (G) 07-00363, (H) 08-00007, (I) 08-00073, and (J) 08-00236. AUCs determined by probit regression (see **Supplemental Methods**).

A





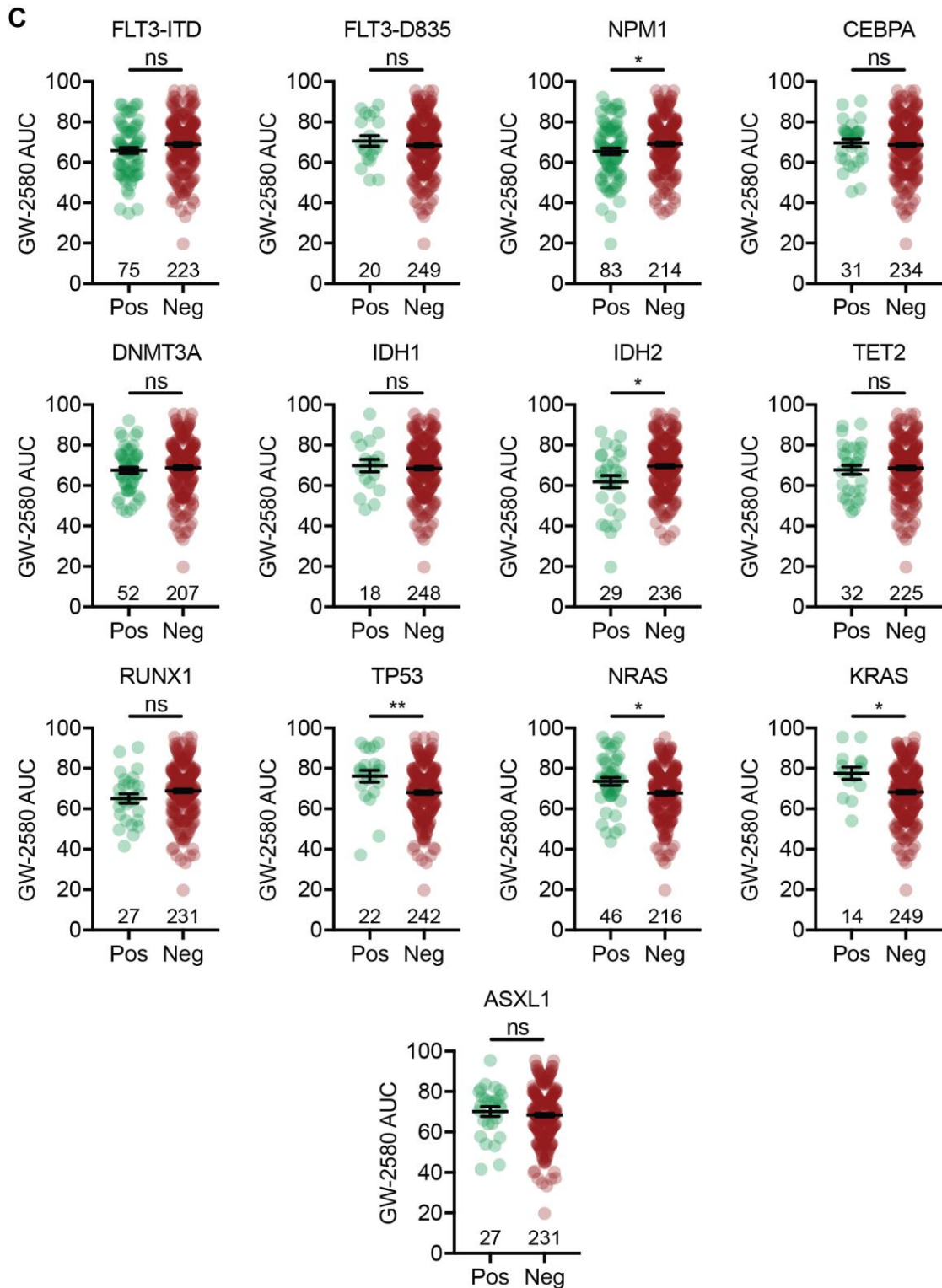


Figure 8.7. Individual correlation graphs of CSF1R inhibitor sensitivity for each clinical and genetic characteristic evaluated in this study.

(A) Comparison of GW-2580 AUC and GW-2580 IC₅₀, specimen type, patient age, patient gender, WBC count, and prognostic risk. Black bars represent mean \pm SEM; statistics determined by Spearman's rank correlation (GW-2580 IC₅₀, age, and WBC count), Mann-Whitney test (gender), and Kruskal-Wallis test with Dunn's multiple comparison's test (specimen type and prognostic risk) if necessary.

(B) Comparison of GW-2580 AUC between patient samples with or without karyotypic abnormalities commonly observed in AML. Black bars represent mean \pm SEM; significance determined by Mann-Whitney test.

(C) Comparison of GW-2580 AUC between mutant or wildtype patient samples in genes commonly mutated in AML. Black bars represent mean \pm SEM; significance determined by Mann-Whitney test.

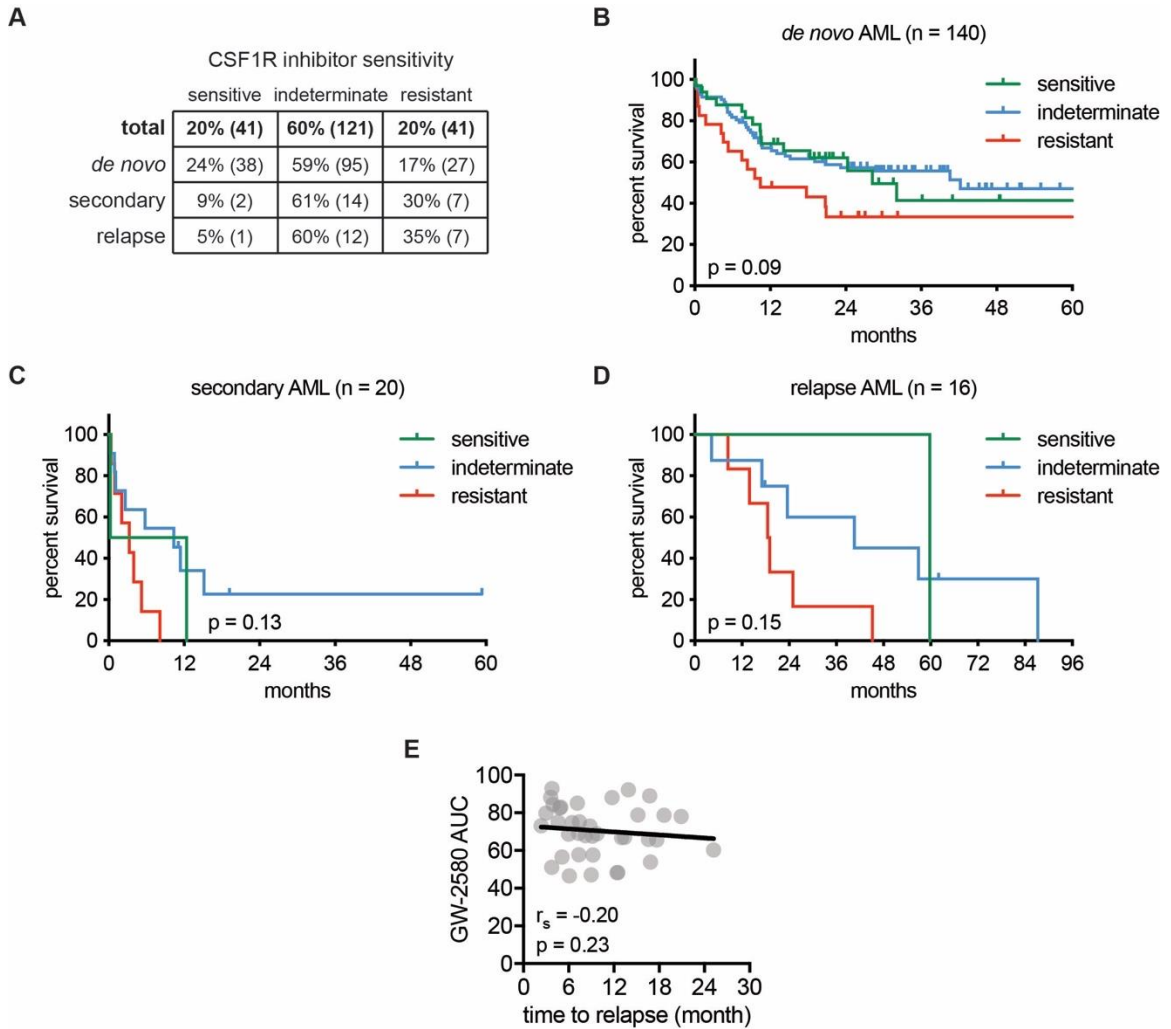


Figure 8.8. No correlation between CSF1R inhibitor sensitivity and differences in overall survival or disease presentation.

(A) Table comparing the distribution of the CSF1R inhibitor sensitivity subgroups across *de novo* (n = 161), secondary (n = 23), and relapsed (n = 21) AML patient samples that had associated clinical data.

(B-D) Kaplan-Meier survival curve of patients with both clinical and survival data whose disease at the time of sample collection presented as (B) *de novo* (n = 140), (C) secondary (n = 20), and (D) relapsed (n = 16) AML, divided into the corresponding CSF1R inhibitor sensitivity subgroups. Significance determined by log-rank test.

(E) Comparison between time to relapse for the AML patient population (n = 37 patients with eventual relapse) among the CSF1R inhibitor sensitivity subgroups. Significance determined by Spearman's rank correlation.

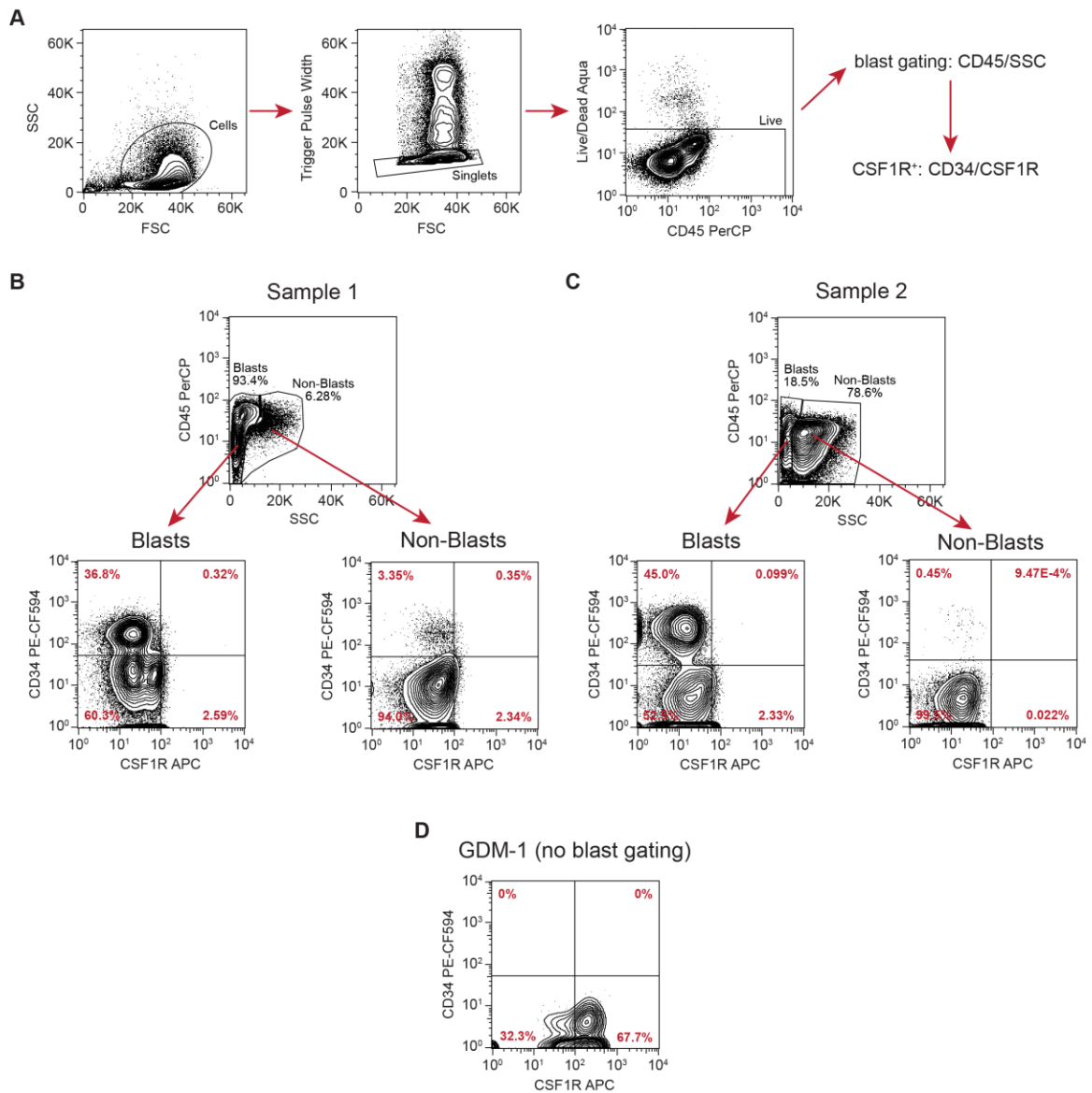
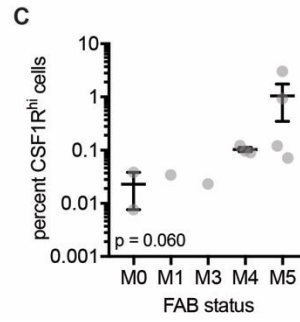
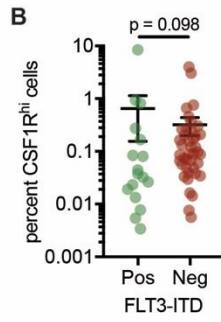
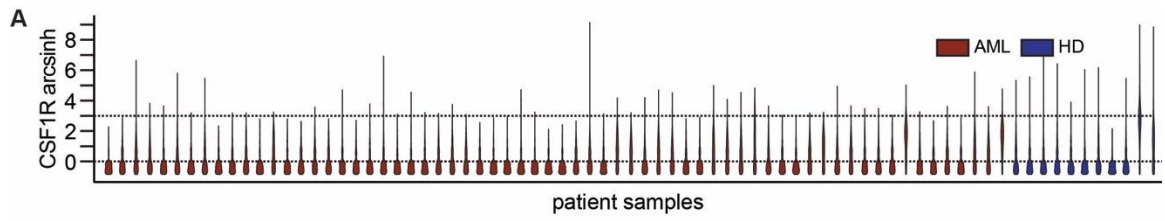


Figure 8.9. CSF1R is not expressed on leukemia blasts from primary AML patient samples.

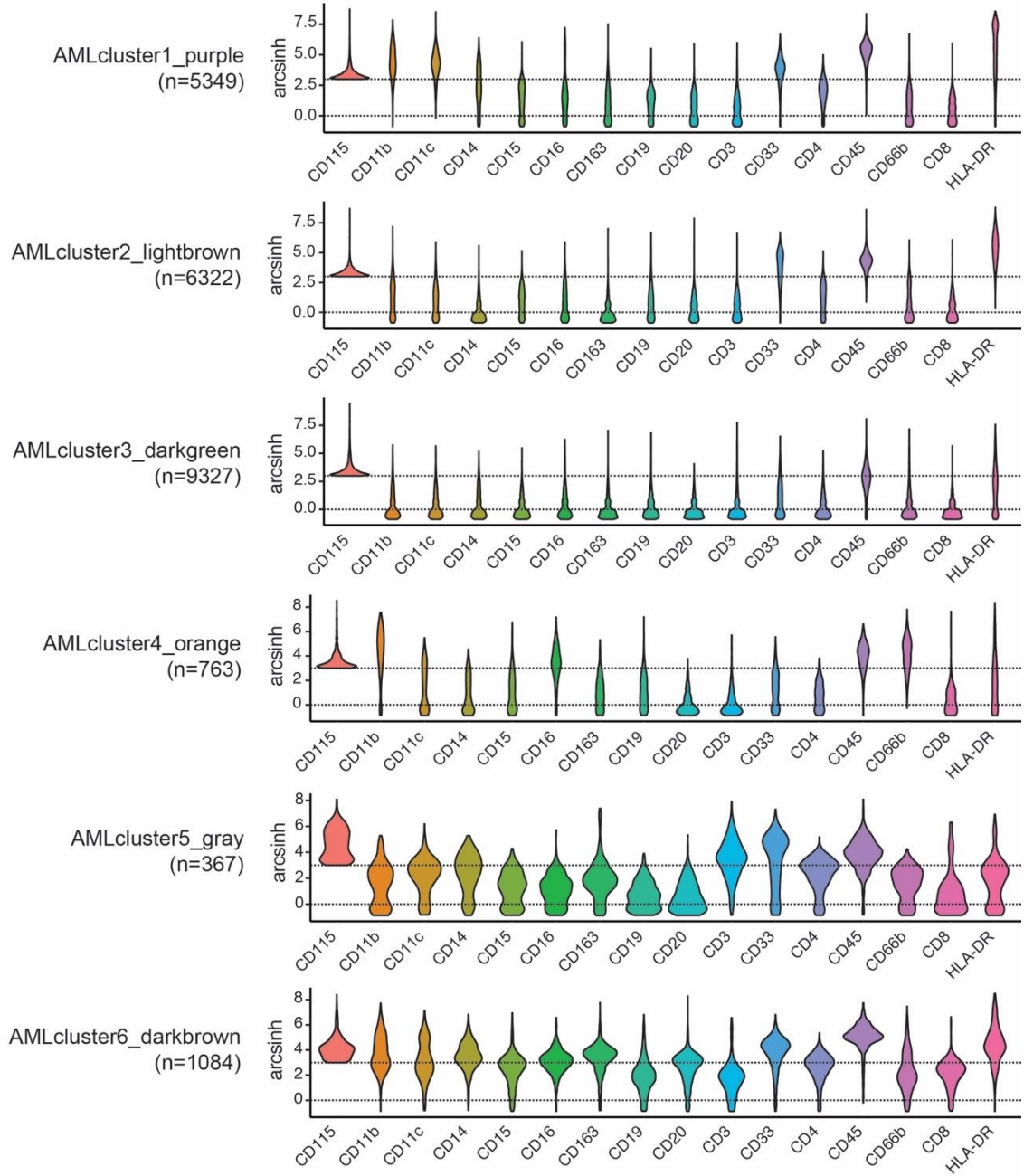
(A) Gating strategy for flow cytometry analysis of primary AML patient samples to identify CSF1R⁺ cells.

(B-C) Overall, CSF1R is not expressed on the CD34⁺ leukemia blasts from two primary AML patient samples, (B) Sample 1 and (C) Sample 2.

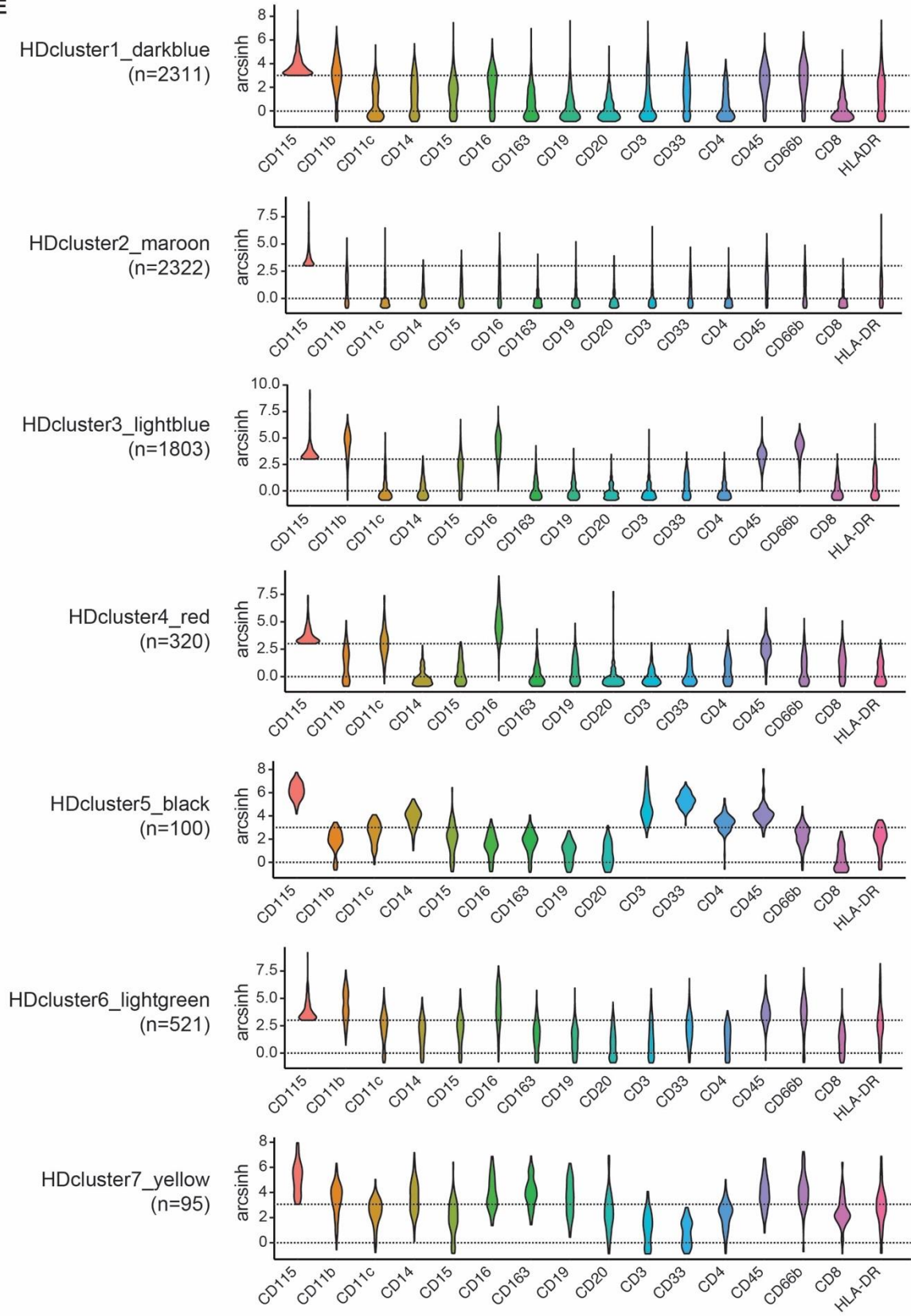
(D) As a positive control, CSF1R is expressed on a significant proportion of GDM-1 cells, an AML cell line with an activating mutation in CSF1R (Y571D).



D



E



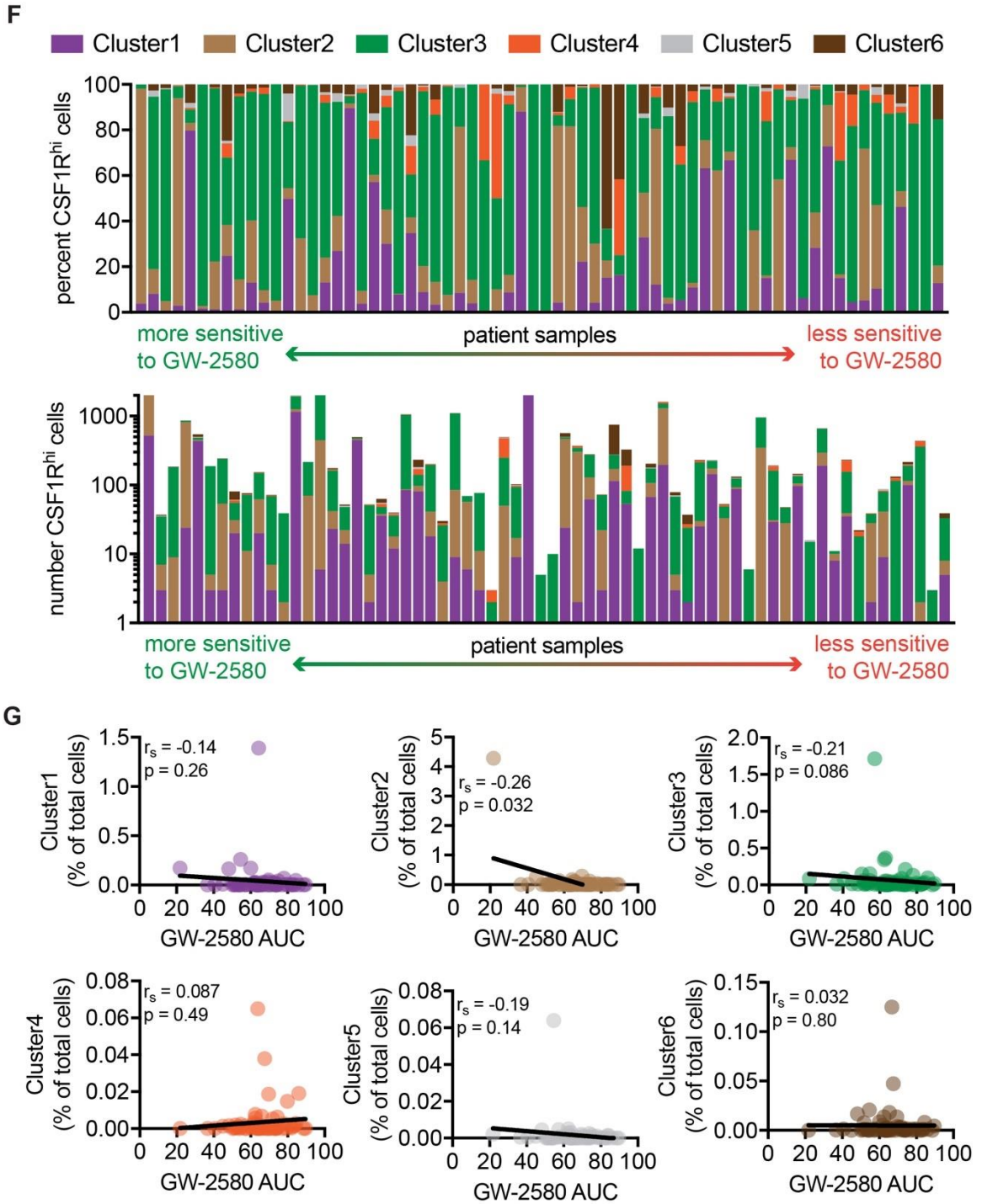


Figure 8.10. CSF1R^{hi} cells cluster into unique subgroups in AML patient samples that correlate differently with *ex vivo* GW-2580 response.

(A) Violin plots of CSF1R expression intensity in AML patient samples (n = 66) and healthy donors (n = 11).

(B-C) Association between percentage of CSF1R^{hi} cells and (B) FLT3-ITD status (n = 58 patient samples) or (C) FAB morphology (n = 11). Significance for (B) determined by Mann-Whitney test; significance for (C) determined by Kruskal-Wallis test.

(D-E) Violin plots of cell-surface marker expression intensity for CSF1R^{hi} cell subgroups in (D) AML samples and (E) healthy donors.

(F) Percentage and number of CSF1R^{hi} cell subgroups for AML patient samples, ranked in order of GW-2580 AUC.

(G) Correlation between CSF1R^{hi} cell subgroup percentage and GW-2580 AUC for each CSF1R^{hi} subgroup in AML patient samples. Significance determined by Spearman's rank correlation.

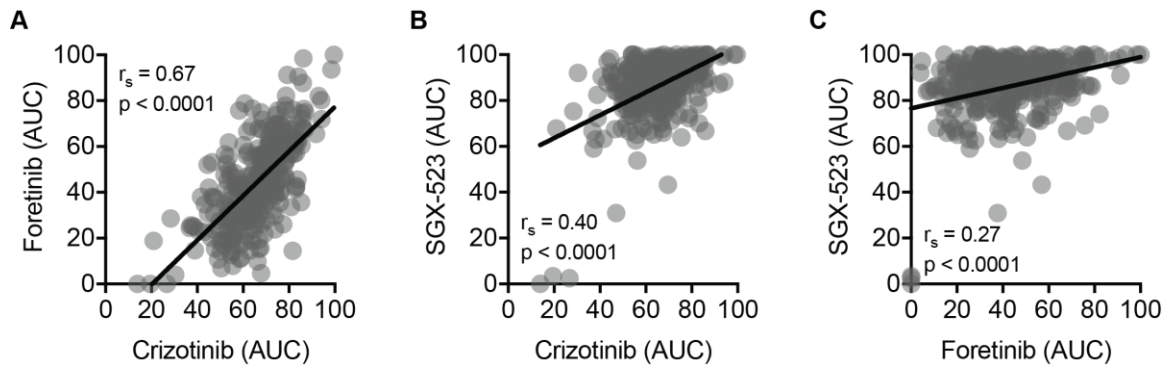


Figure 8.11. Significant correlation exists between inhibitors of MET in AML patient samples.

(A-C) Correlation between the area under the curve for MET inhibitors (A) crizotinib and foretinib, (B) crizotinib and SGX-523, and (C) foretinib and SGX-523 in AML patient samples ($n = 300$). Significance determined by Spearman's rank correlation.

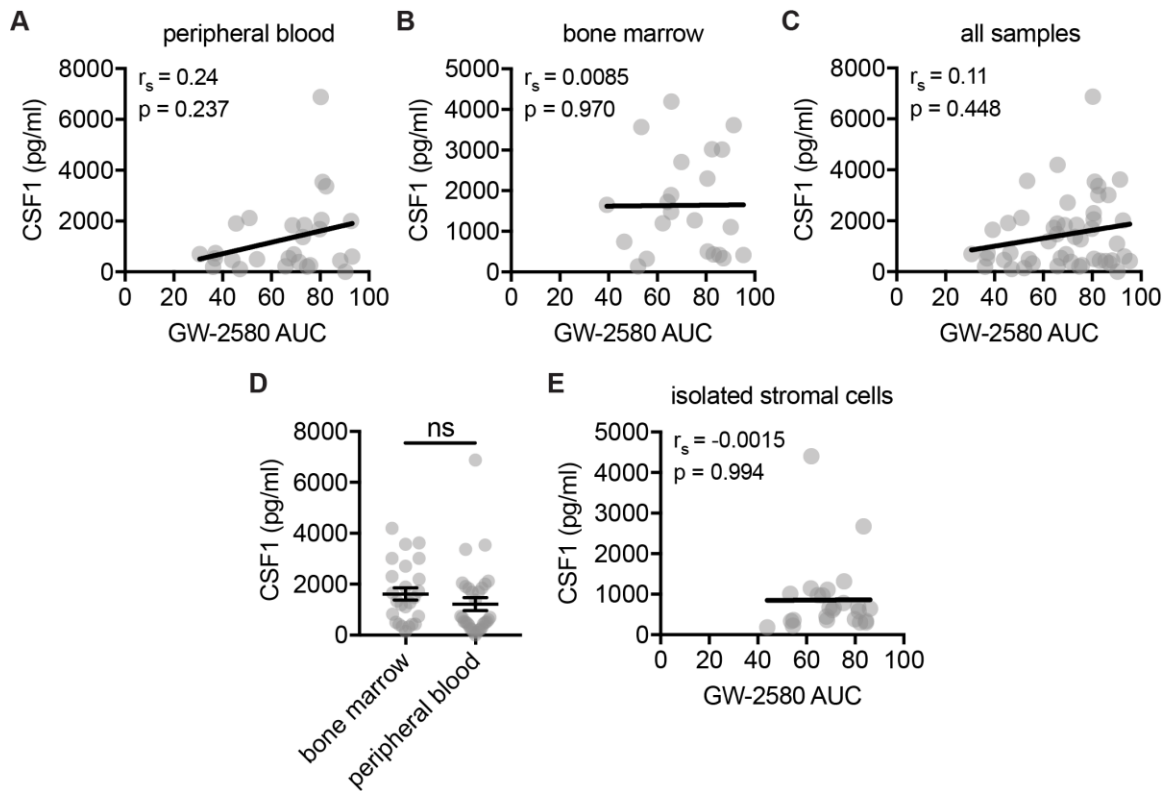


Figure 8.12. CSF1R inhibitor sensitivity is not associated with CSF1 levels in AML patient samples or sample-derived stromal cells.

(A-C) No significant correlation between CSF1 concentration in patient plasma and GW-2580 sensitivity for primary AML patient samples isolated from (A) peripheral blood ($n = 27$) and (B) bone marrow ($n = 22$), or from (C) both sample types combined.

(D) No difference between CSF1 concentration in plasma from bone marrow and peripheral blood samples.

(E) No correlation observed between CSF1 levels secreted from stromal cells isolated from primary AML patient samples, and the GW-2580 sensitivity of those samples (see Supplemental Methods).

9 Discussion

The results described in this dissertation identify colony stimulating factor 1 receptor (CSF1R) as a promising therapeutic target that eliminates the tumor microenvironment in chronic lymphocytic leukemia (CLL) and acute myeloid leukemia (AML) patient samples. The research was compiled into two manuscripts, one characterizing CSF1R in CLL, the other CSF1R in AML. For each manuscript, a discussion of the implications of these findings on their corresponding subtype-specific fields of leukemia research was included, and has been faithfully replicated in this dissertation (see section 7.5 Discussion for CSF1R in CLL and section 8.8 Discussion for CSF1R in AML). Therefore, a more thorough discussion integrating these two projects—a discussion about their similarities and differences, their collective contributions on the field of tumor microenvironment research, and intriguing future directions and experiments—will be included here.

One of the most prominent similarities is the comparable percentage of CLL and AML samples that demonstrate sensitivity to CSF1R inhibitors. For CLL, roughly one-quarter of *ex vivo* patient samples showed sub-micromolar sensitivity to two CSF1R-specific inhibitors, GW-2580 and ARRY-382 (Figure 7.1), sensitivity values that correspond roughly to the physiologically relevant concentrations in animal studies. Additionally, for AML, roughly one-quarter of *ex vivo* patient samples were considered “hits” using the RNAi-assisted protein target identification (RAPID) siRNA functional screen (Figure 8.1B). Notably, CLL patient samples were not evaluated using the RAPID screen because CLL cells have limited survival

ex vivo and cannot sufficiently withstand the required electroporation step (see Electroporation of siRNA Library BioRad (AML Patient Sample) Protocol).

Although additional research is required to directly correlate *ex vivo* screening data with clinical trial results in patients with CLL and AML, the percentage of sensitive samples observed during my research is similar to the percentage demonstrated in clinical trials from other cancer types. Two common endpoint measurements for clinical trials are (1) the objective response rate (ORR), or the percentage of patients whose disease decreases or disappears (achieves partial or complete response); and (2) the clinical benefit rate, or the percentage of patients whose disease decreases or remains stable over time. Based on preliminary published data from the CSF1/CSF1R clinical trials in patients with various solid tumors, Hodgkin's lymphoma, and glioblastoma, the average ORR and CBR, and the corresponding standard error of the mean, is 4.42 ± 6.02 (n = 7) and 32.3 ± 19.3 (n = 6), respectively (see Table 6.1). These results suggest that the predicted outcome of a minority of leukemia patients responding to CSF1R inhibitor treatment might be more universal across cancer subtypes.

In terms of better understanding this minority of leukemia patients, or predicting patient sample response to CSF1R inhibitor treatment, it is worth noting that the conclusions were similar in both CLL and AML projects. I identified no singular genetic and clinical characteristics that could biologically explain CSF1R inhibitor sensitivity. This underscores the universality of targeting the tumor microenvironment, that CSF1R inhibitors are effective across AML and CLL regardless of their genetic or cytogenetic abnormalities. Notably, the AML patient

samples utilized in my dissertation research were part of the Beat AML Project and had detailed clinical annotations and next-generation sequencing. Consequently, I made substantially more detailed comparisons between patient characteristics and CSF1R inhibitor sensitivity, including evaluating prognostic risk guidelines that combined multiple genetic abnormalities, overall survival data, and time to relapse.

Based on some of these comparisons, I hypothesized that AML samples with CSF1R inhibitor resistance might represent a later stage of leukemia development than sensitive samples. Because I observed a significant correlation between multiple adverse-risk mutations or cytogenetic abnormalities and CSF1R inhibitor resistance (Figure 8.2), I postulated that the disease in these patients becomes generally resistant to any kind of treatment (see Discussion). In addition, I discovered that relapsed AML samples have significantly higher GW-2580 area under the curve (AUC) than that of *de novo* or transformed AML samples (Figure 8.2B). This is a similar correlation observed in CLL between treatment-naïve and relapsed samples (Figure 7.7E). Additionally, although overall survival data was not available for CLL patients, I hypothesize that there would be no association between survival and CSF1R inhibitor sensitivity, as observed in AML patients.

One of the most promising future directions for this dissertation research is the multicenter phase II clinical trial currently in development at Oregon Health & Science University. The clinical trial is based largely on the preliminary data that inspired the development of these two projects (i.e. the appearance of CSF1R-inhibitor-sensitive AML and CLL samples in the functional screening data). Reciprocally, these projects themselves have inspired correlative studies to be

conducted throughout the course of the trial. Ultimately, the clinical trial will evaluate the effectiveness of an as-yet-undisclosed CSF1R small-molecule inhibitor in AML and CLL patients, based on the classification of “sensitive” versus “insensitive” groups by patient sample functional screening.

The primary endpoint for the clinical trial is objective response rate (ORR), and the secondary endpoints are the incidence of treatment-related toxicity (identified as Grade 3 or higher), duration of response, 12-month progression-free survival, and 12-month overall survival. To be included in the trial, patients must have histologically confirmed CLL or AML (acute promyelocytic leukemia patients are excluded), including a bone marrow biopsy and aspirate or lymph node biopsy. They must be at least 18 years old with normal organ and bone marrow function, no uncontrolled infections or active hepatitis, and an ECOG (Eastern Cooperative Oncology Group) performance grade ≤ 2 (Karnofsky grade ≥ 60).²⁵⁶ CLL patients must have received at least two prior therapies and possess measurable relapsed or refractory disease in accordance with the 2008 International Workshop on Chronic Lymphocytic Leukemia guidelines.²⁵⁷ AML patients must have relapsed or refractory disease, having received at least one prior therapy.

Patients will be assessed throughout the trial with bone marrow biopsies collected after treatment cycles 1-3, and then Q3 cycles, where hematologic response and transfusion dependence will be measured. Serial samples will be obtained over time to evaluate any changes that might occur within the tumor (gene expression or genetic/cytogenetic abnormalities), or within the microenvironment, that could contribute to treatment resistance. The purpose of obtaining these samples is to

determine if a clinical or genetic signature can be identified in patients to predict response, and to ascertain how resistance can develop in patients.

Notably, according to the clinical trial protocol, a “sensitive” sample is one whose half maximal inhibitory concentration (IC50) for a particular drug is <20% of the median for all patient samples tested with that drug. This measurement has been the standard methodology by which our lab has quantified the functional screening data, established before I began my dissertation research.¹⁹⁵ Now, based upon the results of my research, I would recommend modifying this standard in a couple of strategic ways. First, I would consider replacing IC50 with AUC, since AUC is a better single parameter for combining potency and efficacy, provided that the drug range being evaluated is held constant.²⁴² Although IC50 is more recognizable clinically, it might not necessarily be the optimal pharmacokinetic “driver for efficacy,” or the variable that correlates best with patient response, so multiple mathematical representations of drug sensitivity should be considered in preclinical profiling.²⁵⁸

Second, I would suggest replacing that definition of “sensitivity” with other definitions or conventions used in this dissertation. Specifically, the definition could be replaced by the overall percentage of CSF1R^{hi} cells (as determined by CyTOF^m; Figure 8.3) or its relative sensitivity percentile (by AUC) when compared to the majority of other patient samples (Figure 8.2). Ultimately, conducting a

^m Relying on CyTOF for clinical treatment would be challenging due to the time-consuming nature of CyTOF analysis, and defining an exact percentage cutoff would require additional, more precise experiments. However, modifying the antibody for traditional fluorescence-based flow cytometry, which is conducted routinely for patients in clinic, could be an effective substitute.

comprehensive analysis of the incoming trial data will determine the best long-term strategy of evaluating sensitivity.

Throughout the duration of the trial, various monitoring and correlative studies will be conducted. First, the pharmacokinetics of the CSF1R inhibitor will be evaluated by measuring the plasma inhibitory activity (PIA), which is the percent decrease of the phospho-CSF1R band by immunoblotting after drug treatment compared to a baseline measurement.²⁵⁹ This is not only crucial information for the drug manufacturer to assist in developing that drug for other indications, but also for evaluating the functional screening data. Correlating results from *in vitro* (or *ex vivo*) and *in vivo* drug experiments can be challenging and vary depending on the type of inhibitor,²⁶⁰ and the clinical trial would provide excellent data on correlating the IC50 or AUC from our *ex vivo* patient sample functional screening with the appropriate clinical dose for the same patient. As an extension of this monitoring study, and partially as a confirmation of the predictive power of the *ex vivo* functional screening assay, any measured change to patient sample sensitivity before and after CSF1R inhibition treatment will be correlated with patient response to treatment.

Second, the effect of CSF1R inhibitor treatment will be evaluated on immune cell subpopulations (cytotoxic T cells, etc.) by CyTOF, especially to evaluate the potential reversal of reprogramming or anergy induction by the CSF1R-expressing cells. As previously mentioned, immune cell subpopulations can be reprogrammed by TAMs and other supportive monocytes/macrophages (see section 7.3 Introduction for CLL and section 8.4 Introduction for AML). This analysis has particular clinical interest because the effectiveness of anti-CSF1R treatments is

currently being investigated in clinical trials in combination with immunotherapy agents.¹²² Simultaneously blocking the tumor-promotional effect of CSF1R-expressing cells and stimulating immune function and anti-tumor response could have significant lasting benefit for CSF1R-inhibitor-sensitive patients.

Third, the downstream signaling within CSF1R-expressing cells will be measured using a combination of plasma membrane phosphoproteomics (by CyTOF) and single-cell RNA (scRNA) sequencing. The results from these experiments should be compared to the signaling changes in blood cells from healthy donors after CSF1R inhibitor treatment. This will help determine if reprogrammed CSF1R-expressing cells have differential activation of regulatory pathways, and if these pathways are differentially perturbed after exposure to CSF1R inhibitors.

These studies also address a remaining question from this dissertation research—namely, whether differential regulatory pathways are being activated in reprogrammed CSF1R-expressing cells. To answer this question, it is first important to understand what is currently known about reprogrammed supportive monocytes/macrophages. For CLL, as mentioned previously (see CSF1R in chronic lymphocytic leukemia), the extent of phenotypic reprogramming in nurse-like cells has been only partly studied, although it has gained more attention in recent studies.^{157,160,216} However, highly CSF1R-expressing nurse-like cells do not appear to constitute the entire population of nurse-like cells,¹⁵⁷ and if they represent a subpopulation of nurse-like cells, the degree to which phenotypic reprogramming has impacted these cells remains unknown.

To address the extent of phenotypic reprogramming in CSF1R-expressing cells, I recommend scRNA sequencing of CSF1R-expressing cells in AML and CLL patients, preferably before and after CSF1R inhibitor treatment. Recently, there were prominent scRNA sequencing studies performed on CLL patient samples.^{261,262} However, in both of these studies, the patient sample cells were sorted by flow cytometry to select only CLL cells (CD19+/CD5+) prior to sequencing, and therefore any supportive cells (including CSF1R-expressing cells) would have been eliminated from the downstream analysis.

I take inspiration from recent studies on other cancer types, which provide examples of effective methodological approaches to address this question. To conduct comprehensive immune and tumor cell profiling, Chung et al performed scRNA sequencing on 515 cells from 11 patients with breast cancer.²⁶³ Using chromosomal gene expression patterns and a tumor-purity analysis method called ESTIMATE,²⁶⁴ the researchers identified 175 tumor-associated immune cells, further subdividing them into B cells, T cells, and macrophages, based on established gene ontology terms.²⁶⁵ Another study conducted by Müller et al more directly compared phenotypic differences in human glioma TAMs with macrophages isolated from mouse models of glioma and from normal human tissue.²⁶⁶ They alternately perform CD11b+ selection and no selection on glioma cells, identifying TAMs by positive macrophage-associated gene expression and exclusion of somatic tumor mutations.²⁶⁶

Based on these methodologies, I recommend performing a CSF1R selection on patient samples and analyze the scRNA sequencing results under two conditions:

(1) before and after CSF1R inhibitor treatment; and (2) between leukemia patient samples and healthy donors. I found that CSF1R inhibitors eliminate nurse-like cells from culturing onto plastic in *ex vivo* patient samples (Figure 7.4). However, the consequence of CSF1R inhibitors on AML patient samples is unknown. There are two possible mechanisms of action for CSF1R inhibitors in AML patients: (1) CSF1R inhibitors are eliminating CSF1R-expressing cells, thereby depleting their secretion of essential growth factors; or (2) CSF1R inhibitors are reprogramming CSF1R-expressing cells, transitioning them away from a tumor-promotional phenotype and preventing their secretion of growth factors. Because there is no well-characterized population of “nurse-like cells” in AML, nor are there long-term culturing assays designed to isolate supportive cells from the surrounding tumor cells, conducting CyTOF experiments before and after CSF1R inhibitor treatment would provide an essential, definitive answer to this lingering question.

The results from these sequencing studies would inspire additional downstream experiments. Depending on the transcriptional pathways that are identified, one could manipulate primary patient samples *ex vivo* using various specific monoclonal antibodies or cytokines/growth factors and determine if CSF1R-expressing cell reprogramming can be reversed, or determine how normal CSF1R-expressing cells can be reprogrammed into tumor-supportive monocytes/macrophages. These studies could enable the transition from *ex vivo* patient sample studies into patient-derived xenograft (PDX) mouse models, in which primary patient samples would be injected into mice along with reprogrammed

CSF1R-expressing monocytes, opening up entirely new offshoots of research possibilities.

Fourth, the effectiveness of combining CSF1R small-molecule inhibitors with other targeted small-molecule inhibitors will be evaluated. It should be noted that the “targeted” small-molecule inhibitors to which I am referring generally target multiple kinases other than their intended primary target. While there are some CSF1R small-molecule inhibitors that are extremely specific for CSF1R (e.g. GW-2580 and ARRY-382), other inhibitors designated as “CSF1R inhibitors” are less specific, especially against other Class-III receptor tyrosine kinases (e.g. JNJ-28312141 and most inhibitors currently in clinical trials¹²²; see Figure 8.1C).

There are promising targeted therapies to combine with CSF1R small-molecule inhibitors. In CLL patient samples, I demonstrated the synergistic combination of GW-2580 with both ibrutinib and idelalisib (Figure 7.5). As previously mentioned, these two therapies have increased the survival rate for CLL patients and are rapidly becoming standard-of-care treatment strategies. This raises the likelihood of combining these therapies with CSF1R inhibitors if this preliminary clinical trial succeeds, and, if so, these results will encourage inclusion in future clinical applications.

Other research from our lab performed similar functional screening of hundreds of samples from patients with various hematological malignancies, with samples being exposed to multiple combinations of molecularly targeted therapies. The results of this screening were recently published by Kurtz et al, in which 58 AML samples and 42 CLL samples were screened against 48 drug combinations.²¹⁹

Notably, the CSF1R-specific inhibitor ARRY-382 was featured in 7 combinations, paired against venetoclax (selective inhibitor of B-cell lymphoma 2, or BCL-2, an anti-apoptotic protein), panobinostat (histone deacetylase, or HDAC, inhibitor), JQ1 (bromodomain inhibitor), quizartinib (FLT3 inhibitor, although it inhibits other Class-III receptor tyrosine kinases, including CSF1R), palbociclib (inhibitor of cyclin-dependent kinases 4 and 6, or CDK4/6), idelalisib (as mentioned above, a phosphatidylinositol-3-kinase delta isoform specific, or PI3k δ , inhibitor), and trametinib (inhibitor of mitogen-activated protein kinase kinase, or MEK).²¹⁹

From this functional screening data, 3 significantly effective inhibitor combinations were found involving ARRY-382 for AML and CLL patients: idelalisib and ARRY-382 (for both AML and CLL samples), venetoclax and ARRY-382 (AML only), and trametinib and ARRY-382 (AML only).²¹⁹ As previously mentioned, I demonstrated that the combination with idelalisib is effective in a different set of CLL patient samples, thus providing external validation of these newly published findings. The combination with venetoclax is intriguing for multiple reasons. The effectiveness of venetoclax was recently demonstrated AML both as a monotherapy and in combination with other inhibitors,²⁶⁷ and there are currently three clinical trials recruiting patients to combine venetoclax with other targeted therapies (ClinicalTrials.gov ID codes NCT02670044, NCT02670044, and NCT02391480). Moreover, venetoclax was shown to be effective in CLL patients with relapsed/refractory disease and 17p deletion,²⁶⁸ resulting in a Breakthrough Therapy designation by the US Food and Drug Administration (FDA) in 2016. The third inhibitor combination with trametinib remains understudied, although the

results of a phase 1/2 clinical trial examining the effectiveness of trametinib on relapsed or refractory myeloid malignancies found preferential efficacy against RAS-mutant AML.²⁶⁹ Further research would be required to confirm these effective combinations and identify the mechanism of action underlying their synergy.

Importantly, the results from the Kurtz et al combination screening are not comprehensive. Although I did not personally evaluate the potential synergy of CSF1R inhibitors with other targeted therapies in AML patient samples, the survey of clinical and genetic characteristics of patient samples does hypothesize one additional combination. I observed that the presence of IDH2 mutations correlates significantly with CSF1R inhibitor response (Figure 8.2), suggesting that a combination of CSF1R inhibitors with IDH2 inhibitors might be effective in AML patients. Moreover, the population of AML patients that could be impacted by this combination is not trivial. IDH2 is the fourth most frequently mutated gene in AML, impacting roughly 10% of AML patients.²⁴ My results suggest that the number of IDH2-mutant patients whose samples exhibit *ex vivo* sensitivity to CSF1R inhibitors is ~5% (frequency of IDH2-mutant patients whose samples are within the top 20th percentile of CSF1R sensitivity; see Figure 8.2). I recommend evaluating this combination in our *ex vivo* functional screening, which would prompt further studies into uncovering the underlying mechanism.

It should be mentioned that although this dissertation describes the effectiveness of CSF1R-specific small-molecule inhibitors against primary AML and CLL patient samples, I did not evaluate the effectiveness of CSF1R neutralizing antibodies. Currently, there are 5 CSF1R small-molecule inhibitors and 5

CSF1/CSF1R monoclonal antibodies being evaluated in clinical trials for cancer patients.¹²² Based on dozens of multiple *in vitro* and *in vivo* studies from researchers across many different cancer subtypes, there is no evidence of any pharmacological difference between these two categories of CSF1R-targeted therapies in terms of effectiveness or clinical tolerance, and both are often described interchangeably.¹²² Consequently, I predict I would observe a similar efficacy profile for neutralizing antibodies in *ex vivo* patient sample screenings. Moreover, because the monoclonal antibodies would be administered intravenously, and because the bloodstream is the home of the tumor itself in leukemia patients, the phenomenon of reduced tissue perfusion common to monoclonal antibodies would not be a significant issue.

There are notable differences in the experiments performed on CLL and AML patient samples, and many of these disparities are based on distinct biological differences between the CSF1R dependencies in both leukemia subtypes. For example, we published data where we performed CD14+ depletion in CLL patient samples (Figure 7.4 and

Figure 7.9). We showed that the percentage of CD14+ cells correlated with CSF1R inhibitor sensitivity, and patient samples with greater sensitivity showed a more significant decrease in cell viability upon CD14+ depletion. These results inspired CD14+ depletion experiments on primary AML patient samples. However, I observed no preferential decrease in cell viability or reduction in CSF1R inhibitor sensitivity in CSF1R-inhibitor-sensitive samples (data not shown).

Initially, I assumed that the phenotype of CSF1R-expressing cells would be similar between CLL and AML patient samples. However, our CyTOF data showed that CD14 is co-expressed on a small majority of CSF1R^{hi} reprogrammed AML cells (Figure 8.3), which was unexpected. Performing depletion studies on more commonly co-expressed cell surface markers such as HLA-DR and CD33, markers that are indicative of tumor-specific phenotypic reprogramming and were found to correlate significantly with CSF1R inhibitor sensitivity, might produce similar results to CD14 depletion in CLL patient samples. Later, we attempted a CSF1R-specific cell depletion by conjugating a biotinylated CSF1R antibody with streptavidin-coated magnetic beads, although technical challenges and time limitations prevented these studies from achieving success; perhaps employing alternative techniques, such as cell sorting by flow cytometry, would prove more effective.

Anticipating reviewer comments regarding the CSF1R in AML project following the manuscript submission, I conducted rescue experiments on primary AML patient samples (data not shown). These experiments address the possibility that the cytokines and growth factors secreted by CSF1R^{hi} supportive monocytes/macrophages by themselves can rescue tumor cell viability after exposure to CSF1R inhibitors. I exposed primary AML patient cells either to recombinant HGF, MCP-1, and IL-8 (at the maximum concentrations used in the growth factor assay described in Carey et al²²⁶), or media conditioned by immortalized HS-5 human marrow stromal cell line. These cells were subsequently exposed to dose-escalating concentrations of GW-2580 and incubated for 72 hours, after which cell viability was assessed.

I observed a rescue of growth for HS-5-conditioned media, which contains a multitude of cytokines and growth factors, as well as rescue of slight CSF1R inhibitor sensitivity from the aforementioned cytokines at least one patient sample. This observation suggests that HGF, MCP-1 and IL-8 are not the only supportive signals provided by the supportive monocytes/macrophages. Additional experiments could address this question more definitively, including adding antibodies blocking the effects of the cytokines in AML cells and measuring their impact on cell viability. Moreover, the aforementioned scRNA sequencing of CSF1R^{hi} cells could provide important answers to the pathways that are upregulated in these supportive cells and what combination of growth factors they are producing to enhance leukemia cell survival.

10 Appendix

10.1 Detailed Protocols Used in Dissertation Research

This appendix contains more comprehensive versions of the protocols described in the CSF1R in AML portion of this dissertation. Although these protocols are discussed in Methods and Supplemental Methods, due to the limited space requirements for scientific manuscripts, they do not have sufficient detail to completely recreate the experiments. To replicate the work contained within this dissertation, or to more thoroughly analyze or understand it, having access to these detailed protocols is critically important.

Some of these protocols are copied directly from standardly implemented practices in the Druker/Tyner labs (e.g. “Processing Patient Peripheral Blood and Bone Marrow Samples Protocol” and “Electroporation of siRNA Library BioRad (AML Patient Sample) Protocol”), and the others were developed and written by me, unless otherwise indicated. There are two components of computational data analysis that have not been included in this section but are been described in significant detail in Supplemental Methods. The first is accessing the AML patient sample information from the Beat AML database, which was performed by Kevin Watanabe-Smith; and the second is evaluating the AML patient survival data, which was performed by Mara Rosenberg. Both of these forms of analysis were conducted in R, a statistical programming language, and R Markdown files detailing the exact computational instructions for analyzing and acquiring the data are available upon request from both researchers.

This appendix does not contain more comprehensive protocols from the CSF1R in CLL portion of this dissertation, mostly because many of those experiments—the CD14 depletion of mononuclear blood cells from CLL patient samples, the combination experiments using CSF1R inhibitors and targeted small-molecule inhibitors—were performed by Tyler Sweeney, and that information is contained in his personal records and lab notebooks.

10.1.1 *Processing Patient Peripheral Blood and Bone Marrow Samples Protocol*

This protocol is a reformatted version of the standard patient sample processing protocol used in the Tyner/Druker labs. It was last updated on February 9th, 2016, and edited by Christina Tognon, Kara Johnson, and Jeffrey Tyner.

Notes on Best Practices and the Patient Sample Database

Patient Sample Viability

- Patient samples collected at OHSU can be stored over night at 4°C.
- It can take 4-6 hrs to process a sample depending upon the size and what needs to be done with it.
- If a sample is FedEx-ed in, it should be processed the same day.
- Samples arriving from overseas may also be viable and must be processed the same day.
- *If samples are left too long before processing it may not affect initial viability but will impact viability at a later time point.*

Entering Patient Sample Information into the Database

1. If sample is from OHSU, contact Brian Junio (junio@ohsu.edu) with the MRN and initials of the patient and consent/HIPAA forms if you have them. If you pick up consent and HIPAA forms, make sure initials, signatures and dates are in the appropriate place.
2. Enter database computer system using your own login. Go through: OHSU--Database—Beat AML (LLS SCOR) Web Portal—Login (https://octri.ohsu.edu/lls_scor/login).
3. Check the MRN (Medical Record Number) to see if patient has been seen previously.
4. View Related—Hem Malignancy—Specimen—Create New—Specimen. A form will open.
5. Assign a Lab ID number (current year 000 sample #; ie 16-00021). Ensure the number has not been previously used.
6. Record the same information in the LLS database. NOTE: Date Received = processing date.

Nomenclature for Database

- Must try to use the same nomenclature when entering values for specimen volumes, cell yields, etc.
- There is no way to make these into pull-down menu format, since they are

simply numbers that will be different every time.

Please use the following formats when entering sample information:

- Volume of initial specimen: just the number, no "ml" afterwards
- Resuspension volume: same as above
- Dilution for cell count: the actual ratio, ie "1:200" instead of "200"
- Cell concentration: the actual number, not a shorthand. ie 5000000 instead of 5e6
- Cell Viability (%): just the value, no % sign (i think we were ok on this one)
- Total Viable Cells: same as cell concentration, the actual number, not shorthand
- Plasma: Cell concentration, just the number, no "ml" afterwards (for example 1.0 or 0.5). Entered under the cell number field on the derivative upload sheet, and not in the cell concentration field under Specimen.

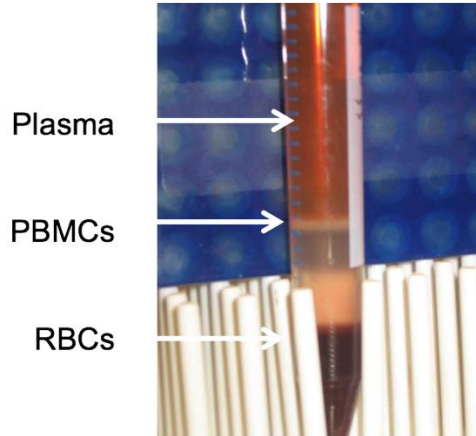
Protocol

Isolating mononuclear cells

1. Collect plasma from both peripheral blood and bone marrow by spinning the tube(s) at 2500rpm for 10min to separate out the plasma. Move the plasma into a barcoded cryotube (0.5 - 1ml/tube) and flash freeze. Mix the remaining cells and proceed to next step.
2. Prepare centrifuge tubes with Ficoll-Paque (Pharmacia). Place 4ml Ficoll in 15ml conical tubes. Often samples require two or more of these. For samples with a larger starting volume or apheresis samples, place 20ml Ficoll in 50ml conical tube.
3. Dilute peripheral blood 1:1, bone marrow 1:4 or apheresis 1:10 with warmed IMDM (GibcoBRL).
4. Carefully layer 10ml diluted sample on top of Ficoll layer. If using 50ml conical layer up to 25ml diluted sample on top of Ficoll layer.

NOTE: If sample contains significant clotting, do not add the clots to the Ficoll. To maximize MNC recovery from the clots, pipet the clots into a separate 50ml falcon tube, add 20-25ml of patient wash solution and vortex briefly. Incubate this tube on ice for 5-10min, vortex briefly again, and filter mixture into a new 50ml tube using a 70um cell strainer (BD Bio). Remove the filter and spin down the filtrate at 1200rpm for 10min. Aspirate off supernatant and proceed with RBC lysis protocol as usual. These MNC cells may then be resuspended with their corresponding sample's other Ficoll cells prior to counting.

5. Centrifuge at 1300rpm, 20min, no brake, at RT. RBCs will move down through the Ficoll and nucleated cells will stay on top of the Ficoll layer.
6. Aspirate top plasma to within 2mls of interphase or Buffy coat layer containing the peripheral blood mononuclear cells (PBMCs), which appear as a white band on the interphase layer (see below image).



7. With a 5ml pipet, draw up the mononuclear cells and transfer to a clean 50ml tube. Try to minimize the amount of Ficoll taken up. Bring up volume to 50mls with IMDM to wash out residual Ficoll. NOTE: Tubes containing blood should be disposed of in red biohazard waste bag. Deface patient information before throwing tubes out.
8. Centrifuge mononuclear cells 1100rpm, 10mins, low brake, at RT.
NOTE: You can use 1200 rpm. If cell counts are high (probably $>5 \times 10^8$), sometimes an extra 5 min is needed to pellet all cells.
9. **RBC Lysis:** ALL STEPS MUST BE PERFORMED ON ICE. Resuspend the sample in 5-20ml cold, sterile 1X ACK lysis buffer (Patient sample TC room refrigerator). Mix by inverting several times. Incubate on ice 15-20 min.

10X LYSIS REAGENT BUFFER (ACK)

- 41.3g NH_4Cl
- 5g KHCO_3
- 0.1g EDTA

Dissolve in 500ml H_2O and filter sterilize with 0.2 μm filter unit. To make 1X working solution, dilute 10X in sterile H_2O .

10. Centrifuge at 1100rpm, 10min, low brake, at RT.
NOTE: You can add IMDM to 50mls after ACK and then spin instead of a second wash step (step 11).
11. Aspirate ACK buffer and resuspend white blood cell pellet in IMDM. Repeat spin.

12. Aspirate supernatant avoiding the cell pellet and resuspend in 3-20mls IMDM or Inhibitor media. (NOTE: Inhibitor media is RPMI with 10% FBS (20% for CLL). Add β ME (0.7ul per 100ml media) and sterile filter.) Volume depends upon size of pellet, although shoot for $1-5 \times 10^7$ cells/ml.
13. Count cells by with Guava Viacount, diluting 1:10 or greater depending on pellet size. Concentrated cells: dilute 1:200 or 1:100. Count viable and nonviable cells. Determine total cell number as well as cell number per ml and % viability. Record numbers in database.

**Based on the total number of cells in sample process according to the following:
(IN ORDER OF PRIORITY)**

- i) **Genomic Pellet:** 2.5 million cells or less, maximum 5 million.
 - ii) **GTC lysate (for RNA):** minimum 2.5 million cells, maximum 10 million.
 - iii) **Inhibitor Plates:** 15 million cells per 3 plates, 20 million for 4 plates. Generally try to stick to the ratio of 10,000cells/25ul, making sure to have extra volume for plating with EpMotion.
 - iv) **siRNA plate:** 30 million cells.
 - v) **Frozen Viables:** 10 million cells per vial.
 - vi) **Additional Cell Pellets:** 10 million cells per vial.
14. Tubes should be labeled with the sample number, date, and type of sample processed (**Plasma:** Plasma, **GTC lysate:** GTC, **cell pellet:** CP, **frozen viable:** FV, and **number of cells if frozen viable or cell pellet**).
 15. Determine the number of cells/volume to be transferred for each sample type and the aliquot cells to the appropriate tubes.
 16. Cell pellets:
 - a. Place cells into barcoded tubes, spin at 5000rpm for 5mins.
 - b. Aspirate the supernatant and flash freeze dried pellets in liquid nitrogen.
 - c. Scan barcode into database and store at -80°C .
 17. GTC lysates:
 - a. Prepare GTC lysis buffer by adding 100ul β ME per 10mls RLT buffer from the Qiagen RNeasy kit. This buffer is stable for 1 month after the addition of β ME. (Aliquots are found in a box in the sterile H₂O cabinet in the TC room)

- b. Place a minimum of 2.5 million cells (5-10 million preferred) in a bar coded tube. Pellet at 5000rpm for 5min. Remove as much liquid as possible.
- c. VIGOROUSLY break the pellet by vortexing or pipetting.
- d. Add 350-500ul (350ul if less than 5×10^6 cells, 500ul for anything over 5×10^6) GTC lysis buffer and VORTEX IMMEDIATELY AND VIGOROUSLY. Flash freeze, scan barcode into database and store at -80°C .

18. Frozen Viables: Cells are frozen in 90% FBS, 10% DMSO.

- a. Centrifuge cells to be frozen at 1000rpm for 2-3 mins and aspirate supernatant.
- b. Make up 10% DMSO/90% FBS solution. Use 1ml/vial of cells. Place vials in Mr. Frosty and place at -80°C overnight. Remove the next day, scan the bar codes and move to liquid nitrogen storage. Mark appropriate sheet with location of sample by ID number.

PATIENT WASH SOLUTION

- To 500mls Dulbecco's PBS, Ca, Mg free, 500ml
- Add: Human Albumin Solution 4.5% 10ml
- Recombinant human DNase (Pulmozyme) 5ml
- MgCl_2 (1.25M; 500X) 1ml

Store at 4°C .

19. Inhibitor Plate

- a. Take out plates from -20 freezer (All 4 plates now found in patient sample -20 freezer) and place in 37°C incubator for a minimum of 1 hr. Do not stack plates while thawing.
- b. After they have thawed completely spin at 3500 rpm, 15 sec at RT.
- c. For patient samples, resuspend 15 million cells in 35ml or 20 million cells in 50ml of the appropriate media (see below).
- d. Plating cells with Multidrop:
 - i. Turn on Multidrop
 - ii. Set the following parameters:
 - i. 384 well plate (standard)
 - ii. 25ul dispense volume
 - iii. flow rate: medium
 - iii. Prepare tubing for dispensing:
 - i. Aliquot 40mls PBS to a clean 50ml tube.

- ii. Prime with 5mls 70% ethanol to clear and sterilize tubing
- iii. Prime with 10mls PBS
- iv. Prime with 10mls culture media (R10 or R20), then air to clear tubing
- iv. Prime with patient sample until sample begins to come through. Place first plate on tray and hit start. Once dispensing is completed, check to be sure all wells look filled. Remove patient sample plate and repeat for remaining plates.
- v. Wash according to instructions on sheet on TC hood.

OR

- e. Plating cells with EPmotion:
 - i. Open the program: “3 plates 300 uL tool” (in folder “Inhibitor Plates 384”)
 - ii. Place 300ul tip box and inhibitor plates in the appropriate location as shown on program. NOTE: Place an empty trough in the second trough rack, position 6. This will be used for the first dispense after every aspiration to assure even dispense into the inhibitor plates.
 - iii. Put troughs in position 6 & 7 of the rack holder. Mix cells and put into the trough in position 7. Be very careful when adding the cells/media because 35mls will fill the trough very close to the top.
 - iv. Run the program, making sure to de-select levels, tips and locations. Record volume level of cells/media in trough 7 as 34ml.
 - v. When program is finished, make sure to wash out the troughs and put in ‘non-sterile’ box. Wash & clean the tip box lid.
 - vi. Place plates in the 37°C incubator for 3 days.

20. Perform MTS assay

- a. Using Multidrop:
 - i. Turn on Multidrop.
 - ii. Set the following parameters:
 - 1. 384 well plate (standard)
 - 2. 5ul dispense volume
 - 3. flow rate: medium

- iii. Put MTS into a 50ml tube. You will need 2mls MTS per plate, plus ~5mls for priming.
 - iv. Prepare tubing for dispensing:
 - v. Prime with 10% bleach solution to sterilize tubes.
 - vi. Prime with 70% ethanol. Then prime with ddH₂O Bottle 2.
 - vii. Prime with MTS until you see it flowing through.
 - viii. Add MTS to plates. Inspect each plate individually to make sure that no well is missing MTS, and if necessary, add 5 uL of MTS to those wells.
 - ix. Mix on 384well setting with MixMate and place back in incubator until ready to read. Make sure to pop all large bubbles before reading using either an insulin syringe or a hair dryer.
 - x. Clean Multidrop tubing as instructed on sheet.
- b. Using EPmotion:
- i. Open the program: MTS 3 or 4 plates (in folder Inhibitor Plates 384)
 - ii. Take a sterile trough and add 8-9 mL of MTS solution (in cold room common stock shelf, 2.5-3.0 ml per plate).
 - iii. Place trough in position 7 and plates & 50 uL tips in the appropriate locations
 - iv. Run the program deselecting levels & locations
 - v. Once finished, place each plate individually on the Eppendorf MixMate and mix each plate with the '384' settings selected.
 - vi. Inspect each plate individually to make sure that no well is missing MTS, if necessary, add 5 uL of MTS to those wells.
 - vii. Incubate until ready to read. Make sure to pop all large bubbles before reading using either an insulin syringe or a hair dryer.

INHIBITOR PLATE CELL RESUSPENSION SOLUTION

Myeloid Samples:

- 10% FBS RPMI
- B-mercap (use 3.5ul per 500mls media; if making less volume of inhibitor media, make a 1:10 dilution of B-mercap)

CLL Samples:

- 20% FBS RPMI
- B-mercap (use 3.5ul per 500mls media, if making less volume of inhibitor media make a 1:10 dilution of B-mercap)

10.1.2 Electroporation of siRNA Library BioRad (AML Patient Sample) Protocol

This protocol is a reformatted version of the standard patient sample processing protocol used in the Tyner/Druker labs. It was last updated on February 9th, 2016, and edited by Christina Tognon, Kara Johnson, and Jeffrey Tyner.

1. Pipette patient sample media (RPMI + 10% FBS + 3.5ul BME per 500ml media) into three 96-well plates (90ul per well) and place in incubator.
 - a. NOTE: This can be done using the EpMotion. The programs are called: “3 plates 90 ul” or “6 plates 90 ul” depending on the number of samples.
2. Add 3×10^7 patient sample cells to 50ml PBS.
3. Spin at 1000 rpm for 10 mins.
4. While this is spinning, thaw an aliquot of the 6ul siRNA library. Once thawed, spin at 3500 rpm for 15 sec. Leave the centrifuge break off and let the siRNA library slow down while waiting for cells to finish spinning.
5. Resuspend cells in 10.2ml cold siPort Buffer and transfer to trough.
6. Aliquot 100ul into each well of the siRNA library (except A1), making sure to mix well.
7. Transfer entire content from each well with multi-channel pipette (set at 150ul).
8. Add 106ul blank siPORT buffer to A1.
9. Inspect the plate to make sure each well is fully covered in liquid by gently shaking plate. Pop any remaining bubbles with pipette tips.
10. Select the appropriate protocol by:
 - a. User Protocols → User Directory → Jeff
 - b. Select AMLPTSAMPLE (for Myeloid samples).
 - c. The settings for myeloid samples are: 276 V, 5.0 ms, 2x. Before pulsing your sample, check that the correct setting is loaded for your sample.
11. Place the plate in the plate handler, making sure to push down on plate until it is fully inserted. Leave the plate lid on and close the lid of the plate handler.
12. When ready, press pulse.
13. Remove the 3 plates with media from the incubator and get the P20 and P200 multi-channel pipettes. For each row mix well with the P200 multi-channel pipette set at 50ul and then transfer 12-14ul (for myeloid samples) from electroporation plate into each of the 3 plates with media.
14. Incubate for 4 days, after which perform an MTS.
15. For MTS assay, add 20ul MTS solution (located on the cold room common shelf). Mix well after adding (no need for MixMate).
16. Return to incubator. Check color development regularly and read once color has developed. Readings can be done up to 24 hr after addition of MTS if necessary.

10.1.3 CSF1R Flow Cytometry Staining Protocol

This protocol describes staining CLL and AML primary patient sample cells with a variety of hematopoietic-population-staining cell surface marker and CSF1R antibodies by flow cytometry. It was developed in conjunction with Angela Rofelty, based on a protocol by Anupriya Agarwal.

NOTE: Healthy normal cells are stored as frozen viables (5E6 cells) in liquid nitrogen, labeled "D.E. Control, 5e6 PBMC, 6.27.16". Use normal control for the following: unstained (1E5 cells), single channels (9 tubes at 5E4 cells each), and FMO CSF1R or CD14 (1E5 cells).

NOTE: Request 10-20E6 patient sample cells for each sort. Process normal and tumor cells using this protocol. Allow 1.5 hr for entire staining protocol.

1. Centrifuge cells at 1500 rpm for 5 min.
2. Wash cells in 5ml staining buffer (PBS + 0.5% BSA). Centrifuge at 1500 rpm for 5 min.
3. Resuspend control cells at 1E6 cells/ml and divide into staining tubes:
 - a. Unstained: 1E5 cells in 100ul
 - b. Single stains: 5E4 cells in 50ul
 - c. FMO: 1E5 cells in 100ul
4. Resuspend tumor sample at 10E6 cells/ml.
5. Create the following antibody dilutions in staining buffer. (For single stain tubes, add 2.5ul of each diluted antibody.)

Marker	Channel	Dilution	Volume Added (ul)
Live/Dead	Aqua	1:10	2.5
CD33	PerCP/Cy5.5	1:10	2.5
CSF1R	APC	1:50	2.5
CD34 (AML)	PE-CF594	1:50	2.5
CD64 (CLL)	PE	1:20	2.5
CD14	APC-H7	1:10	2.5
CD19	V450	1:10	2.5
CD90 (AML)	PE/Cy7	1:100	2.5
CD5 (CLL)	PE/Cy7	1:50	2.5
CD3	FITC	1:20	2.5
CD45	PerCP	none	2.5

6. (The FMO tubes, which exclude CSF1R APC or CD14 APC-H7, can be maintained at 1E6 cells/ml, or 1E5 cells in 100ul. To each 100ul cell suspension, add 40ul master mix (if master mix is depleted, add 5uL of each diluted antibody):

FMO AML Master Mix			
Marker	Channel	Dilution	Volume Added (ul)
Live/Dead	Aqua	1:10	5
CD33	PerCP/Cy5.5	1:10	5
CD34	PE-CF594	1:50	5
CD14	APC-H7	1:10	5
CD19	V450	1:10	5
CD90	PE/Cy7	1:100	5
CD3	FITC	1:20	5
CD45	PerCP	N/A	5
		Total	40
FMO CLL Master Mix			
Marker	Channel	Dilution	Volume Added (ul)
Live/Dead	Aqua	1:10	5
CD33	PerCP/Cy5.5	1:10	5
CD64	PE	1:20	5
CD14	APC-H7	1:10	5
CD19	V450	1:10	5
CD5	PE/Cy7	1:50	5
CD3	FITC	1:20	5
CD45	PerCP	N/A	5
		Total	40

7. Maintain combination staining tubes at a concentration of 10E6 cells/ml. (The final volume will be ~1ml). To each tube, add 44ul (for AML) or 45.5ul (for CLL) of master mix. If master mixes are depleted, add following volumes of undiluted antibody directly to the staining tube:

AML FACS Antibody Mix		
Marker	Channel	Volume Added (ul)
Live/Dead	Aqua	5
CD33	PerCP/Cy5.5	5
CSF1R	APC	2
CD34	PE-CF594	1
CD14	APC-H7	2.5
CD19	V450	5
CD90	PE/Cy7	1
CD3	FITC	2.5
CD45	PerCP	20
	Total	44

CLL FACS Antibody Mix		
Marker	Channel	Volume Added (ul)
Live/Dead	Aqua	5
CD33	PerCP/Cy5.5	5
CSF1R	APC	2
CD64	PE	2.5
CD14	APC-H7	2.5
CD19	V450	5
CD5	PE/Cy7	1
CD3	FITC	2.5
CD45	PerCP	20
	Total	45.5

8. Incubate tubes at 25C in the dark for 30 min.
9. Add 1ml staining wash buffer to each tube. Centrifuge at 1500 rpm for 5 min.
10. Decant liquid. Resuspend combination tubes (10E6 cels) in 200ul staining buffer.
11. Cover tubes and store at 4C until time for sorting.

List of Antibodies and their Catalog Numbers/Manufacturer

Marker	Channel	Catalog Number	Manufacturer
Live/Dead	Aqua	L34957	Thermo Fisher
CD33	PerCP/Cy5.5	341640	BD Biosciences
CSF1R	APC	347306	BioLegend
CD34 (AML)	PE-CF594	562383	BD Biosciences
CD64 (CLL)	PE	558592	BD Biosciences
CD14	APC-H7	643077	BD Biosciences
CD19	V450	644492	BD Biosciences
CD90 (AML)	PE/Cy7	561558	BD Biosciences
CD5 (CLL)	PE/Cy7	348790	BD Biosciences
CD3	FITC	349201	BD Biosciences
CD45	PerCP	304025	BioLegend

10.1.4 CSF1R Inhibition and Stimulation (RNA and Conditioned Media) Protocol

This protocol explains how to dose primary AML patient sample cells with CSF1R inhibitors (ARRY-382 and GW-2580), CSF1 (the ligand to CSF1R), and GM-CSF (a control cytokine for monocyte/macrophage activation).

1. Dilute 10E6 primary AML patient sample cells to 1E6 cells/ml (10ml) in R10 media.
2. In a 12-well dish, label 10 wells with the following labels: “untreated” (x2), “+ARRY” (x2), “+GW” (x2), “+CSF1” (x2), and “+GM-CSF” (x2).
3. Pipette 1ml diluted primary patient sample cells into each labeled well.
4. Add the following inhibitors/cytokines to the labeled wells:
 - a. 1ul ARRY-382 (stored at 10mM; 10uM final)
 - b. 1ul GW-2580 (stored at 10mM; 10uM final)
 - c. 10ul GM-CSF (stored at 10ng/ul; 100ng/ml final)
 - d. 1ul CSF1 (stored at 100ng/ul; 100ng/ml final)
5. On the 12-well plate, write down the date/time that the cells will need to be harvested (48 hrs after cell inhibition/stimulation).
6. Cover plate with adhesive covering and incubate at 37C for 48 hours.

After 48 hours but before beginning next step, label 20 Eppendorf tubes with the following information: patient sample ID (on each tube, listed as ##-###; e.g. “17-209”), condition (“unt 1”, “unt 2”, “ARRY 1”, “ARRY 2”, “GW 1”, “GW 2”, “CSF1 1”, “CSF1 2”, “GM-CSF 1”, “GM-CSF 2”), and (“CM” for conditioned media; “RNA” for RNA).

Here is an example of the labeling scheme: Tube 1: 17-209, unt 1, CM. Tube 2:17-209, unt 1, RNA. Tube 3: 17-209, unt 2, CM. Tube 4: 17-209, unt 2, RNA. Etc.

7. After incubation, remove adhesive covering. For each well, mix the contents well using a p1000 pipette and place into the “RNA” tube for each condition.
8. Spin down tubes at 5000 rpm for 2 min.
9. For each condition, pipette 750ul conditioned media into its “CM” tube.
10. Completely aspirate all of the remaining conditioned media in the “RNA” tubes.
11. Fill bottom of ice bucket with liquid nitrogen and place next to tissue culture hood.
12. Add 150ul RNA lysis buffer (RLT + BME, found in the patient sample processing room) to each tube. Mix thoroughly by pipetting up and down.
13. Flash-freeze all 20 tubes by placing them into the liquid nitrogen.
14. After completely frozen, transfer the tubes into -80C for long-term storage.

10.1.5 Magnetic 30-Plex Luminex Protocol

This protocol is a slightly modified version of standard protocol for the Human Cytokine Magnetic 30-Plex Panel (Pub #MAN0009850). Modifications were based on discussion with Anupriya Agarwal.

NOTE: Before starting, reserve one hour of time on Day 2 for the Luminex 200 machine. Email flow cytometry core member to alert them of the reservation. Make sure to have ready the technical data sheet from the Luminex kit (which contains the lot number and the lot-specific cytokine concentrations) and the plate layout.

Day 1: Sample prep

1. Thaw all conditioned media samples on ice.
2. Once thawed, invert tubes to mix and spin at 16000 rpm for 10 min.
3. Pipette 65ul (50ul + extra) conditioned media samples into 96-well plate according to pre-determined plate layout.
4. Incubate plate on ice until needed (Step 16).
5. Return conditioned media samples to -80C.

Day 1: Assay protocol

NOTE: Allow all reagents to reach room temperature before use.

- *Don't invert the plate unless it's on the magnetic separator*
- *Protect the fluorescent beads and RPE reagents from light when possible.*
- *Set orbital shaker to proper speed (500-600 rpm) to avoid splashing liquid on lid.*
- *Mix the magnetic beads well before use.*

Preparing standards

6. Create standard mixture (2.5ml RPMI (no FBS) and 2.5ml Assay Diluent) and mix well.
7. Pipette 500ul mixture onto lyophilized cytokines in standard vials (Human 16-Plex Standard and Human 14-Plex Standard). Do not mix yet. **Incubate for 10 mins** at 25C.
 - a. While incubating, label 9 tubes: STD1 to STD8 (standards 1-8) and BLK (blank).
 - b. Add 300ul standard mixture to STD2 to STD8 and BLK.

8. Gently mix each vial to ensure complete reconstitution and **incubate for 5 min** at 25C.
9. Pipette entire contents of each vial into STD1. Mix thoroughly.
10. Pipette 150ul from STD1 to STD2, then STD2 to STD3, etc., making 1:3 serial dilutions of the standard. Mix thoroughly and change pipettes tips between steps.

NOTE: Reconstitute standards 1 hr before use.

Make 1X Wash Solution

- Add 15ml Wash Solution Concentrate (20X) to 285ml ddH₂O and mix well.
- Solution is stable for 2 wks at 25C.

NOTE: If Wash Solution Concentrate has formed precipitate at the bottom, incubate in 37C bead bath and mix until fully dissolved. If precipitate still remains after solution is diluted, incubate in 37C bead bath until precipitate dissolves.

Washing guidelines

1. Place the plate containing beads and 200ul 1X Wash Solution onto the magnetic separator.
2. Allow the beads to settle for 30-60 sec.
3. Turn the magnetic separator and plate (held securely together) upside down, decant the fluid, and blot excess liquid on a stack of dry paper towels.

NOTE: Blotting excess liquid is important to avoid cross contamination from droplets.

4. Separate the plate from the magnetic separator before adding wash solution or any reagent to the plate.

Adding beads/sample

11. Vortex the Antibody Bead (1X) for 30 sec, then sonicate in water bath (in FACS room) for 30 sec immediately before use.
12. Add 25ul Antibody Bead (1X) into each well in assay run. Cover plate with aluminum foil.
13. Wash assay wells twice with 200ul 1X Wash Solution. (see “Washing guidelines”).
14. Add 50ul Incubation Buffer into each well.

15. Add 100ul diluted standards and blanks into standard wells.
16. Add 100ul blank into blank/background wells.
17. Add 50ul Assay Diluent followed by 50ul sample into the sample wells.
Transfer samples from 96-well plate to Luminex plate using p200 multichannel pipette.
18. Cover plate with an opaque lid and **incubate for 2 hr** at 25C under agitation on an orbital plate shaker.

Cytokine detection

19. Prepare 1X Biotinylated Detector Antibody in a conical tube by adding 100ul Biotin Diluent and 10ul 10X Biotinylated Antibody per assay well, e.g. for entire plate (96 wells), add 10ml Biotin Diluent and 10ul 10X Biotinylated Antibody.
20. Place the plate onto magnetic separator for 30-60 sec, then decant liquid.
21. Wash the wells twice with 200ul 1X Wash Solution (see “Washing guidelines”).
22. Add 100ul 1X Biotinylated Detector Antibody to each well. Cover and **incubate the plate for 1 hr** at 25C on orbital plate shaker.
23. Prepare 1X Streptavidin-RPE solution in a conical tube by adding 100ul RPE-Diluent and 10ul 10X Streptavidin-RPE per assay well. Protect solution from light.
24. Decant liquid and wash the wells twice with 200ul 1X Wash Solution.
25. Add 100ul 1X Streptavidin-RPE solution to each assay well. Cover and **incubate the plate for 30 min** at 25C on orbital plate shaker.
26. Place the plate onto magnetic separator for 30-60 sec, then decant liquid.
27. Wash the wells 3 times with 200ul 1X Wash Solution.
28. Add 150ul 1X Wash Solution and cover/store plate overnight in the dark at 4C.

Day 2: Reading assay

1. Remove existing wash solution from overnight plate. Replace with 150ul fresh 1X Wash Solution.
2. Place plate on orbital plate shaker for 2-3 mins before analysis.
3. Give plate to flow cytometry core member, along with the lot number and a plate diagram showing which wells have been used.
4. Analyze the collected data.

10.1.6 Stromal Cell Isolation Protocol

This protocol describes how to isolate stromal cells from the red blood cell pellet of a primary acute myeloid leukemia patient sample. Developed with assistance from Elie Traer and Shelton Viola.

NOTE: This protocol begins after obtaining the bone marrow aspirate from an AML patient.

1. After MNCs have been collected from Ficoll-separated bone marrow, aspirate the remaining supernatant and Ficoll, leaving only the red blood cell pellet.
2. Resuspend the red blood cell pellet in 12mL ACK lysis buffer.
3. Mix by pipetting and incubate on ice for 20 min.
4. After incubation, centrifuge at 1500 rpm for 5 min.
5. Aspirate supernatant and resuspend cell pellet in 10 mL stromal growth media (MEM-alpha with 20% fetal bovine serum, 2% L-Glutamine, 1% Pen-Strep, and 0.1% Fungizone).
6. Plate cells in 10cm dish. This stage is "Passage 0".
7. Incubate cells for 48 hr. After incubation, aspirate culture media to remove any non-adherent cells.
8. Following initial media replacement, allow cells to incubate for 2 wks, changing culture media every 7 days. By day 14, adherent cells should adopt a fibroblast-like morphology and form small colonies in the dish. If this does not occur, discard the sample.
9. Allow cells to culture until reaching ~80% confluency, then passage the sample into one 15cm dish as follows:
 - a. Wash 10cm dish with 3 mL sterile PBS and aspirate.
 - b. Add 2mL trypsin to dish and incubate at 37C until cells have lifted off of the dish (this time can vary widely between samples. Check using microscope every 5 min).
 - c. Wash cells off the dish with 3mL of media, then centrifuge at 1500 rpm for 5 min.
 - d. Resuspend cells in 15mL culture media and plate in 15cm dish.
 - e. After plating in one 15cm dish, the sample is then at "Passage 1".
10. Allow the sample to reach ~80% confluency, then split the sample into two 15 cm dishes. The sample is then at "Passage 2".
 - a. Note: Allow the cells one month to expand during Passage 1. If the sample is not ready to be passaged after one month, the stroma is considered senescent and should be discarded.
11. Once both dishes have reached ~80% confluency, wash the cells in PBS and add 13 mL exosome-depleted α 20 to each dish (Exosome-depleted FBS is

- made using the exosome isolation protocol listed below). Incubate for three days.
12. After three days of incubation, remove the culture media and centrifuge the media at 1500 rpm for 5 min to remove cells/debris. Store the supernatant at 4C.
 - a. Remove 3ml media and pipette into three 1.5ml Eppendorf tubes (1ml per tube). Store at -80C for cytokine analysis.
 13. Add 13 mL of fresh exosome-depleted α 20 to each dish and incubate for an additional three days.
 14. After incubation, remove the culture media, centrifuge to remove cells and debris, and combine with the supernatant collected three days prior, for a total of approximately 50mL of conditioned media from each sample.
 - a. Isolate exosomes using Exosome Isolation Protocol. Media can be stored at 4C before exosome isolation.
 15. Harvest both dishes of stroma as follows:
 - a. Wash each dish with 5mL PBS.
 - b. Add 4mL trypsin to each plate and incubate until cells become non-adherent. (The time is variable but tends to increase with the total time the sample has been in culture).
 - c. Wash each dish with 5 mL of media and collect all stromal cells in one 50 mL conical tube. Centrifuge the stroma at 1500 rpm for 5 minutes).
 16. Resuspend stroma in 1 mL of α 20 and divide into the following three derivatives:
 - a. Cell pellet: transfer 250uL of stromal cell suspension into a 1.5 mL Eppendorf tube. Centrifuge at 5000 rpm for 5 min and aspirate supernatant. Flash freeze and store at -80C.
 - b. RNA isolation: transfer 250uL of stromal cell suspension into a 1.5 mL Eppendorf tube. Centrifuge at 5000 rpm for 5 min and aspirate supernatant. Resuspend cell pellet in 700uL QIAzol lysis reagent and store at -80C.
 - c. Frozen Viable: Transfer the remaining 500uL of stromal cell suspension to a cryovial. Add 400uL of filter-sterile FBS and 100uL of DMSO. Freeze in Mr. Frosty overnight, then store in liquid nitrogen.

NOTE: Cells can be passaged until Passage 6, after which they should be either frozen down or discarded. Each 15cm dish yields between 5E5 and 1E6 cells. To freeze down cells, use one 15cm dish in 1ml freezing media.

11 References

1. Siegel RL, Miller KD, Jemal A. Cancer statistics, 2018. *CA Cancer J Clin.* 2018;68(1):7–30.
2. World Health Organization Classification of Tumours: Pathology and Genetics of Tumours of Haematopoietic and Lymphoid Tissues. Lyon, France: IARC; 2001.
3. Swerdlow SH, Campo E, Pileri SA, et al. The 2016 revision of the World Health Organization classification of lymphoid neoplasms. *Blood.* 2016;127(20):2375–2390.
4. Quintanilla-Martinez L. The 2016 updated WHO classification of lymphoid neoplasias. *Hematol Oncol.* 2017;35 Suppl 1:37–45.
5. Teras LR, DeSantis CE, Cerhan JR, et al. 2016 US lymphoid malignancy statistics by World Health Organization subtypes. *CA Cancer J Clin.* 2016.
6. Arber DA, Orazi A, Hasserjian R, et al. The 2016 revision to the World Health Organization classification of myeloid neoplasms and acute leukemia. *Blood.* 2016;127(20):2391–2405.
7. Dores GM, Devesa SS, Curtis RE, Linet MS, Morton LM. Acute leukemia incidence and patient survival among children and adults in the United States, 2001-2007. *Blood.* 2012;119(1):34–43.
8. Ohanian M, Faderl S, Ravandi F, et al. Is acute myeloid leukemia a liquid tumor? *Int. J. Cancer.* 2013;133(3):534–543.
9. Kandoth C, McLellan MD, Vandin F, et al. Mutational landscape and significance across 12 major cancer types. *Nature.* 2013;502(7471):333–339.

10. Downing JR, Wilson RK, Zhang J, et al. The Pediatric Cancer Genome Project. *Nat. Genet.* 2012;44(6):619–622.
11. Zhang J, Walsh MF, Wu G, et al. Germline Mutations in Predisposition Genes in Pediatric Cancer. *N. Engl. J. Med.* 2015;373(24):2336–2346.
12. Hanahan D, Weinberg R. Hallmarks of cancer: the next generation. *Cell.* 2011;144(5):646–74.
13. Landau DA, Carter SL, Getz G, Wu CJ. Clonal evolution in hematological malignancies and therapeutic implications. *Leukemia.* 2014;28(1):34–43.
14. Hanahan D, Coussens LM. Accessories to the crime: functions of cells recruited to the tumor microenvironment. *Cancer Cell.* 2012;21(3):309–322.
15. O'Donnell MR, Abboud CN, Altman J, et al. Acute myeloid leukemia. *J Natl Compr Canc Netw.* 2011;9(3):280–317.
16. Bennett JM, Catovsky D, Daniel MT, et al. Proposals for the classification of the acute leukaemias. French-American-British (FAB) co-operative group. *Br J Haematol.* 1976;33(4):451–458.
17. Lee EJ, Pollak A, Leavitt RD, Testa JR, Schiffer CA. Minimally differentiated acute nonlymphocytic leukemia: a distinct entity. *Blood.* 1987;70(5):1400–1406.
18. Bloomfield CD, Brunning RD. FAB M7: acute megakaryoblastic leukemia--beyond morphology. *Ann. Intern. Med.* 1985;103(3):450–452.
19. Behm FG. Classification of Acute Leukemias. *Treatment of Acute Leukemias.* 2003;(2):43–58.

20. Döhner H, Estey EH, Amadori S, et al. Diagnosis and management of acute myeloid leukemia in adults: recommendations from an international expert panel, on behalf of the European LeukemiaNet. *Blood*. 2010;115(3):453–474.
21. Röllig C, Bornhäuser M, Thiede C, et al. Long-term prognosis of acute myeloid leukemia according to the new genetic risk classification of the European LeukemiaNet recommendations: evaluation of the proposed reporting system. *J. Clin. Oncol.* 2011;29(20):2758–2765.
22. Döhner H, Estey E, Grimwade D, et al. Diagnosis and management of AML in adults: 2017 ELN recommendations from an international expert panel. *Blood*. 2017;129(4):424–447.
23. Wang M, Yang C, Zhang L, Schaar DG. Molecular Mutations and Their Cooccurrences in Cytogenetically Normal Acute Myeloid Leukemia. *Stem Cells Int.* 2017;2017(5):6962379–11.
24. Cancer Genome Atlas Research Network. Genomic and epigenomic landscapes of adult de novo acute myeloid leukemia. *N. Engl. J. Med.* 2013;368(22):2059–2074.
25. Papaemmanuil E, Gerstung M, Bullinger L, et al. Genomic Classification and Prognosis in Acute Myeloid Leukemia. *N. Engl. J. Med.* 2016;374(23):2209–2221.
26. Hallek M. Chronic lymphocytic leukemia: 2017 update on diagnosis, risk stratification, and treatment. *Am. J. Hematol.* 2017;92(9):946–965.

27. Kikushige Y, Ishikawa F, Miyamoto T, et al. Self-renewing hematopoietic stem cell is the primary target in pathogenesis of human chronic lymphocytic leukemia. *Cancer Cell*. 2011;20(2):246–259.
28. Landau DA, Tausch E, Taylor-Weiner AN, et al. Mutations driving CLL and their evolution in progression and relapse. *Nature*. 2015;526(7574):525–530.
29. Seiffert M, Dietrich S, Jethwa A, et al. Exploiting biological diversity and genomic aberrations in chronic lymphocytic leukemia. *Leuk. Lymphoma*. 2012;53(6):1023–1031.
30. Quesada V, Conde L, Villamor N, et al. Exome sequencing identifies recurrent mutations of the splicing factor SF3B1 gene in chronic lymphocytic leukemia. *Nature Publishing Group*. 2011;44(1):47–52.
31. Puente XS, Pinyol M, Quesada V, et al. Whole-genome sequencing identifies recurrent mutations in chronic lymphocytic leukaemia. *Nature*. 2011;475(7354):101–105.
32. Puente XS, Beà S, Valdés-Mas R, et al. Non-coding recurrent mutations in chronic lymphocytic leukaemia. *Nature*. 2015;526(7574):519–524.
33. Rai KR, Sawitsky A, Cronkite EP, et al. Clinical staging of chronic lymphocytic leukemia. *Blood*. 1975;46(2):219–234.
34. Binet JL, Auquier A, Dighiero G, et al. A new prognostic classification of chronic lymphocytic leukemia derived from a multivariate survival analysis. *Cancer*. 1981;48(1):198–206.

35. Rai KR. A critical analysis of staging in CLL. *Chronic Lymphocytic Leukemia: Recent Progress and Future Directions*. 1987;253–264.
36. Pflug N, Bahlo J, Shanafelt TD, et al. Development of a comprehensive prognostic index for patients with chronic lymphocytic leukemia. *Blood*. 2014;124(1):49–62.
37. International CLL-IPI working group. An international prognostic index for patients with chronic lymphocytic leukaemia (CLL-IPI): a meta-analysis of individual patient data. *Lancet Oncol*. 2016;17(6):779–790.
38. Molica S, Shanafelt TD, Giannarelli D, et al. The chronic lymphocytic leukemia international prognostic index predicts time to first treatment in early CLL: Independent validation in a prospective cohort of early stage patients. *Am. J. Hematol*. 2016;91(11):1090–1095.
39. Appelbaum FR, Gundacker H, Head DR, et al. Age and acute myeloid leukemia. *Blood*. 2006;107(9):3481–3485.
40. Sanz MA, Grimwade D, Tallman MS, et al. Management of acute promyelocytic leukemia: recommendations from an expert panel on behalf of the European LeukemiaNet. *Blood*. 2009;113(9):1875–1891.
41. Lancet JE. New agents: great expectations not realized. *Best Pract Res Clin Haematol*. 2013;26(3):269–274.
42. Stilgenbauer S. Prognostic markers and standard management of chronic lymphocytic leukemia. *Hematology Am Soc Hematol Educ Program*. 2015;2015(1):368–377.

43. Hallek M, Fischer K, Fingerle-Rowson G, et al. Addition of rituximab to fludarabine and cyclophosphamide in patients with chronic lymphocytic leukaemia: a randomised, open-label, phase 3 trial. *Lancet*. 2010;376(9747):1164–1174.
44. Weigel RJ, McDougall IR. The role of radioactive iodine in the treatment of well-differentiated thyroid cancer. *Surg. Oncol. Clin. N. Am.* 2006;15(3):625–638.
45. HEIDELBERGER C, CHAUDHURI NK, DANNEBERG P, et al. Fluorinated pyrimidines, a new class of tumour-inhibitory compounds. *Nature*. 1957;179(4561):663–666.
46. Jordan VC, Koerner S. Tamoxifen (ICI 46,474) and the human carcinoma 8S oestrogen receptor. *Eur. J. Cancer*. 1975;11(3):205–206.
47. Jordan VC. Fourteenth Gaddum Memorial Lecture. A current view of tamoxifen for the treatment and prevention of breast cancer. *Br. J. Pharmacol.* 1993;110(2):507–517.
48. DeVita VT, Chu E. A history of cancer chemotherapy. 2008;68(21):8643–8653.
49. O'Brien SG, Guilhot F, Larson RA, et al. Imatinib compared with interferon and low-dose cytarabine for newly diagnosed chronic-phase chronic myeloid leukemia. *N. Engl. J. Med.* 2003;348(11):994–1004.
50. Druker BJ, Guilhot F, O'Brien SG, et al. Five-year follow-up of patients receiving imatinib for chronic myeloid leukemia. *N. Engl. J. Med.* 2006;355(23):2408–2417.

51. Imai K, Takaoka A. Comparing antibody and small-molecule therapies for cancer. *Nat. Rev. Cancer.* 2006;6(9):714–727.
52. Han TH, Zhao B. Absorption, distribution, metabolism, and excretion considerations for the development of antibody-drug conjugates. *Drug Metab. Dispos.* 2014;42(11):1914–1920.
53. Estey E, Levine RL, Löwenberg B. Current challenges in clinical development of “targeted therapies”: the case of acute myeloid leukemia. *Blood.* 2015;125(16):2461–2466.
54. Duque-Afonso J, Cleary ML. The AML salad bowl. *Cancer Cell.* 2014;25(3):265–267.
55. Stone RM, Mandrekar SJ, Sanford BL, et al. Midostaurin plus Chemotherapy for Acute Myeloid Leukemia with a FLT3 Mutation. *N. Engl. J. Med.* 2017;377(5):454–464.
56. Stein EM, DiNardo CD, Pollyea DA, et al. Enasidenib in mutant IDH2 relapsed or refractory acute myeloid leukemia. *Blood.* 2017;130(6):722–731.
57. Percival M-E, Estey E. Emerging treatments in acute myeloid leukemia: current standards and unmet challenges. *Clin Adv Hematol Oncol.* 2017;15(8):632–642.
58. Hillmen P, Skotnicki AB, Robak T, et al. Alemtuzumab compared with chlorambucil as first-line therapy for chronic lymphocytic leukemia. *J. Clin. Oncol.* 2007;25(35):5616–5623.

59. Stevenson FK, Krysov S, Davies AJ, Steele AJ, Packham G. B-cell receptor signaling in chronic lymphocytic leukemia. *Blood*. 2011;118(16):4313–4320.
60. Brown JR, Byrd JC, Coutre SE, et al. Idelalisib, an inhibitor of phosphatidylinositol 3-kinase p110 δ , for relapsed/refractory chronic lymphocytic leukemia. *Blood*. 2014;123(22):3390–3397.
61. Jones JA, Robak T, Brown JR, et al. Efficacy and safety of idelalisib in combination with ofatumumab for previously treated chronic lymphocytic leukaemia: an open-label, randomised phase 3 trial. *Lancet Haematol*. 2017;4(3):e114–e126.
62. Herman SEM, Gordon AL, Hertlein E, et al. Bruton tyrosine kinase represents a promising therapeutic target for treatment of chronic lymphocytic leukemia and is effectively targeted by PCI-32765. *Blood*. 2011;117(23):6287–6296.
63. Byrd JC, Brown JR, O'Brien S, et al. Ibrutinib versus ofatumumab in previously treated chronic lymphoid leukemia. *N. Engl. J. Med*. 2014;371(3):213–223.
64. Burger JA, Keating MJ, Wierda WG, et al. Safety and activity of ibrutinib plus rituximab for patients with high-risk chronic lymphocytic leukaemia: a single-arm, phase 2 study. *Lancet Oncol*. 2014;15(10):1090–1099.
65. Jain P, Keating MJ, Wierda WG, et al. Long-term Follow-up of Treatment with Ibrutinib and Rituximab in Patients with High-Risk Chronic Lymphocytic Leukemia. *Clin. Cancer Res*. 2017;23(9):2154–2158.

66. Chanan-Khan A, Cramer P, Demirkan F, et al. Ibrutinib combined with bendamustine and rituximab compared with placebo, bendamustine, and rituximab for previously treated chronic lymphocytic leukaemia or small lymphocytic lymphoma (HELIOS): a randomised, double-blind, phase 3 study. *Lancet Oncol.* 2016;17(2):200–211.
67. Jaglowski SM, Jones JA, Nagar V, et al. Safety and activity of BTK inhibitor ibrutinib combined with ofatumumab in chronic lymphocytic leukemia: a phase 1b/2 study. *Blood.* 2015;126(7):842–850.
68. Balkwill F, Mantovani A. Inflammation and cancer: back to Virchow? *Lancet.* 2001;357(9255):539–545.
69. Grivennikov SI, Greten FR, Karin M. Immunity, inflammation, and cancer. *Cell.* 2010;140(6):883–899.
70. Stewart T, Tsai SC, Grayson H, Henderson R, Opelz G. Incidence of de-novo breast cancer in women chronically immunosuppressed after organ transplantation. *Lancet.* 1995;346(8978):796–798.
71. Gallagher B, Wang Z, Schymura MJ, Kahn A, Fordyce EJ. Cancer incidence in New York State acquired immunodeficiency syndrome patients. *Am. J. Epidemiol.* 2001;154(6):544–556.
72. Birbrair A, Frenette PS. Niche heterogeneity in the bone marrow. *Ann. N. Y. Acad. Sci.* 2016;1370(1):82–96.
73. Kunisaki Y, Bruns I, Scheiermann C, et al. Arteriolar niches maintain haematopoietic stem cell quiescence. *Nature.* 2013;502(7473):637–643.

74. Asada N, Kunisaki Y, Pierce H, et al. Differential cytokine contributions of perivascular haematopoietic stem cell niches. *Nat. Cell Biol.* 2017;19(3):214–223.
75. Quail DF, Joyce JA. Microenvironmental regulation of tumor progression and metastasis. *Nat. Med.* 2013;19(11):1423–1437.
76. Qian B-Z, Pollard JW. Macrophage diversity enhances tumor progression and metastasis. *Cell.* 2010;141(1):39–51.
77. Almand B, Clark JI, Nikitina E, et al. Increased production of immature myeloid cells in cancer patients: a mechanism of immunosuppression in cancer. *The Journal of Immunology.* 2001;166(1):678–689.
78. Fang H, Declerck YA. Targeting the tumor microenvironment: from understanding pathways to effective clinical trials. *Cancer Res.* 2013;73(16):4965–4977.
79. Hodi FS, O'Day SJ, McDermott DF, et al. Improved survival with ipilimumab in patients with metastatic melanoma. *N. Engl. J. Med.* 2010;363(8):711–723.
80. Hwu P. Treating cancer by targeting the immune system. *N. Engl. J. Med.* 2010;363(8):779–781.
81. Wolchok JD, Kluger H, Callahan MK, et al. Nivolumab plus ipilimumab in advanced melanoma. *N. Engl. J. Med.* 2013;369(2):122–133.
82. Callahan MK, Kluger H, Postow MA, et al. Nivolumab Plus Ipilimumab in Patients With Advanced Melanoma: Updated Survival, Response, and

- Safety Data in a Phase I Dose-Escalation Study. *J. Clin. Oncol.* 2018;36(4):391–398.
83. Hamid O, Robert C, Daud A, et al. Safety and tumor responses with lambrolizumab (anti-PD-1) in melanoma. *N. Engl. J. Med.* 2013;369(2):134–144.
84. Vonderheide RH, Glennie MJ. Agonistic CD40 antibodies and cancer therapy. *Clin. Cancer Res.* 2013;19(5):1035–1043.
85. Beatty GL, Chiorean EG, Fishman MP, et al. CD40 agonists alter tumor stroma and show efficacy against pancreatic carcinoma in mice and humans. *Science.* 2011;331(6024):1612–1616.
86. Qian B-Z, Li J, Zhang H, et al. CCL2 recruits inflammatory monocytes to facilitate breast-tumour metastasis. *Nature.* 2011;475(7355):222–225.
87. Robinson WA, Stanley ER, Metcalf D. Stimulation of bone marrow colony growth in vitro by human urine. *Blood.* 1969;33(3):396–399.
88. Stanley ER, Heard PM. Factors regulating macrophage production and growth. Purification and some properties of the colony stimulating factor from medium conditioned by mouse L cells. *J. Biol. Chem.* 1977;252(12):4305–4312.
89. Stanley ER, Chen DM, Lin HS. Induction of macrophage production and proliferation by a purified colony stimulating factor. *Nature.* 1978;274(5667):168–170.
90. Guilbert LJ, Stanley ER. Specific interaction of murine colony-stimulating factor with mononuclear phagocytic cells. *J. Cell Biol.* 1980;85(1):153–159.

91. Donner L, Fedele LA, Garon CF, Anderson SJ, Sherr CJ. McDonough feline sarcoma virus: characterization of the molecularly cloned provirus and its feline oncogene (v-fms). *J. Virol.* 1982;41(2):489–500.
92. Rettenmier CW, Chen JH, Roussel MF, Sherr CJ. The product of the c-fms proto-oncogene: a glycoprotein with associated tyrosine kinase activity. *Science.* 1985;228(4697):320–322.
93. Sherr CJ, Rettenmier CW, Sacca R, et al. The c-fms proto-oncogene product is related to the receptor for the mononuclear phagocyte growth factor, CSF-1. *Cell.* 1985;41(3):665–676.
94. Coussens L, Van Beveren C, Smith D, et al. Structural alteration of viral homologue of receptor proto-oncogene fms at carboxyl terminus. *Nature.* 1986;320(6059):277–280.
95. Stanley ER, Chitu V. CSF-1 receptor signaling in myeloid cells. *Cold Spring Harb Perspect Biol.* 2014;6(6):a021857–a021857.
96. Lin H, Lee E, Hestir K, et al. Discovery of a cytokine and its receptor by functional screening of the extracellular proteome. *Science.* 2008;320(5877):807–811.
97. Wei S, Nandi S, Chitu V, et al. Functional overlap but differential expression of CSF-1 and IL-34 in their CSF-1 receptor-mediated regulation of myeloid cells. *J. Leukoc. Biol.* 2010;88(3):495–505.
98. Dai X-M, Zong X-H, Sylvestre V, Stanley ER. Incomplete restoration of colony-stimulating factor 1 (CSF-1) function in CSF-1-deficient

- Csf1op/Csf1op mice by transgenic expression of cell surface CSF-1. *Blood*. 2004;103(3):1114–1123.
99. Dai X-M, Ryan GR, Hapel AJ, et al. Targeted disruption of the mouse colony-stimulating factor 1 receptor gene results in osteopetrosis, mononuclear phagocyte deficiency, increased primitive progenitor cell frequencies, and reproductive defects. *Blood*. 2002;99(1):111–120.
100. Hwang S-J, Choi B, Kang S-S, et al. Interleukin-34 produced by human fibroblast-like synovial cells in rheumatoid arthritis supports osteoclastogenesis. *Arthritis Res. Ther.* 2012;14(1):R14.
101. Tian Y, Shen H, Xia L, Lu J. Elevated serum and synovial fluid levels of interleukin-34 in rheumatoid arthritis: possible association with disease progression via interleukin-17 production. *J. Interferon Cytokine Res.* 2013;33(7):398–401.
102. Nandi S, Cioce M, Yeung Y-G, et al. Receptor-type protein-tyrosine phosphatase ζ is a functional receptor for interleukin-34. *J. Biol. Chem.* 2013;288(30):21972–21986.
103. Krysinska H, Hoogenkamp M, Wilson N, et al. A two-step, PU.1-dependent mechanism for developmentally regulated chromatin remodeling and transcription of the *c-fms* gene. *Mol. Cell. Biol.* 2007;27(3):878–887.
104. Laslo P, Spooner CJ, Warmflash A, et al. Multilineage transcriptional priming and determination of alternate hematopoietic cell fates. *Cell*. 2006;126(4):755–766.

105. Pixley FJ, Stanley ER. CSF-1 regulation of the wandering macrophage: complexity in action. *Trends Cell Biol.* 2004;14(11):628–638.
106. Munugalavadla V, Borneo J, Ingram DA, Kapur R. p85alpha subunit of class IA PI-3 kinase is crucial for macrophage growth and migration. *Blood.* 2005;106(1):103–109.
107. Yu W, Chen J, Xiong Y, et al. Macrophage proliferation is regulated through CSF-1 receptor tyrosines 544, 559, and 807. *J. Biol. Chem.* 2012;287(17):13694–13704.
108. Bourette RP, Myles GM, Choi JL, Rohrschneider LR. Sequential activation of phosphatidylinositol 3-kinase and phospholipase C-gamma2 by the M-CSF receptor is necessary for differentiation signaling. *EMBO J.* 1997;16(19):5880–5893.
109. Grasset M-F, Gobert-Gosse S, Mouchiroud G, Bourette RP. Macrophage differentiation of myeloid progenitor cells in response to M-CSF is regulated by the dual-specificity phosphatase DUSP5. *J. Leukoc. Biol.* 2010;87(1):127–135.
110. Wilson NJ, Cross M, Nguyen T, Hamilton JA. cAMP inhibits CSF-1-stimulated tyrosine phosphorylation but augments CSF-1R-mediated macrophage differentiation and ERK activation. *FEBS J.* 2005;272(16):4141–4152.
111. McMahon KA, Wilson NJ, Marks DC, et al. Colony-stimulating factor-1 (CSF-1) receptor-mediated macrophage differentiation in myeloid cells: a

- role for tyrosine 559-dependent protein phosphatase 2A (PP2A) activity. *Biochem. J.* 2001;358(Pt 2):431–436.
112. Lee AW, Mao Y, Penninger JM, Yu S. Gab2 promotes colony-stimulating factor 1-regulated macrophage expansion via alternate effectors at different stages of development. *Mol. Cell. Biol.* 2011;31(22):4563–4581.
113. Wynn TA, Chawla A, Pollard JW. Macrophage biology in development, homeostasis and disease. *Nature.* 2013;496(7446):445–455.
114. Gautier EL, Shay T, Miller J, et al. Gene-expression profiles and transcriptional regulatory pathways that underlie the identity and diversity of mouse tissue macrophages. *Nat. Immunol.* 2012;13(11):1118–1128.
115. Gordon S. Alternative activation of macrophages. *Nat. Rev. Immunol.* 2003;3(1):23–35.
116. Sica A, Mantovani A. Macrophage plasticity and polarization: in vivo veritas. *J. Clin. Invest.* 2012;122(3):787–795.
117. Martín-Moreno AM, Roncador G, Maestre L, et al. CSF1R Protein Expression in Reactive Lymphoid Tissues and Lymphoma: Its Relevance in Classical Hodgkin Lymphoma. *PLoS ONE.* 2015;10(6):e0125203.
118. Domínguez-Soto A, Sierra-Filardi E, Puig-Kröger A, et al. Dendritic cell-specific ICAM-3-grabbing nonintegrin expression on M2-polarized and tumor-associated macrophages is macrophage-CSF dependent and enhanced by tumor-derived IL-6 and IL-10. *J. Immunol.* 2011;186(4):2192–2200.

119. Xue J, Schmidt SV, Sander J, et al. Transcriptome-based network analysis reveals a spectrum model of human macrophage activation. *Immunity*. 2014;40(2):274–288.
120. Coussens LM, Pollard JW. Leukocytes in mammary development and cancer. *Cold Spring Harb Perspect Biol*. 2011;3(3):a003285–a003285.
121. Zhang Q-W, Liu L, Gong C-Y, et al. Prognostic significance of tumor-associated macrophages in solid tumor: a meta-analysis of the literature. *PLoS ONE*. 2012;7(12):e50946.
122. Cannarile MA, Weisser M, Jacob W, et al. Colony-stimulating factor 1 receptor (CSF1R) inhibitors in cancer therapy. *J Immunother Cancer*. 2017;5(1):53.
123. Moskowitz CH, Younes A, de Vos S, et al. CSF1R Inhibition by PLX3397 in Patients with Relapsed or Refractory Hodgkin Lymphoma: Results From a Phase 2 Single Agent Clinical Trial. *Blood*. 2012;120(21):1638–1638.
124. Bendell JC, Tolcher AW, Jones SF, et al. Abstract A252: A phase 1 study of ARRY-382, an oral inhibitor of colony-stimulating factor-1 receptor (CSF1R), in patients with advanced or metastatic cancers. *Mol. Cancer Ther*. 2014;12(11_Supplement):A252–A252.
125. Sharma N, Wesolowski R, Reebel L, et al. A phase 1b study to assess the safety of PLX3397, a CSF-1 receptor inhibitor, and paclitaxel in patients with advanced solid tumors. *J Clin Oncol*. 2014;32(15_suppl):TPS3127–TPS3127.

126. Butowski NA, Colman H, De Groot JF, et al. A phase 2 study of orally administered PLX3397 in patients with recurrent glioblastoma. *J Clin Oncol.* 2014;32(15_suppl):2023–2023.
127. Tresckow von B, Morschhauser F, Ribrag V, et al. An Open-Label, Multicenter, Phase I/II Study of JNJ-40346527, a CSF-1R Inhibitor, in Patients with Relapsed or Refractory Hodgkin Lymphoma. *Clin. Cancer Res.* 2015;21(8):1843–1850.
128. Gomez-Roca CA, Cassier PA, Italiano A, et al. Phase I study of RG7155, a novel anti-CSF1R antibody, in patients with advanced/metastatic solid tumors. *J Clin Oncol.* 2015;33(15_suppl):3005–3005.
129. Lundqvist A, van Hoef V, Zhang X, et al. 31st Annual Meeting and Associated Programs of the Society for Immunotherapy of Cancer (SITC 2016): part one. *J Immunother Cancer.* 2016;4(1):82.
130. Brahmer J, Rasco D, Chen M, et al. Abstract B143: A phase 1a/1b study of FPA008 in combination with nivolumab in patients with selected advanced cancers. *Cancer Immunol Res.* 2016;4(1 Supplement):B143–B143.
131. Papadopoulos K, Gluck L, Martin LP, et al. Abstract CT137: First-in-human study of AMG 820, a monoclonal anti-CSF-1R (c-fms) antibody, in patients (pts) with advanced solid tumors. *Cancer Res.* 2016;76(14 Supplement):CT137–CT137.
132. Butowski N, Colman H, De Groot JF, et al. Orally administered colony stimulating factor 1 receptor inhibitor PLX3397 in recurrent glioblastoma: an

- Ivy Foundation Early Phase Clinical Trials Consortium phase II study.
Neuro-oncology. 2016;18(4):557–564.
133. Manji GA, Patwardhan P, Lee SM, et al. Phase 1/2 study of combination therapy with pexidartinib and sirolimus to target tumor-associated macrophages in malignant peripheral nerve sheath tumors. *J Clin Oncol*. 2016;34(15_suppl):TPS11070–TPS11070.
134. Wainberg ZA, Eisenberg PD, Sachdev JC, et al. Phase 1/2a study of double immune suppression blockade by combining a CSF1R inhibitor (pexidartinib/PLX3397) with an anti PD-1 antibody (pembrolizumab) to treat advanced melanoma and other solid tumors. *J Clin Oncol*. 2016;34(4_suppl):TPS465–TPS465.
135. Ridge SA, Worwood M, Oscier D, Jacobs A, Padua RA. FMS mutations in myelodysplastic, leukemic, and normal subjects. *Proceedings of the National Academy of Sciences*. 1990;87(4):1377–1380.
136. Lilljebjörn H, Ågerstam H, Orsmark-Pietras C, et al. RNA-seq identifies clinically relevant fusion genes in leukemia including a novel MEF2D/CSF1R fusion responsive to imatinib. *Leukemia*. 2014;28(4):977–979.
137. Ben-Bassat H, Korkesh A, Voss R, Leizerowitz R, Polliack A. Establishment and characterization of a new permanent cell line (GDM-1) from a patient with myelomonoblastic leukemia. 1982;6(6):743–752.

138. Chase A, Schultheis B, Kreil S, et al. Imatinib sensitivity as a consequence of a CSF1R-Y571D mutation and CSF1/CSF1R signaling abnormalities in the cell line GDM1. *Leukemia*. 2008;23(2):358–364.
139. Takeuchi S, Sugito S, Uemura Y, et al. Acute megakaryoblastic leukemia: establishment of a new cell line (MKPL-1) in vitro and in vivo. *Leukemia*. 1992;6(6):588–594.
140. Gu T-L, Mercher T, Tyner JW, et al. A novel fusion of RBM6 to CSF1R in acute megakaryoblastic leukemia. *Blood*. 2007;110(1):323–333.
141. Aikawa Y, Katsumoto T, Zhang P, et al. PU.1-mediated upregulation of CSF1R is crucial for leukemia stem cell potential induced by MOZ-TIF2. *Nat. Med*. 2010;16(5):580–5– 1p following 585.
142. Perez-Campo FM, Costa G, Lie-A-Ling M, Kouskoff V, Lacaud G. The MYSTERIOUS MOZ, a histone acetyltransferase with a key role in haematopoiesis. *Immunology*. 2013;139(2):161–165.
143. Yeh Y-M, Hsu S-J, Lin P-C, et al. The c.1085A>G Genetic Variant of CSF1R Gene Regulates Tumor Immunity by Altering the Proliferation, Polarization, and Function of Macrophages. *Clin. Cancer Res*. 2017;23(20):6021–6030.
144. 1000 Genomes Project Consortium, Auton A, Brooks LD, et al. A global reference for human genetic variation. *Nature*. 2015;526(7571):68–74.
145. Collins RJ, Verschuer LA, Harmon BV, et al. Spontaneous programmed death (apoptosis) of B-chronic lymphocytic leukaemia cells following their culture in vitro. *Br J Haematol*. 1989;71(3):343–350.

146. Panayiotidis P, Jones D, Ganeshaguru K, Foroni L, Hoffbrand AV. Human bone marrow stromal cells prevent apoptosis and support the survival of chronic lymphocytic leukaemia cells in vitro. *Br J Haematol.* 1996;92(1):97–103.
147. Lagneaux L, Delforge A, Bron D, De Bruyn C, Stryckmans P. Chronic lymphocytic leukemic B cells but not normal B cells are rescued from apoptosis by contact with normal bone marrow stromal cells. *Blood.* 1998;91(7):2387–2396.
148. Whitlock CA, Witte ON. Long-term culture of B lymphocytes and their precursors from murine bone marrow. *Proceedings of the National Academy of Sciences.* 1982;79(11):3608–3612.
149. Witte PL, Robinson M, Henley A, et al. Relationships between B-lineage lymphocytes and stromal cells in long-term bone marrow cultures. *Eur. J. Immunol.* 1987;17(10):1473–1484.
150. Burger JA, Burger M, Kipps TJ. Chronic lymphocytic leukemia B cells express functional CXCR4 chemokine receptors that mediate spontaneous migration beneath bone marrow stromal cells. *Blood.* 1999;94(11):3658–3667.
151. Burger JA, Tsukada N, Burger M, et al. Blood-derived nurse-like cells protect chronic lymphocytic leukemia B cells from spontaneous apoptosis through stromal cell-derived factor-1. *Blood.* 2000;96(8):2655–2663.
152. Ysebaert L, Fournié J-J. Genomic and phenotypic characterization of nurse-like cells that promote drug resistance in chronic lymphocytic leukemia. *Leuk. Lymphoma.* 2011;52(7):1404–1406.

153. Boissard F, Fournié J-J, Laurent C, Poupot M, Ysebaert L. Nurse like cells: chronic lymphocytic leukemia associated macrophages. *Leuk. Lymphoma*. 2015;56(5):1570–1572.
154. Boissard F, Fournie JJ, Quillet-Mary A, Ysebaert L, Poupot M. Nurse-like cells mediate ibrutinib resistance in chronic lymphocytic leukemia patients. *Blood Cancer J*. 2015;5(10):e355–e355.
155. Nishio M, Endo T, Tsukada N, et al. Nurselike cells express BAFF and APRIL, which can promote survival of chronic lymphocytic leukemia cells via a paracrine pathway distinct from that of SDF-1alpha. *Blood*. 2005;106(3):1012–1020.
156. Burger JA, Quiroga MP, Hartmann E, et al. High-level expression of the T-cell chemokines CCL3 and CCL4 by chronic lymphocytic leukemia B cells in nurselike cell cocultures and after BCR stimulation. *Blood*. 2009;113(13):3050–3058.
157. Polk A, Lu Y, Wang T, et al. Colony-Stimulating Factor-1 Receptor Is Required for Nurse-like Cell Survival in Chronic Lymphocytic Leukemia. *Clin. Cancer Res*. 2016;22(24):6118–6128.
158. Haegel H, Thioudellet C, Hallet R, et al. A unique anti-CD115 monoclonal antibody which inhibits osteolysis and skews human monocyte differentiation from M2-polarized macrophages toward dendritic cells. *MAbs*. 2013;5(5):736–747.
159. Bertilaccio MTS, Scielzo C, Simonetti G, et al. A novel Rag2^{-/-}-gammac^{-/-} xenograft model of human CLL. *Blood*. 2010;115(8):1605–1609.

160. Galletti G, Scielzo C, Barboglio F, et al. Targeting Macrophages Sensitizes Chronic Lymphocytic Leukemia to Apoptosis and Inhibits Disease Progression. *Cell Rep.* 2016;14(7):1748–1760.
161. Miller KD, Siegel RL, Lin CC, et al. Cancer treatment and survivorship statistics, 2016. *CA Cancer J Clin.* 2016;66(4):271–289.
162. Dohner H, Stilgenbauer S, Benner A, et al. Genomic aberrations and survival in chronic lymphocytic leukemia. *N. Engl. J. Med.* 2000;343(26):1910–1916.
163. Choi MY, Kipps TJ. Inhibitors of B-cell receptor signaling for patients with B-cell malignancies. *Cancer J.* 2012;18(5):404–410.
164. Komohara Y, Jinushi M, Takeya M. Clinical significance of macrophage heterogeneity in human malignant tumors. *Cancer Sci.* 2014;105(1):1–8.
165. Ruffell B, Affara NI, Coussens LM. Differential macrophage programming in the tumor microenvironment. *Trends Immunol.* 2012;33(3):119–126.
166. Boissard F, Laurent C, Ramsay AG, et al. Nurse-like cells impact on disease progression in chronic lymphocytic leukemia. *Blood Cancer J.* 2016;6(1):e381–e381.
167. Burger JA, Tsukada N, Burger M, et al. Blood-derived nurse-like cells protect chronic lymphocytic leukemia B cells from spontaneous apoptosis through stromal cell-derived factor-1. *Blood.* 2000;96(8):2655–2663.
168. Bhattacharya N, Diener S, Idler IS, et al. Non-malignant B cells and chronic lymphocytic leukemia cells induce a pro-survival phenotype in CD14+ cells from peripheral blood. *Leukemia.* 2011;25(4):722–726.

169. Filip AA, Ciseł B, Koczkodaj D, et al. Circulating microenvironment of CLL: are nurse-like cells related to tumor-associated macrophages? *Blood Cells Mol Dis.* 2013;50(4):263–270.
170. Friedman DR, Sibley AB, Owzar K, et al. Relationship of blood monocytes with chronic lymphocytic leukemia aggressiveness and outcomes: a multi-institutional study. *Am. J. Hematol.* 2016;91(7):687–691.
171. Van Overmeire E, Stijlemans B, Heymann F, et al. M-CSF and GM-CSF Receptor Signaling Differentially Regulate Monocyte Maturation and Macrophage Polarization in the Tumor Microenvironment. *Cancer Res.* 2016;76(1):35–42.
172. Hampe A, Shamoon BM, Gobet M, Sherr CJ, Galibert F. Nucleotide sequence and structural organization of the human FMS proto-oncogene. *Oncogene Res.* 1989;4(1):9–17.
173. Byrne PV, Guilbert LJ, Stanley ER. Distribution of cells bearing receptors for a colony-stimulating factor (CSF-1) in murine tissues. *J. Cell Biol.* 1981;91(3 Pt 1):848–853.
174. Rieger MA, Hoppe PS, Smejkal BM, Eitelhuber AC, Schroeder T. Hematopoietic cytokines can instruct lineage choice. *Science.* 2009;325(5937):217–218.
175. Priceman SJ, Sung JL, Shaposhnik Z, et al. Targeting distinct tumor-infiltrating myeloid cells by inhibiting CSF-1 receptor: combating tumor evasion of antiangiogenic therapy. *Blood.* 2010;115(7):1461–1471.

176. Hanna BS, McClanahan F, Yazdanparast H, et al. Depletion of CLL-associated patrolling monocytes and macrophages controls disease development and repairs immune dysfunction in vivo. *Leukemia*. 2016;30(3):570–579.
177. Polk A, Lu Y, Wang T, et al. Colony-stimulating Factor-1 Receptor is Required for Nurse-like Cell Survival in Chronic Lymphocytic Leukemia. *Clin. Cancer Res.* 2016.
178. Conway JG, McDonald B, Parham J, et al. Inhibition of colony-stimulating-factor-1 signaling in vivo with the orally bioavailable cFMS kinase inhibitor GW2580. *Proceedings of the National Academy of Sciences*. 2005;102(44):16078–16083.
179. Munk Pedersen I, Reed J. Microenvironmental interactions and survival of CLL B-cells. *Leuk. Lymphoma*. 2004;45(12):2365–2372.
180. Ramsay AG, Clear AJ, Fatah R, Gribben JG. Multiple inhibitory ligands induce impaired T-cell immunologic synapse function in chronic lymphocytic leukemia that can be blocked with lenalidomide: establishing a reversible immune evasion mechanism in human cancer. *Blood*. 2012;120(7):1412–1421.
181. Chou T-C. Theoretical basis, experimental design, and computerized simulation of synergism and antagonism in drug combination studies. *Pharmacol. Rev.* 2006;58(3):621–681.

182. Furman RR, Sharman JP, Coutre SE, et al. Idelalisib and rituximab in relapsed chronic lymphocytic leukemia. *N. Engl. J. Med.* 2014;370(11):997–1007.
183. Byrd JC, Furman RR, Coutre SE, et al. Three-year follow-up of treatment-naïve and previously treated patients with CLL and SLL receiving single-agent ibrutinib. *Blood.* 2015;125(16):2497–2506.
184. Woyach JA, Furman RR, Liu T-M, et al. Resistance mechanisms for the Bruton's tyrosine kinase inhibitor ibrutinib. *N. Engl. J. Med.* 2014;370(24):2286–2294.
185. Maddocks KJ, Ruppert AS, Lozanski G, et al. Etiology of Ibrutinib Therapy Discontinuation and Outcomes in Patients With Chronic Lymphocytic Leukemia. *JAMA Oncol.* 2015;1(1):80–87.
186. Mantovani A, Ming WJ, Balotta C, Abdeljalil B, Bottazzi B. Origin and regulation of tumor-associated macrophages: the role of tumor-derived chemotactic factor. *Biochim. Biophys. Acta.* 1986;865(1):59–67.
187. Ruffell B, Chang-Strachan D, Chan V, et al. Macrophage IL-10 blocks CD8+ T cell-dependent responses to chemotherapy by suppressing IL-12 expression in intratumoral dendritic cells. *Cancer Cell.* 2014;26(5):623–637.
188. Tsukada N, Burger JA, Zvaifler NJ, Kipps TJ. Distinctive features of “nurselike” cells that differentiate in the context of chronic lymphocytic leukemia. *Blood.* 2002;99(3):1030–1037.

189. Galletti G, Caligaris-Cappio F, Bertilaccio MTS. B cells and macrophages pursue a common path toward the development and progression of chronic lymphocytic leukemia. *Leukemia*. 2016;30(12):2293–2301.
190. Steidl C, Lee T, Shah SP, et al. Tumor-associated macrophages and survival in classic Hodgkin's lymphoma. *N. Engl. J. Med.* 2010;362(10):875–885.
191. Koh YW, Park C, Yoon DH, Suh C, Huh J. CSF-1R expression in tumor-associated macrophages is associated with worse prognosis in classical Hodgkin lymphoma. *Am. J. Clin. Pathol.* 2014;141(4):573–583.
192. Shiao SL, Ruffell B, DeNardo DG, et al. TH2-Polarized CD4(+) T Cells and Macrophages Limit Efficacy of Radiotherapy. *Cancer Immunol Res.* 2015;3(5):518–525.
193. Cotechini T, Medler TR, Coussens LM. Myeloid Cells as Targets for Therapy in Solid Tumors. *Cancer J.* 2015;21(4):343–350.
194. Fiorcari S, Maffei R, Audrito V, et al. Ibrutinib modifies the function of monocyte/macrophage population in chronic lymphocytic leukemia. *Oncotarget.* 2016;7(40):65968–65981.
195. Tyner JW, Yang WF, Bankhead A, et al. Kinase pathway dependence in primary human leukemias determined by rapid inhibitor screening. *Cancer Res.* 2013;73(1):285–296.
196. Chou TC, Talalay P. Quantitative analysis of dose-effect relationships: the combined effects of multiple drugs or enzyme inhibitors. *Adv. Enzyme Regul.* 1984;22:27–55.

197. Reich M, Liefeld T, Gould J, et al. GenePattern 2.0. *Nat. Genet.* 2006;38(5):500–501.
198. Davis MI, Hunt JP, Herrgard S, et al. Comprehensive analysis of kinase inhibitor selectivity. *Nat. Biotechnol.* 2011;29(11):1046–1051.
199. Wright AD, Lee A, Boys ML, et al. A potent and selective cFMS inhibitor regulates the tumor macrophage microenvironment leading to tumor growth inhibition. *AACR.* 2011;71(8 Supplement):1–1.
200. Edwards DK V, Rofelty A, Agarwal A, et al. CSF1R Inhibition Targets AML Cells By Depleting Supportive Microenvironmental Signal from CD14+ Monocytes. *Blood.* 2015;126(23):3824–3824.
201. Jan M, Majeti R. Clonal evolution of acute leukemia genomes. *Oncogene.* 2013;32(2):135–140.
202. Tabe Y, Konopleva M. Advances in understanding the leukaemia microenvironment. *Br J Haematol.* 2014;164(6):767–778.
203. Tabe Y, Konopleva M. Role of Microenvironment in Resistance to Therapy in AML. *Curr Hematol Malig Rep.* 2015;10(2):96–103.
204. Colmone A, Freudiger CW, Min W, et al. Leukemic cells create bone marrow niches that disrupt the behavior of normal hematopoietic progenitor cells. *Science.* 2008;322(5909):1861–1865.
205. Raaijmakers MHGP, Mukherjee S, Guo S, et al. Bone progenitor dysfunction induces myelodysplasia and secondary leukaemia. *Nature.* 2010;464(7290):852–857.

206. Duhrsen U, Hossfeld DK. Stromal abnormalities in neoplastic bone marrow diseases. *Ann. Hematol.* 1996;73(2):53–70.
207. Hanoun M, Zhang D, Mizoguchi T, et al. Acute myelogenous leukemia-induced sympathetic neuropathy promotes malignancy in an altered hematopoietic stem cell niche. *Cell Stem Cell.* 2014;15(3):365–375.
208. Zambetti NA, Ping Z, Chen S, et al. Mesenchymal Inflammation Drives Genotoxic Stress in Hematopoietic Stem Cells and Predicts Disease Evolution in Human Pre-leukemia. *Cell Stem Cell.* 2016;19(5):613–627.
209. Schepers K, Pietras EM, Reynaud D, et al. Myeloproliferative neoplasia remodels the endosteal bone marrow niche into a self-reinforcing leukemic niche. *Cell Stem Cell.* 2013;13(3):285–299.
210. Kode A, Manavalan JS, Mosialou I, et al. Leukaemogenesis induced by an activating β -catenin mutation in osteoblasts. *Nature.* 2014;506(7487):240–244.
211. Le Dieu R, Taussig DC, Ramsay AG, et al. Peripheral blood T cells in acute myeloid leukemia (AML) patients at diagnosis have abnormal phenotype and genotype and form defective immune synapses with AML blasts. *Blood.* 2009;114(18):3909–3916.
212. Zhou Q, Munger ME, Veenstra RG, et al. Coexpression of Tim-3 and PD-1 identifies a CD8⁺ T-cell exhaustion phenotype in mice with disseminated acute myelogenous leukemia. *Blood.* 2011;117(17):4501–4510.
213. Schnorfeil FM, Lichtenegger FS, Emmerig K, et al. T cells are functionally not impaired in AML: increased PD-1 expression is only seen at time of

- relapse and correlates with a shift towards the memory T cell compartment. *J Hematol Oncol*. 2015;8(1):93.
214. Mantovani A, Marchesi F, Malesci A, Laghi L, Allavena P. Tumour-associated macrophages as treatment targets in oncology. *Nat Rev Clin Oncol*. 2017;14(7):399–416.
215. Mouchemore KA, Pixley FJ. CSF-1 signaling in macrophages: pleiotrophy through phosphotyrosine-based signaling pathways. *Crit Rev Clin Lab Sci*. 2012;49(2):49–61.
216. Edwards DK V, Sweeney DT, Ho H, et al. Targeting of colony-stimulating factor 1 receptor (CSF1R) in the CLL microenvironment yields antineoplastic activity in primary patient samples. *Oncotarget*. 2018.
217. Al-Matary YS, Botezatu L, Opalka B, et al. Acute myeloid leukemia cells polarize macrophages towards a leukemia supporting state in a Growth factor independence 1 dependent manner. *Haematologica*. 2016;101(10):1216–1227.
218. Tyner JW, Tyner JW, Yang WF, et al. Kinase pathway dependence in primary human leukemias determined by rapid inhibitor screening. *Cancer Res*. 2013;73(1):285–296.
219. Kurtz SE, Eide CA, Kaempf A, et al. Molecularly targeted drug combinations demonstrate selective effectiveness for myeloid- and lymphoid-derived hematologic malignancies. *Proc. Natl. Acad. Sci. U.S.A.* 2017;114(36):E7554–E7563.

220. Tyner JW, Walters DK, Willis SG, et al. RNAi screening of the tyrosine kinome identifies therapeutic targets in acute myeloid leukemia. *Blood*. 2008;111(4):2238–2245.
221. Tyner JW, Deininger MW, Loriaux MM, et al. RNAi screen for rapid therapeutic target identification in leukemia patients. *Proc. Natl. Acad. Sci. U.S.A.* 2009;106(21):8695–8700.
222. Lamble AJ, Dietz M, Laderas T, McWeeney S, Lind EF. Integrated functional and mass spectrometry-based flow cytometric phenotyping to describe the immune microenvironment in acute myeloid leukemia. *J. Immunol. Methods*. 2017.
223. Finak G, Frelinger J, Jiang W, et al. OpenCyto: an open source infrastructure for scalable, robust, reproducible, and automated, end-to-end flow cytometry data analysis. *PLoS Comput. Biol.* 2014;10(8):e1003806.
224. Hahne F, LeMeur N, Brinkman RR, et al. flowCore: a Bioconductor package for high throughput flow cytometry. *BMC Bioinformatics*. 2009;10:106.
225. Finak G, Langweiler M, Jaimes M, et al. Standardizing Flow Cytometry Immunophenotyping Analysis from the Human ImmunoPhenotyping Consortium. *Sci Rep*. 2016;6:20686.
226. Carey A, Edwards DK V, Eide CA, et al. Identification of Interleukin-1 by Functional Screening as a Key Mediator of Cellular Expansion and Disease Progression in Acute Myeloid Leukemia. *Cell Rep*. 2017;18(13):3204–3218.

227. Li J, Sejas DP, Zhang X, et al. TNF-alpha induces leukemic clonal evolution ex vivo in Fanconi anemia group C murine stem cells. *J. Clin. Invest.* 2007;117(11):3283–3295.
228. Corbin AS, Agarwal A, Loriaux M, et al. Human chronic myeloid leukemia stem cells are insensitive to imatinib despite inhibition of BCR-ABL activity. *J. Clin. Invest.* 2011;121(1):396–409.
229. Roecklein BA, Torok-Storb B. Functionally distinct human marrow stromal cell lines immortalized by transduction with the human papilloma virus E6/E7 genes. *Blood.* 1995;85(4):997–1005.
230. Edwards DK V, Eryildiz F, Tyner JW. RNAi screening of the tyrosine kinome in primary patient samples of acute myeloid leukemia.
231. Watanabe-Smith K, Druker BJ, Tyner JW, Edwards DK V. Automated decision tree to evaluate genetic abnormalities when determining prognostic risk in acute myeloid leukemia. *Haematologica.* 2018;haematol.2018.190926.
232. McGowan-Jordan J, Simons A, Schmid M. ISCN 2016. Basel, Switzerland: S. Karger Publishing; 2016.
233. Huang Q, Chen W, Gaal KK, et al. A rapid, one step assay for simultaneous detection of FLT3/ITD and NPM1 mutations in AML with normal cytogenetics. *Br J Haematol.* 2008;142(3):489–492.
234. Li H, Durbin R. Fast and accurate short read alignment with Burrows-Wheeler transform. *Bioinformatics.* 2009;25(14):1754–1760.

235. McKenna A, Hanna M, Banks E, et al. The Genome Analysis Toolkit: a MapReduce framework for analyzing next-generation DNA sequencing data. *Genome Res.* 2010;20(9):1297–1303.
236. Cibulskis K, Lawrence MS, Carter SL, et al. Sensitive detection of somatic point mutations in impure and heterogeneous cancer samples. *Nat. Biotechnol.* 2013;31(3):213–219.
237. Koboldt DC, Zhang Q, Larson DE, et al. VarScan 2: somatic mutation and copy number alteration discovery in cancer by exome sequencing. *Genome Res.* 2012;22(3):568–576.
238. McLaren W, Pritchard B, Rios D, et al. Deriving the consequences of genomic variants with the Ensembl API and SNP Effect Predictor. *Bioinformatics.* 2010;26(16):2069–2070.
239. Liao Y, Smyth GK, Shi W. The Subread aligner: fast, accurate and scalable read mapping by seed-and-vote. *Nucleic Acids Res.* 2013;41(10):e108.
240. Liao Y, Smyth GK, Shi W. featureCounts: an efficient general purpose program for assigning sequence reads to genomic features. *Bioinformatics.* 2014;30(7):923–930.
241. Lilljebjörn H, Ågerstam H, Orsmark-Pietras C, et al. RNA-seq identifies clinically relevant fusion genes in leukemia including a novel MEF2D/CSF1R fusion responsive to imatinib. *Leukemia.* 2014;28(4):977–979.

242. Fallahi-Sichani M, Honarnejad S, Heiser LM, Gray JW, Sorger PK. Metrics other than potency reveal systematic variation in responses to cancer drugs. *Nat. Chem. Biol.* 2013;9(11):708–714.
243. Tagoh H, Himes R, Leenen PJM, Riggs AD, Hume D. Transcription factor complex formation and chromatin fine structure alterations at the murine c-fms (CSF-1 receptor) locus during maturation of myeloid precursor cells. *Genes Dev.* 2002;16(13):1721–1737.
244. Solito S, Marigo I, Pinton L, et al. Myeloid-derived suppressor cell heterogeneity in human cancers. *Ann. N. Y. Acad. Sci.* 2014;1319:47–65.
245. Eda H, Zhang J, Keith RH, et al. Macrophage-colony stimulating factor and interleukin-34 induce chemokines in human whole blood. *Cytokine.* 2010;52(3):215–220.
246. Noy R, Pollard JW. Tumor-associated macrophages: from mechanisms to therapy. *Immunity.* 2014;41(1):49–61.
247. Ohri CM, Shikotra A, Green RH, Waller DA, Bradding P. Macrophages within NSCLC tumour islets are predominantly of a cytotoxic M1 phenotype associated with extended survival. *Eur. Respir. J.* 2009;33(1):118–126.
248. Zhang M, He Y, Sun X, et al. A high M1/M2 ratio of tumor-associated macrophages is associated with extended survival in ovarian cancer patients. *J Ovarian Res.* 2014;7(1):19.
249. Viale A, Pettazoni P, Lyssiotis CA, et al. Oncogene ablation-resistant pancreatic cancer cells depend on mitochondrial function. *Nature.* 2014;514(7524):628–632.

250. Dumitru CA, Moses K, Trellakis S, Lang S, Brandau S. Neutrophils and granulocytic myeloid-derived suppressor cells: immunophenotyping, cell biology and clinical relevance in human oncology. *Cancer Immunol. Immunother.* 2012;61(8):1155–1167.
251. Bronte V, Brandau S, Chen S-H, et al. Recommendations for myeloid-derived suppressor cell nomenclature and characterization standards. *Nat Commun.* 2016;7:12150.
252. Elliott LA, Doherty GA, Sheahan K, Ryan EJ. Human Tumor-Infiltrating Myeloid Cells: Phenotypic and Functional Diversity. *Front Immunol.* 2017;8:86.
253. Fixe P, Rougier F, Ostyn E, et al. Spontaneous and inducible production of macrophage colony-stimulating factor by human bone marrow stromal cells. *Eur. Cytokine Netw.* 1997;8(1):91–95.
254. Kentsis A, Reed C, Rice KL, et al. Autocrine activation of the MET receptor tyrosine kinase in acute myeloid leukemia. *Nat. Med.* 2012;18(7):1118–1122.
255. Molnarfi N, Benkhoucha M, Bjarnadóttir K, Juillard C, Lalive PH. Interferon- β induces hepatocyte growth factor in monocytes of multiple sclerosis patients. *PLoS ONE.* 2012;7(11):e49882.
256. Oken MM, Creech RH, Tormey DC, et al. Toxicity and response criteria of the Eastern Cooperative Oncology Group. *Am. J. Clin. Oncol.* 1982;5(6):649–655.
257. Hallek M, Cheson BD, Catovsky D, et al. Guidelines for the diagnosis and treatment of chronic lymphocytic leukemia: a report from the International

- Workshop on Chronic Lymphocytic Leukemia updating the National Cancer Institute-Working Group 1996 guidelines. *Blood*. 2008;111(12):5446–5456.
258. Tuntland T, Ethell B, Kosaka T, et al. Implementation of pharmacokinetic and pharmacodynamic strategies in early research phases of drug discovery and development at Novartis Institute of Biomedical Research. *Front Pharmacol*. 2014;5:174.
259. Levis M, Brown P, Smith BD, et al. Plasma inhibitory activity (PIA): a pharmacodynamic assay reveals insights into the basis for cytotoxic response to FLT3 inhibitors. *Blood*. 2006;108(10):3477–3483.
260. Emami J. In vitro - in vivo correlation: from theory to applications. *J Pharm Pharm Sci*. 2006;9(2):169–189.
261. Zhao Z, Goldin L, Liu S, et al. Evolution of multiple cell clones over a 29-year period of a CLL patient. *Nat Commun*. 2016;7:13765.
262. Wang L, Fan J, Francis JM, et al. Integrated single-cell genetic and transcriptional analysis suggests novel drivers of chronic lymphocytic leukemia. *Genome Res*. 2017;27(8):1300–1311.
263. Chung W, Eum HH, Lee H-O, et al. Single-cell RNA-seq enables comprehensive tumour and immune cell profiling in primary breast cancer. *Nat Commun*. 2017;8:15081.
264. Yoshihara K, Shahmoradgoli M, Martínez E, et al. Inferring tumour purity and stromal and immune cell admixture from expression data. *Nat Commun*. 2013;4:2612.

265. Bindea G, Mlecnik B, Tosolini M, et al. Spatiotemporal dynamics of intratumoral immune cells reveal the immune landscape in human cancer. *Immunity*. 2013;39(4):782–795.
266. Müller S, Kohanbash G, Liu SJ, et al. Single-cell profiling of human gliomas reveals macrophage ontogeny as a basis for regional differences in macrophage activation in the tumor microenvironment. *Genome Biol*. 2017;18(1):234.
267. Konopleva M, Pollyea DA, Potluri J, et al. Efficacy and Biological Correlates of Response in a Phase II Study of Venetoclax Monotherapy in Patients with Acute Myelogenous Leukemia. *Cancer Discov*. 2016;6(10):1106–1117.
268. Stilgenbauer S, Eichhorst B, Schetelig J, et al. Venetoclax in relapsed or refractory chronic lymphocytic leukaemia with 17p deletion: a multicentre, open-label, phase 2 study. *Lancet Oncol*. 2016;17(6):768–778.
269. Borthakur G, Popplewell L, Boyiadzis M, et al. Activity of the oral mitogen-activated protein kinase kinase inhibitor trametinib in RAS-mutant relapsed or refractory myeloid malignancies. *Cancer*. 2016;122(12):1871–1879.